University of Glasgow

Kupper, Manuel (2021) *Design of experiments for polyoxometalate syntheses.* MSc(R) thesis.

http://theses.gla.ac.uk/82292/

Copyright and moral rights for this work are retained by the author

A copy can be downloaded for personal non-commercial research or study, without prior permission or charge

This work cannot be reproduced or quoted extensively from without first obtaining permission in writing from the author

The content must not be changed in any way or sold commercially in any format or medium without the formal permission of the author

When referring to this work, full bibliographic details including the author, title, awarding institution and date of the thesis must be given

Enlighten: Theses
https://theses.gla.ac.uk/
research-enlighten@glasgow.ac.uk

Design of Experiments for Polyoxometalate Syntheses

Manuel Kupper

A dissertation submitted to the University of Glasgow for the degree of Master of Science by Research (MScR)

School of Chemistry
College of Science and Engineering

February 2021

Acknowledgements

The work presented here was carried out between May 2019 and February 2021 in the Cronin Group within the School of Chemistry at the University of Glasgow. Without the help and support of many people, this work would not have been possible. In particular, I would like to express my gratitude to the following people:

First and foremost, I thank **Prof. Leroy Cronin** for giving time, guidance, patience and the opportunity to carry out this project in his research group as well making this degree.

Immense thanks to **Jim McIver**, who took care of all the little problems and questions I had as well as to **Dr. Nicola Bell**, who helped me a lot with this project and writing the paper about it. Thanks to **Amanda McGarvey**, who always sorted out my administrative issues in no time and to **Dr. Diana Castro Spencer**, who organised big parts of the equipment I needed. Thanks to **Dr. De-Liang Long**, who helped me with resolving crystal structures.

A special thanks to my friends **Dr. Naomi Johnson, Dr. Stephanie Colón Santos** and soon to be doctors **Marcus Tze-Kiat Ng** and **Andrius Bubliauskas** for proofreading this dissertation.

πάντα ῥεῖ

-Heraclitus of Ephesos

1. Introduction

1.1. Design of Experiments

1.1.1 History

Design of experiments (DOE) was pioneered by Ronald Aylmer Fisher between the late 1910s to the mid of 1930s, who aimed to increase the yield of crop in the UK. Traditional methods, such as the predominant principle of changing *one factor at a time* (OFAT), were insufficient for agricultural work because planting a crop in spring and waiting until autumn to get results was too slow to obtain usable data for subsequent iteration. Therefore, the novelty behind DOE was to replace the traditional approach by changing *multiple factors at a time.* Furthermore, Fisher discovered how valid conclusion could be drawn from experiments even in presence of not actively changed so-called *nuisance factors*. In 1935, the book "*The design of experiments"* laid out the fundamental principles of DOE such as *replication, randomisation, blocking* and *confounding* as well as the analysis of variance to be able to interpret results.[1] Fisher also analysed the effect of nuisance factors in yields, e.g. fluctuation of weather conditions.[2] The initial impact of DOE principles and methods on agricultural science was profound, but more importantly, a whole new field was created.

Other key contributors include George E. P. Box and K. B. Wilson, who introduced the *response surface method* (RSM) which uses a sequence of designed experiments to obtain an optimal response. Later, Box and Wilson suggested a second-degree polynomial model as an approximation to estimate effects, even if little is known about a process.[2]

In the 1980s, the Big Three automobile makers at the forefront of US firms took a renewed interest in these statistical methods. Due to the availability of affordable desktop computers and software capable of handling the numerous calculations that DOE methods require,[3] an emphasis was laid on design of experiments to deal with aspects of *statistical process control* (SPC) and *total quality management* (TQM).[4] In recent times, there has been a paradigm shift to *optimal designs* which are not bound to fixed design structures anymore whilst at the same time reducing the cost of experimentation. [3]

1.1.2 What is Design of Experiments?

Design of Experiments, referred to as DOE, is a branch of applied statistics which is used in a variety of experimental situations such as planning and conducting experiments as well as analysing and interpreting data.[2] It is a mathematical, multipurpose tool used in various fields for identification of important process parameters and their relation to the outputs. This means arranging input variables (X) in such a way that their effects on a measured response (Y) can be calculated relatively easily due to its statistical methodology.

DOE is basically regression analysis that can be used for numerous purposes such as factor comparison, variable screening, system optimisation and robust design.[2] By providing the most information from the least data the design of experiments replaces the idea of changing one factor at a time (OFAT) with changing multiple factors at a time (Figure 1), by enabling the researcher to generate any required data more quickly through a minimum amount of experimentation and herby save cost, time, material and energy.

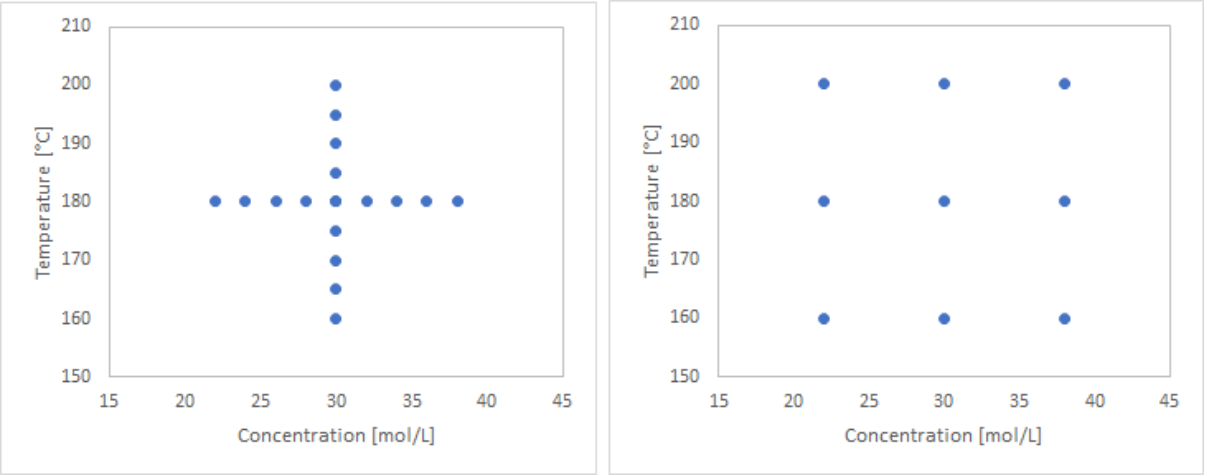

Figure 1

Visual example of how experimental space can be explored using OFAT vs. DOE methods.

In general, DOE differentiates between *controlled inputs* (X) which are the tunable *factors* chosen by the experimenter and *uncontrolled inputs* which are mostly dependent on the environment and can only be either observed or unobserved. Some of the uncontrolled also referred to as nuisance inputs may have an impact on the responses (Y) which would distort the analysis of the controlled input factors and therefore must be eliminated. This is achieved by *randomisation* and *repetition* of the runs whereby sequential errors are removed and changes in the environment e.g. temperature, pressure etc. are neutralised.

Each controlled input is referred to as *factor* and can be represented by a geometric dimension. Thus, one factor equals one dimension which is a line that spans from a low level to a high level. Varying the factor allows selection of multiple points on this line. The range between minimum and maximum levels is called the *design space* and can be expanded to a plane by using two factors giving two dimensions, a cube by three factors and so on as can be seen in Figure 2. Clearly, four dimensions are already difficult to imagine for humans but by continuing to add factors the design space extends into higher and higher dimensions.[3]

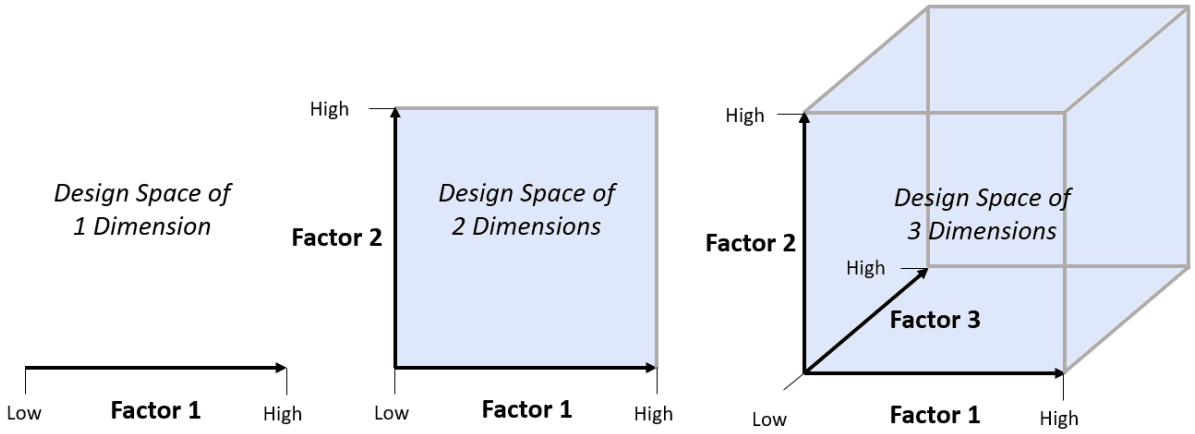

Figure 2

Visual example of how each factor adds respective dimensions to the experimental space.

In addition to determining if some main factors affect the final product significantly more than others, DOE is also capable of unravelling two-factor interactions which have a major effect on the outcome and otherwise would stay undetected. Factor interactions occur when multiple factors work together. They can also generate a significant effect on the outcome in which case their inherent main factors do as well.

In practice, a minimum and a maximum level are defined for each input factor (X) by the experimenter and in some designs, there can also be a third, neutral level in between. By varying multiple factors simultaneously in this manner each data point will provide more information about the surrounding design space than using OFAT methods.[3] This has two major results: the number of experiments is dramatically reduced while the precision of the received information is increased. For example, if k factors are studied at two levels, −1 (low level) and 1 (high level), a factorial design will consist of 2^k experiments.

In DOE, two basic principles contribute to the minimal amount of data required:

1. The so-called *hierarchy ordering principle*,[5] which presumes that higher order effects are more likely to dominate a system than lower order effects. That means main and two-factor interaction effects are considered to have a bigger influence on the process than three- or four-factor interaction effects which herby can be neglected in the analysis and in the planning of the design. By ignoring the lower order effects, e.g. a two-level five-factorial design can be reduced from 32 treatments to only 16 which can be seen comparing Table 1 and Table 2.
2. The *sparsity of effects principle* presumes that the total number of factor effects that dominate the system is small.[5] By applying both principles DOE experiments only identify the drivers of a system, which is a fundamentally different concept from determining all effects to understand and improve a process. [3]

Effects	Average Effect	Main Effects	2-factor Interactions	3-factor Interactions	4-factor Interactions	5-factor Interactions
Runs	1	5	10	10	5	1

Table 1

Number of runs for each effect in a full factorial design with five factors and two levels.

Effects	Average Effect	Main Effects	2-factor Interactions
Runs	1	5	10

Table 2

Number of runs for only higher order effects in a half factorial design with five factors and two levels.

1.1.3 Full Factorial Design (2^k)

In a *full factorial design,* the effects off all main factors and interactions are determined and evaluated. This is possible by carrying out a full set of 2^k runs, where k is the number of factors, and assigning the factors either to a high (1) or a low level (-1) in each run. For example, a *full factorial two level design* for three input factors (2^3) will consist of eight runs. The design is *orthogonal* which means if you multiply any two columns of the design matrix the sum of its treatments is always zero. This is made on purpose to determine all interaction columns. In fact, all 2^k designs are orthogonal.

Firstly, a table is created with the factors in columns and the runs in rows, then the levels are chosen for each factor using the pattern demonstrated in Table 3 starting with the low setting.

Run	Factor X_1	Factor X_2	Factor X_3
1	-1	-1	-1
2	1	-1	-1
3	-1	1	-1
4	1	1	-1
5	-1	-1	1
6	1	-1	1
7	-1	1	1
8	1	1	1

Table 3

A full factorial design matrix with three factors, two levels (1 and -1) in eight runs.

Geometrically each factor is equivalent to one dimension, so for a better understanding the design can be pictured graphically as a cube as shown in Figure 3. Each data point in the cube (1-8) represents one of the runs and the arrows show the direction of increase of the factors from the low (-1) to the high (1) setting.

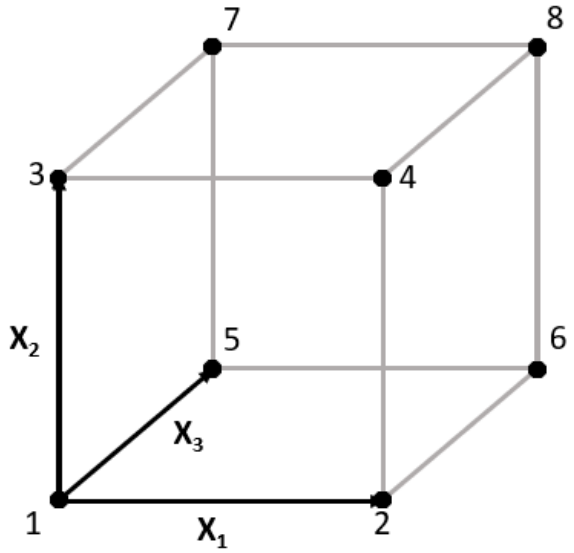

Figure 3

The three-dimensional chemical space a full factorial design with three factors and two levels covers.

Next, the relationship of the outcome (**Y**) with the main factors and all the interactions is interpreted. For simplicity, an example with only two input factors (X_1 and X_2) and four runs is chosen as can be seen in Table 4. The interaction X_1X_2 column is produced by simply multiplying the setting of X_1 with the setting of X_2.

Run	Factor X_1	Factor X_2	Interaction X_1X_2	Response Y (e.g. yield)
1	-1	-1	1	Y_1
2	1	-1	-1	Y_2
3	-1	1	-1	Y_3
4	1	1	1	Y_4

Table 4

A full factorial design matrix with two factors and two levels including a column for the interaction effect of the factors.

A linear relationship is assumed which delivers the following Equation 1:

$$Y = \beta_0 + \beta_1X_1 + \beta_2X_2 + \beta_{12}X_1X_2 \qquad \textit{Equation 1}$$

The next step is to calculate the coefficient values (β_X) of each factor, which, initially, is achieved by setting up four equations, one for each run:

$$Y_1 = \beta_0 + \beta_1(-1) + \beta_2(-1) + \beta_{12}(+1) \quad \textbf{(Run 1)} \qquad \textit{Equation 2}$$

$$Y_2 = \beta_0 + \beta_1(+1) + \beta_2(-1) + \beta_{12}(-1) \quad \textbf{(Run 2)} \qquad \textit{Equation 3}$$

$$Y_3 = \beta_0 + \beta_1(-1) + \beta_2(+1) + \beta_{12}(-1) \quad \textbf{(Run 3)} \qquad \textit{Equation 4}$$

$$Y_4 = \beta_0 + \beta_1(+1) + \beta_2(+1) + \beta_{12}(+1) \quad \textbf{(Run 4)} \qquad \textit{Equation 5}$$

β_0 being the mean of the responses (Y) is determined by addition of all four equations:

$$Y_1 + Y_2 + Y_3 + Y_4 = \beta_0 - \beta_1 - \beta_2 + \beta_{12} + \beta_0 + \beta_1 - \beta_2 - \beta_{12} + \beta_0 - \beta_1 + \beta_2 - \beta_{12} + \beta_0 + \beta_1 + \beta_2 + \beta_{12} \qquad \textit{Equation 6}$$

$$\frac{Y_1 + Y_2 + Y_3 + Y_4}{4} = \beta_0 \qquad \textit{Equation 7}$$

In the same fashion β_1, β_2 and β_{12} are calculated with the only difference being that the equations where the setting is at the low level (-1) are subtracted from the ones with the factors at the high level (1) in the column. Example for β_1:

$$-Y_1 + Y_2 - Y_3 + Y_4 = -\beta_0 + \beta_1 + \beta_2 - \beta_{12} + \beta_0 + \beta_1 - \beta_2 - \beta_{12} - \beta_0 + \beta_1 - \beta_2 + \beta_{12} + \beta_0 + \beta_1 + \beta_2 + \beta_{12} \qquad \textit{Equation 8}$$

$$\frac{-Y_1 + Y_2 - Y_3 + Y_4}{4} = \beta_1$$

These coefficients are the effects of each factor on the final product and the larger their value the greater the influence of a factor on a system.

As the number of runs increases exponentially on addition of more input factors (X), a full factorial design becomes ineffective at some point. Therefore, a *fractional factorial design* or a *Plackett-Burman design (PBD)* is used if five or more factors are examined.[6]

1.1.4 Fractional Factorial Design (2^{k-p})

Fractional factorial designs can be considered as a *fraction* of a *full factorial design* offering a reduced number of experiments without losing much data.[6] They are classified into two broad types: *regular* and *nonregular designs*.

Regular designs have run sizes that equal a power of two, and only full aliasing is present whereas nonregular designs are designs where run sizes are a multiple of 4 and their effects are partial aliased.

Fractional factorial designs can be used if there are too few resources to perform a full factorial design or at the early stages of the experimental research when the goal is to identify significant main effects. This is known as *screening*.

The concept can be illustrated as in Figure 4. Half of the data points at the corners of the cube are eliminated to reduce the number of runs from eight to four which can also be seen by comparing Table 5 and Table 6.

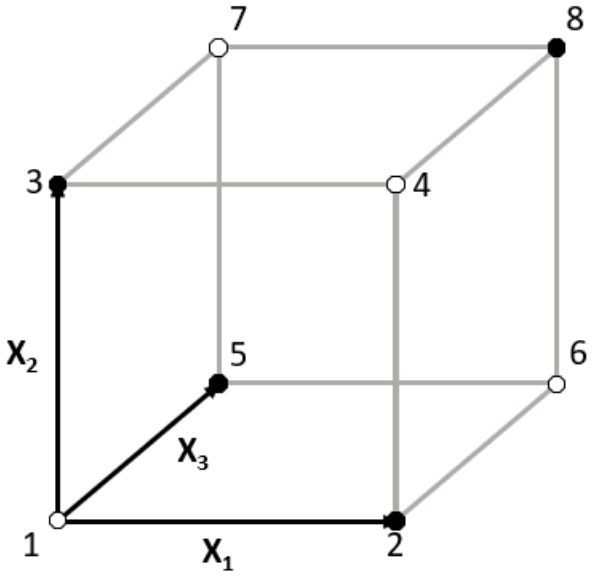

Figure 4

The three-dimensional chemical space a half factorial design with three factors and two levels covers.

Run	X_1	X_2	X_3	Y
1	-1	-1	-1	Y_1
2	1	-1	-1	Y_2
3	-1	1	-1	Y_3
4	1	1	-1	Y_4
5	-1	-1	1	Y_5
6	1	-1	1	Y_6
7	-1	1	1	Y_7
8	1	1	1	Y_8

Table 5

A full factorial design matrix with three factors and two levels.

Run	X_1	X_2	X_3	Y
1 (former 2)	1	-1	-1	Y_1
2 (former 3)	-1	1	-1	Y_2
3 (former 5)	-1	-1	1	Y_3
4 (former 8)	1	1	1	Y_4

Table 6

A half factorial design matrix with three factors and two levels

To compute the main effects from Table 6 it is necessary to subtract the average response of all runs with factors set at -1 (low level) from those set at 1 (high level):

$$\beta_1 = \left(\frac{1}{2}\right)(Y_1 + Y_4) - \left(\frac{1}{2}\right)(Y_2 + Y_3) \qquad \textit{Equation 9}$$

However, these designs entail *confounding* among the factor effects which lead to uncertainty in the interpretation of the results. Confounding, also called aliasing, is used as a general term to indicate that the value of a main effect estimate comes from both the main effect itself and the contamination or bias from other interaction effects. They always occur whenever a fractional factorial design is chosen instead of a full factorial design. The confounding increases the further the number of runs is reduced. Despite this, it is still possible to estimate the main factor and interaction effects from half or even less of the data points due to the two principles of *hierarchy ordering* and *sparsity of effects*, as described in Section 1.1.2.

Design resolution plays an important role and indicates the nature of the confounding in fractional factorial designs. A resolution III design, for example, confounds all main effects with two-factor interactions whereas a resolution IV design confounds main effects only with three-factor interactions but two-factor interactions with other two-factor interactions. However, a resolution V design is preferred due to its advantage of only confounding the main effects with four-factor interactions and the two-factor with three-factor interactions which means confounding can essentially be ignored due to the hierarchy ordering principle. As depicted in Table 7 it can be a difficult choice deciding which 2^{k-p} experimental design is best to use. In general, a higher resolution is always desired because it provides less severe confounding, however for the same number of factors it will require more runs.

		Number of Factors													
		2	**3**	**4**	**5**	**6**	**7**	**8**	**9**	**10**	**11**	**12**	**13**	**14**	**15**
Number of Runs	**4**	2^{2}	2^{3-1}												
	8		2^{3}	2^{4-1}	2^{5-2}	2^{6-3}	2^{7-4}								
	16			2^{4}	2^{5-1}	2^{6-2}	2^{7-3}	2^{8-4}	2^{9-5}	2^{10-6}	2^{11-7}	2^{12-8}	2^{13-9}	2^{14-10}	2^{15-11}
	32				2^{5}	2^{6-1}	2^{7-2}	2^{8-3}	2^{9-4}	2^{10-5}	2^{11-6}	2^{12-7}	2^{13-8}	2^{14-9}	2^{15-10}
	64					2^{6}	2^{7-1}	2^{8-2}	2^{9-3}	2^{10-4}	2^{11-5}	2^{12-6}	2^{13-7}	2^{14-8}	2^{15-9}
	128						2^{7}	2^{8-1}	2^{9-2}	2^{10-3}	2^{11-4}	2^{12-5}	2^{13-6}	2^{14-7}	2^{15-8}
		Full Factorial Design								Resolution IV Design					
		Resolution V (or Higher) Design								Resolution III Design					

Table 7

This table shows the resolutions for different designs depending on their number of factors and their number of runs.

1.1.5 Plackett-Burman Design

Plackett-Burman designs (PBD) are a type of *two-level, nonregular, fractional factorial designs* of which the run sizes are a multiple of four and belong to a wide class of orthogonal arrays.[7] Saturated designs like the PBD ignore interactions, focus on main effects exclusively and make ideal *screening designs* because they reduce the necessary number of runs significantly. One distinctive feature is that PB designs can examine up to $n - 1$ factors in n experiments, where n is a multiple of four, ergo a design with 12 experiments can examine up to eleven factors.[6]

The design is completed with *dummy factors* if the number of examined factors is smaller than *n – 1*. The effects of these imaginary factors can be used in statistical analysis of the main effects[8] and, in principle, are calculated as:

$$E_x = \frac{\sum Y(+) - \sum Y(-)}{n/2} \qquad \textit{Equation 10}$$

Where E_X is the effect of factor X, Σ*Y*(+) and Σ*Y*(−) are the sums of the responses where factor *X* is at the high or low setting and *n* is the number of runs.

The drawback of nonregular designs is their complicated alias patterns, also known as *confounding*, among main effects and interactions. For example, the quite common design in Table 8 which has two levels, eleven factors and twelve runs deals with 55 two-factor interactions. That means every single main effect is aliased with 45 two-factor effects making it extraordinarily difficult to interpret the significance of interactions. That is why PB designs are especially used for screening experiments examining only main effects.

In the example in Table 8 main effects are orthogonal to one another as they are to all two-factor interactions that contain that main effect. However, they are not orthogonal to two-factor interactions that do not contain that main effect. To find the correlation of factor A and interaction BC it is necessary to divide the vector product (sum of columns A and BC = -4) by the number of runs (12) which delivers a quotient of -0.333. Ergo the correlation is mathematically defined as:

$$r_{A,BC} = \frac{\Sigma_{X_A X_{BC}}}{\sqrt{(\Sigma_{X_A^2})(\Sigma_{X_{BC}^2})}} = -0.333 \qquad \textit{Equation 11}$$

As shown above in section 1.1.4, the values for the main factor and the interactions involved [e.g. E(BC)] can be determined by subtracting the average of the responses at the low level (-1) from the average of the responses at the high level (1) which is also called contrast because it compares two averages.[9]

All two-factor interactions that do not include the given main effect are correlated i.e. partially confounded with that main effect. Since factor A is aliased with 45 interactions the correlations for all of those must be calculated which determines the confounding and results in the estimated effect of factor A [$E(A_{est})$]. This can be written as the following equation:

$$E(A_{est}) = E(A) + r_{A,BC}E(BC) + r_{A,BD}E(BD) + \ldots + r_{A,JK}E(JK) \qquad \textit{Equation 12}$$

Once all main factors have been disentangled in this manner, they can be checked for their significance in the system.

Runs	Factor A	Factor B	Factor C	Factor D	Factor E	Factor F	Factor G	Factor H	Factor I	Factor J	Factor K	Response y
1	1	1	-1	1	1	1	-1	-1	-1	1	-1	y_1
2	1	-1	1	1	1	-1	-1	-1	1	-1	1	y_2
3	-1	1	1	1	-1	-1	-1	1	-1	1	1	y_3
4	1	1	1	-1	-1	-1	1	-1	1	1	-1	y_4
5	1	1	-1	-1	-1	1	-1	1	1	-1	1	y_5
6	1	-1	-1	-1	1	-1	1	1	-1	1	1	y_6
7	-1	-1	-1	1	-1	1	1	-1	1	1	1	y_7
8	-1	-1	1	-1	1	1	-1	1	1	1	-1	y_8
9	-1	1	-1	1	1	-1	1	1	1	-1	-1	y_9
10	1	-1	1	1	-1	1	1	1	-1	-1	-1	y_{10}
11	-1	1	1	-1	1	1	1	-1	-1	-1	1	y_{11}
12	-1	-1	-1	-1	-1	-1	-1	-1	-1	-1	-1	y_{12}

Table 8

A Plackett-Burman design matrix with eleven factors, twelve runs and two levels.

Runs/ Factors	1	2	3	4	5	6	7	8	9	10	11	12
A	1	1	-1	1	1	1	-1	-1	-1	1	-1	-1
BC	-1	-1	1	1	-1	1	1	-1	-1	-1	1	1
A*BC	-1	-1	-1	1	-1	1	-1	1	1	-1	-1	-1

Table 9

Visual way of finding the vector product of factor A and interaction BC by multiplying both columns and adding the numerals of A*BC together which equals -4 in this case.

1.2 Polyoxometalates

A polyoxometalate (POM) is a polyatomic ion that consists of at least three transition metal oxyanions linked together by shared oxygen atoms forming mostly anionic clusters that can vary in size from molecular up to nano-scale.[10]

Most POMs are synthesised in an aqueous environment by acid-mediated condensation of simple oxometallate anions $[MO_4]^{n-}$ under one-pot conditions growing larger building blocks and clusters in a self-assembly process and are isolated through crystallisation. Many parameters including pH, temperature, reactant ratio, reactant concentration, ionic strength, and the presence of oxidants, reducing agents or organic ligands can influence the process and the window in which POMs form is rather narrow so reproducibility is a common problem.

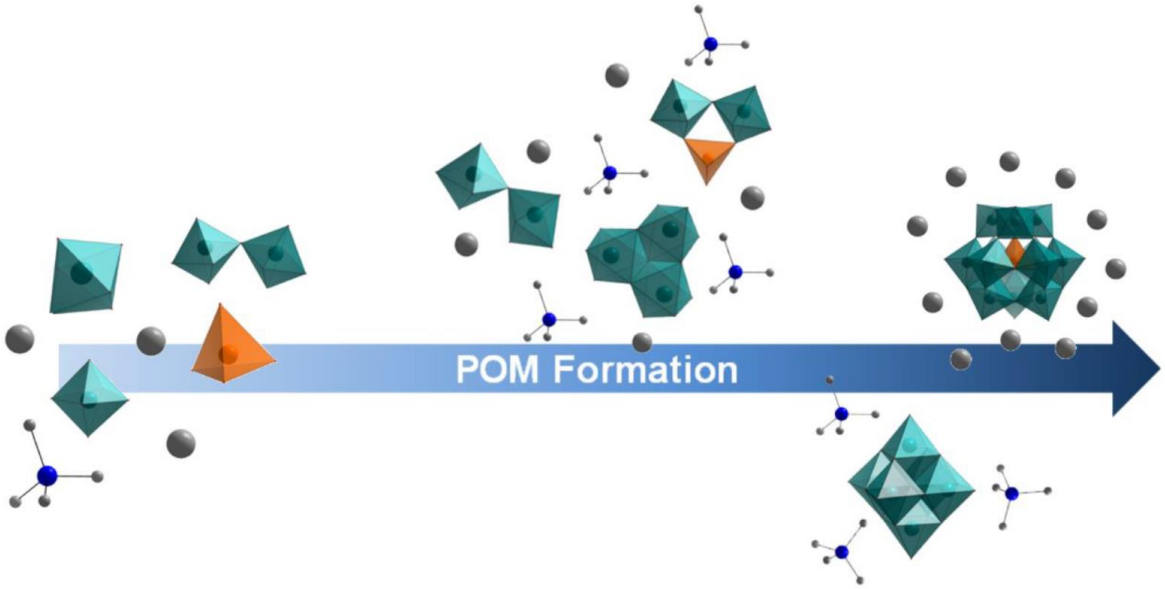

Figure 5

Schematic representation of the synthesis of POM clusters from monomeric oxoanions and simple cations (left) through to intermediate, secondary building units (centre) and finally, to the polyoxometalate-cation complex itself (right).

The transition metals dominating the field are Mo, W and V but also Pd, Nb and Ta in their high oxidation states. The metal-oxygen polyhedra $\{MO_x\}$ are the precursors for building blocks that form clusters and referred to as *addenda*. Atoms which can serve as addenda usually (I) alternate coordination number from four to seven, (II) are among the smaller metal

ions capable of octahedral packing with a high positive charge and (III) are able to form terminal double bonds with unshared oxygen atoms by pπ-dπ interactions.[11]

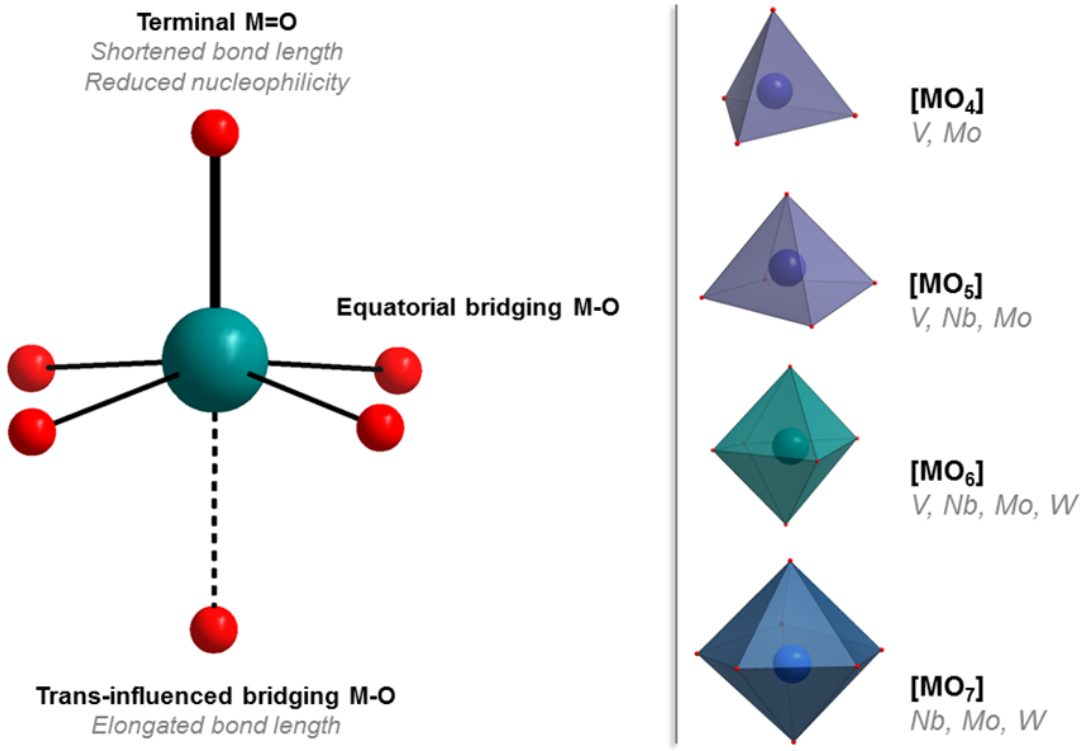

Figure 6

Left: The main structural features of the primary [MO_6] polyhedral unit common to most POM structures and right: a comparison of the possible [MOx] polyhedra found in POM structures.

The oxygen atoms are connected to the central metal atom via a single bond {M-O} as bridging ligands or via double a bond {M=O} as terminal ligands. The shortened bond length of the terminal ligand has an influence on the opposite ligand which shares the same orbital of the central metal atom. The *trans-influence* weakens the stability of the metal-ligand bond if the opposite ligand is much better at donating or accepting electrons. The influence can be structural and distorts the geometry of the polyhedra by increasing the bond length (Figure 7), kinetic by making the ligand more labile or both.[12]

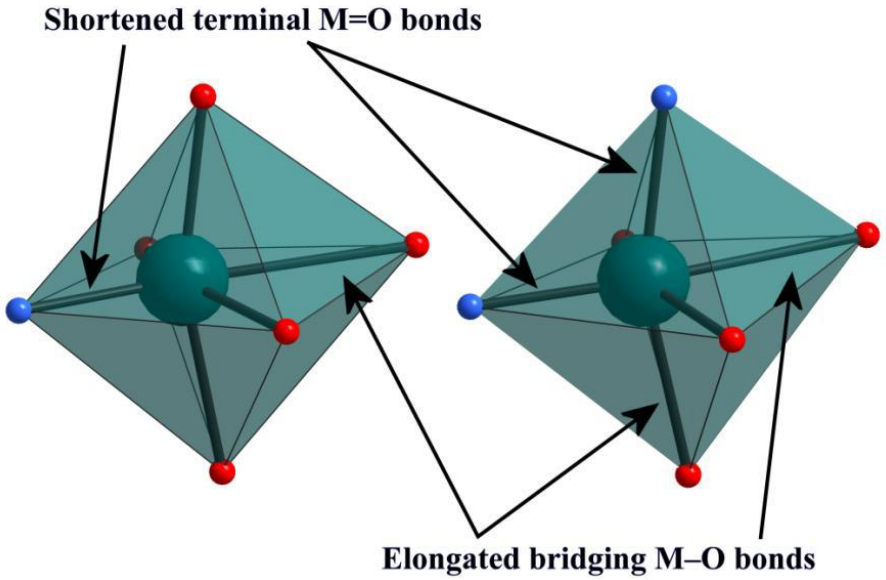

Figure 7

Representation of the *trans*-influence in POM {MO_6} octahedra. (Colour scheme: M = teal, O (terminal) = blue, O (bridging) = red).

Due to the polarisation of the terminal oxygen ligands towards the central metal ions, which means their exposed, external surface is more positive, the basicity of the cluster's external oxidic surface is significantly reduced. So is the probability of protonation and herby the possibility for further condensation with other addenda as well. This explains why POMs do not polymerise into infinite metal-oxides. Consequently, the interior bridging oxygen ligands are more flexible in their addenda, which allow the same POM architecture to accommodate various heteroatoms of different sizes with different bond lengths without any distortion to the cluster's architecture e.g. $[PW_{12}O_{40}]^{3-}$, $[SiW_{12}O_{40}]^{4-}$ and $[CoW_{12}O_{40}]^{5-/6-}$.[13]

However, acid-mediated condensation of individual polyhedra {MO_x} can be achieved resulting in three different ways of sharing oxygen ligands: Corner-, edge- and in some rare cases face-sharing are responsible for different orientations of the polyhedra to one another (Figure 8). POMs can combine a mixture of these geometries as long as each polyhedron does not have more than two unshared terminal oxygens, a concept known as the *Lipscomb Principle*,[14] although there are some molybdate-based structures that break this rule.[15],[16],[17]

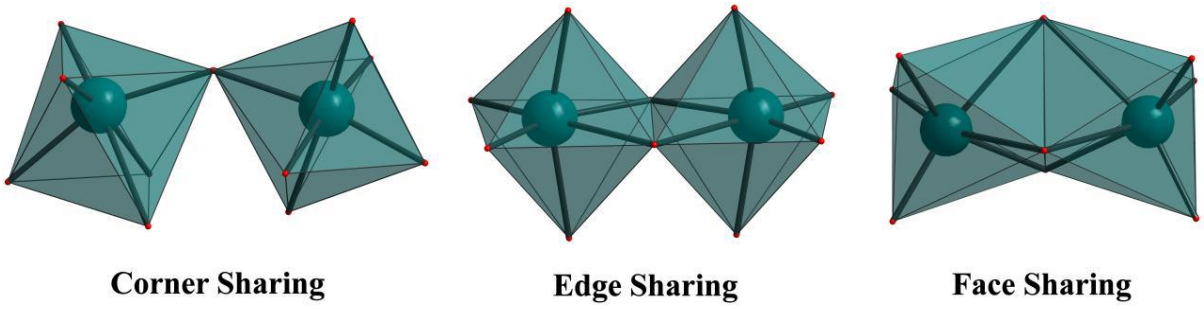

Figure 8

Possible binding modes of [MO_x] polyhedral units sharing either the corner (left), the edge (middle) or the face oxo ligands (right). (Colour scheme: M = teal, O = red).

Based on the number of external M=O bonds three categories of POM clusters were established: *Type I* POMs contain only polyhedra with one terminal M=O bond, whereas *type II* exclusively possesses addenda with two terminal M=O bonds and finally *type III* includes a mixture of both polyhedra.[18] Not only does this classification describe the structural differences between POMs but also their electronic properties. *Type I* and *type III* can undergo reversible redox chemistry because the LUMO in *type I* octahedra is non-bonding, whereas in *type II* octahedra it is anti-bonding and therefore clusters of this type will generally decompose if reduced.[19],[20]

Furthermore, two broad families are recognized, namely *isopolymetalates* which are comprised solely of addenda of transition metal oxides and *heteropolymetalates* which incorporate another type of oxyanion, a so-called heteroatom. Although the heteroatoms are often main group oxyanions such as phosphate, sulphate, silicate etc. they can essentially come from all corners of the periodic table. This can lead to confusion because a second, different transition metal found within a POM cluster can be classified as either a heteroatom or just another addendum. An example of this is the Anderson-Evans-type structure (Figure 9) which can have either a transition metal or a non-metal at its centre and so switches between isopolymetalate and heteropolymetalate.[21]

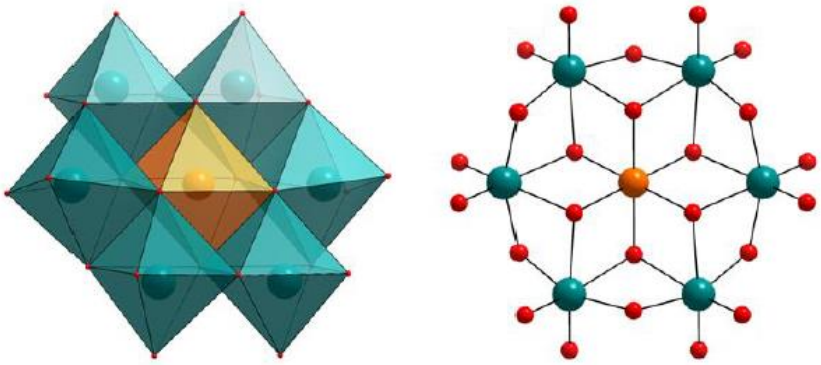

Figure 9

Polyhedral (left) and ball and stick (right) representations of the Anderson-Evans heteropolyoxoanion. (Colour scheme: Heteroatom = orange, M = teal, O = red).

1.2.1 POM Structures

1.2.1.1 The Keggin Structure

The Keggin structure $[XM_{12}O_{40}]^{n-}$ is primarily representative for hetero-12-molybdates and hetero-12-tungstates consisting of four $\{M_3O_{13}\}$ triads (Figure 10) tetrahedrally organised around a central heteroatom $\{XO_4\}$ where X = P, Ge, Si[22] or As and many more.[23] Its tetrahedral heterogroup is encapsulated within the $\{M_{12}O_{36}\}$ shell. The $\{MO_6\}$ octahedra within each triad are edge-sharing whereas the triads themselves are connected by corner-sharing to each other.

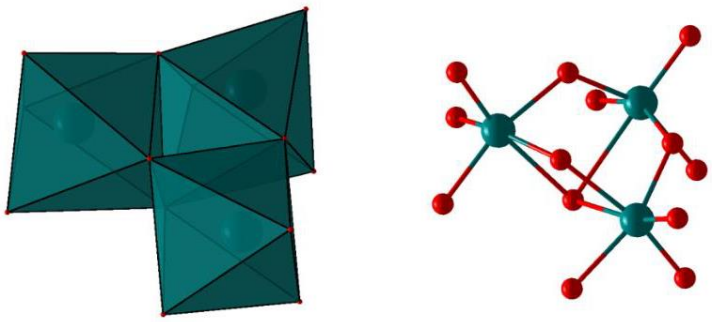

Figure 10

Polyhedral (left) and ball and stick (right) representations of the $\{M_3O_{13}\}$ triad which forms the basis of each Keggin cluster in (Colour scheme: M = teal, O = red).

This results in every single addendum in the cluster having only one terminal M=O bond and therefore the Keggin structure categorised as a type I POM (Figure 11).

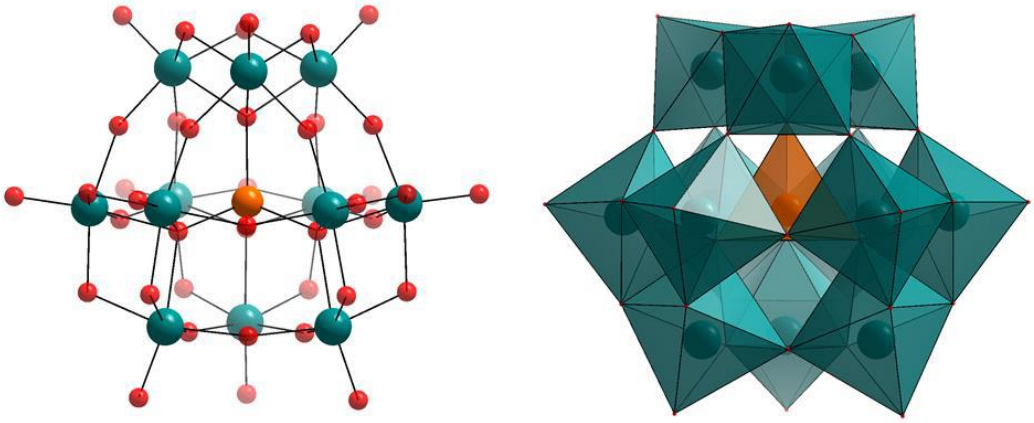

Figure 11

Ball and stick (left) and polyhedral (right) representations of the Keggin heteropolyoxoanion. (Colour scheme: Heteroatom = orange, M = teal, O = red).

One interesting feature of this architecture is its ability to form a series of related isomers by rotating the $\{M_3O_{13}\}$ triads by 60° around the oxygen atom that links three of the octahedra with the heteroatom. Four geometric isomers can be obtained from the α-Keggin in that way which adopt the prefixes β-, γ-, δ- and ε- from the Greek alphabet as can be seen in Figure 12.

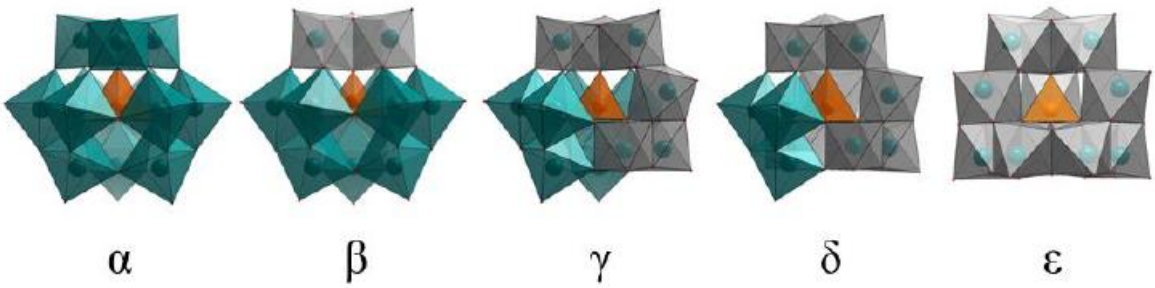

Figure 12

Depiction of the geometrical isomerism possible in the Keggin cluster showing the five, theoretically possible geometric isomers of the Keggin archetype. (Colour scheme: Heteroatom = orange, M = teal, rotated caps = grey).

As mentioned above the most common central addenda atoms are W and Mo[22] although even p-block elements like Al[24] and Ge[25] are documented to form assemblies similar to the Keggin structure which, however, do not precisely count as POMs. Still, these findings opened the way for the concept of Keggin configomers[26] i.e. that in principle the $\{M_{12}O_{36}\}$ shell can

adopt a variety of architectures that differ with the ratio from edge-sharing to corner-sharing polyhedra.

Furthermore, other elements for example vanadium can form different kegginoids such as *extended Keggin structures* like the $[XV_{18}O_{42}]^{n-}$ where X = SO_4 and VO_4.[27] This species can be derived from the hypothetical, highly negative and thus highly reactive $[V_{12}O_{36}]^{12-}$ shell made of $\{VO_5\}$ polyhedra by addition of six [16] cations at the unoccupied square faces (Figure 13) forming a rhombicuboctahedron.

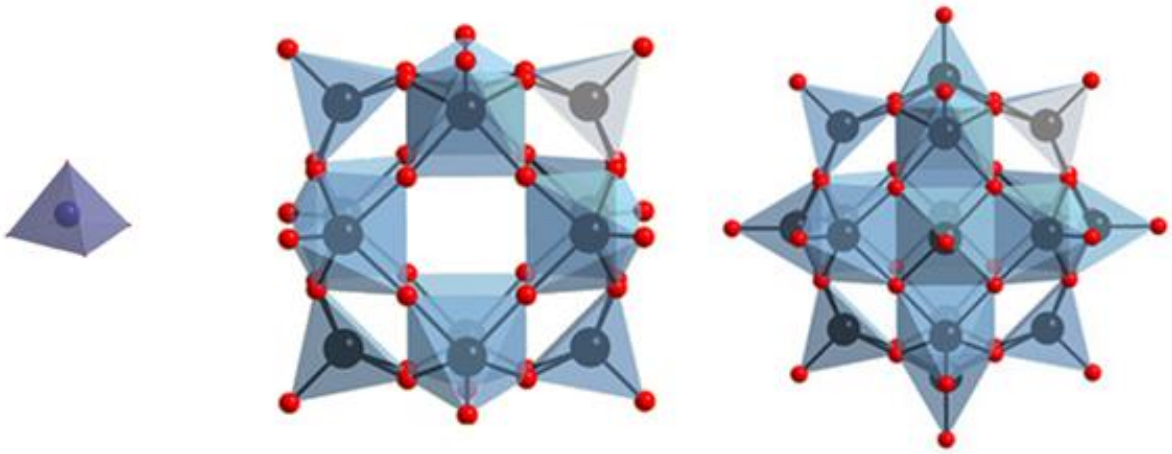

Figure 13

Polyhedral representation of the $[MO_5]$ precursor (left), the $\{V_{12}O_{36}\}$ shell (middle) and the $\{V_{18}O_{42}\}$ shell (right) kegginoid structure. (Colour scheme: V = blue, O = red, $[MO_5]$ precursor = purple).

This results in a tetrahedral central ion being spherically surrounded by 18 vanadium atoms and 24 oxygen atoms. All vanadium atoms in the shell are interconnected by the 24 corner-sharing oxygen atoms and in addition from 18 terminal oxygen bonds which point away from the cluster's centre. The twelve vanadium polyhedra belonging to the "Keggin basic unit" are distorted octahedra by forming weak bonds with the tetrahedral central ion's four oxygen atoms.[27]

1.2.1.2 Lacunary POMs

A POM cluster with a complete shell, which means that all its addenda atoms are present, is called a *plenary* structure. However, it is possible to remove one or more addenda and thus generate a *lacunary* POM. These structures are generally less stable than their plenary

counterparts because the absence of an addendum creates an oxygen rich area where the exposed oxygen ligands are more reactive and energetically unfavourable. This means that lacunary structures can be used to form mixed metal POMs by filling the lacuna with other addenda, heteroatoms or create more complex architectures by condensation of lacunary units and linking clusters through transition metals.

Lacunary derivatives are usually obtained by taking a plenary POM and raising the pH to destabilise the cluster enough to cause partial decomposition, however some lacunary structures can be synthesised in one-pot reactions under unfavourable conditions for the plenary cluster formation.[28]

1.2.1.3 Lacunary Keggin Structures

The ability to produce various stable lacunary structures from different isomers makes the Keggin cluster especially interesting and versatile in POM chemistry, although only derivatives with tungsten addenda and a few heteroatoms such as Si[28] or Ge[29] are reported.

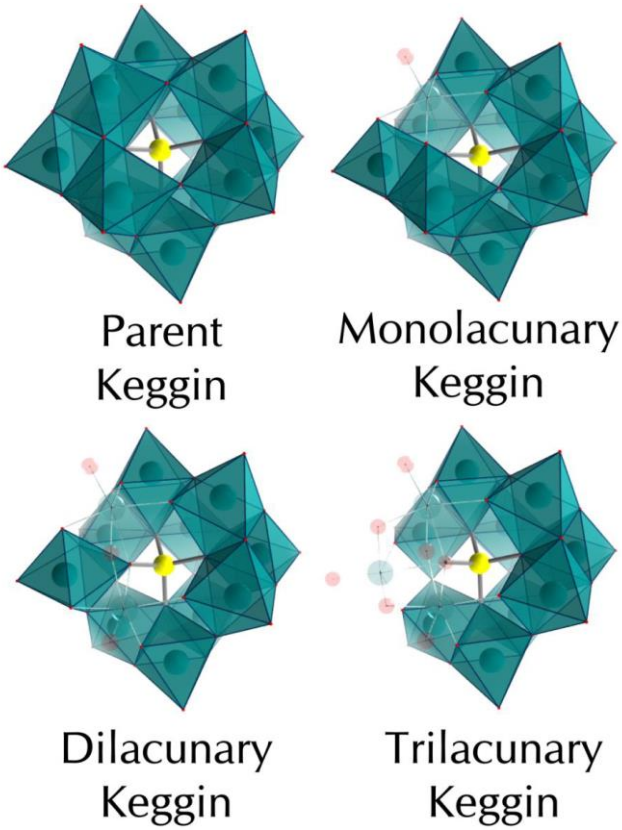

Figure 14

Polyhedral representation of the lacunary structures based on the Keggin structure, showing sequential removal of addenda atoms starting from the parent cluster resulting in $\{W_{11}\}$, $\{W_{10}\}$ and $\{W_9\}$ species (Colour scheme: Heteroatom = yellow, M = teal, O = red, removed addenda = transparent).

Seven different stable and isolable species can be synthesised with Si alone[28] (Figure 15), most of them directly by reacting sodium tungstate with sodium metasilicate.

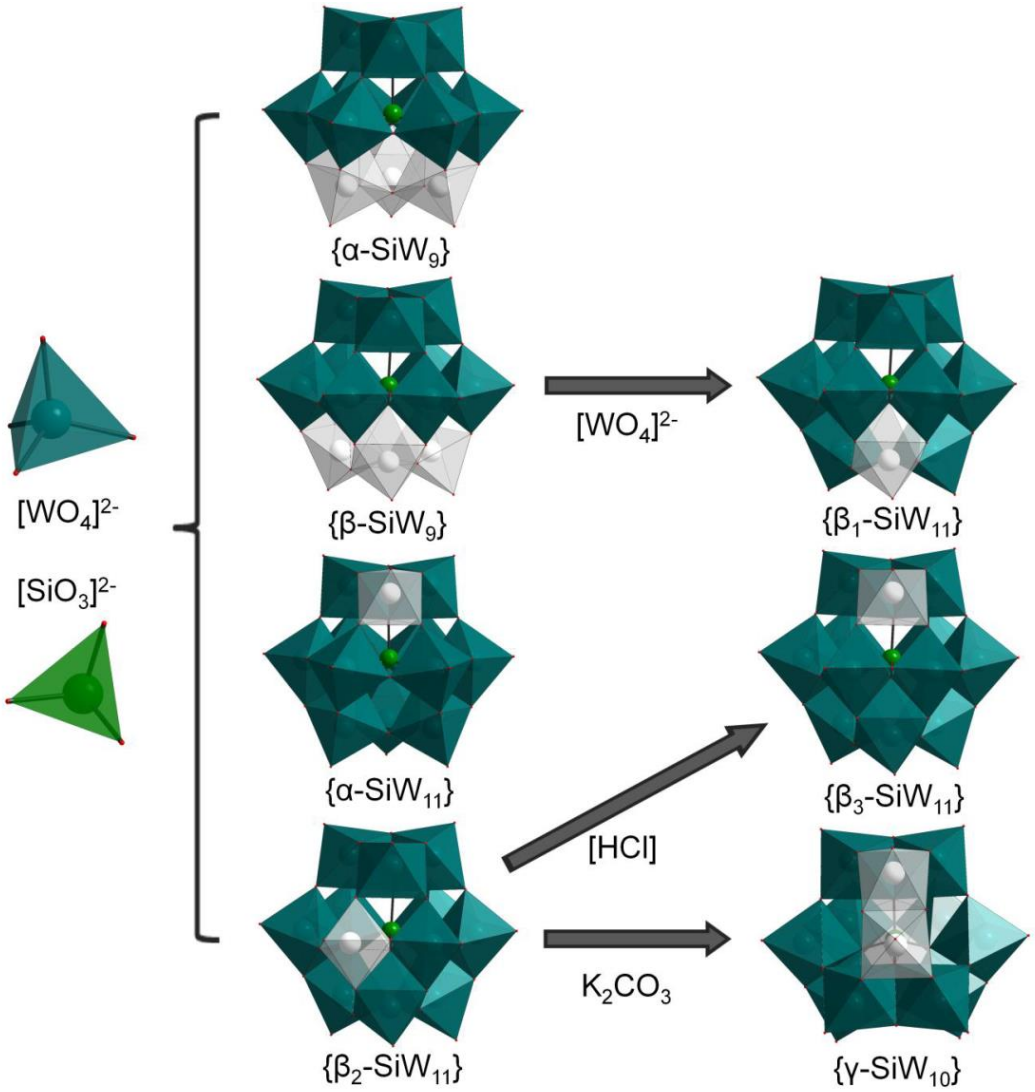

Figure 15

Polyhedral representation of the various Keggin lacuna that can be synthesised as isolated species. (Colour scheme: Si = dark green, W = teal, O = red, vacant position = white).

To distinguish which addendum is missing in the structure of a certain isomer further identifiers are required. In the case of the β-isomer of the Keggin cluster the triad that is rotated by 60° is the point of reference. If one position of the rotated triad itself is vacant the

structure receives the prefix β_3, if one of the addenda that connect to the rotated triad is removed it is β_2 and if an octahedron is missing that does not share an oxygen bond with the rotated triad it is named β_1.

Furthermore, trilacunary species receive an additional identifier depending on whether the three lacunary positions are exclusively from one triad or from three different ones. There is no documentation about two positions missing from one triad and the third one from another. Therefore, two types can be distinguished: *A-type lacunary POMs* have vacant positions on different triads and *B-type POMs* have a complete triad removed.[30]

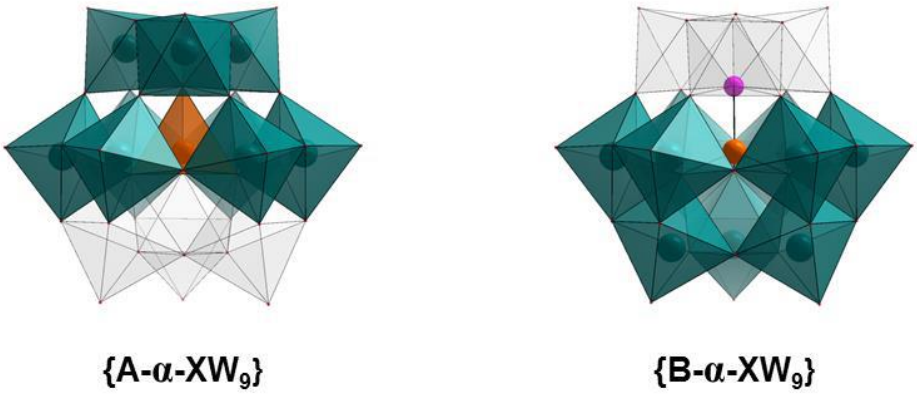

Figure 16

Polyhedral representation of the A- and B-type isomerism possible across $\{XW_9\}$ lacunary species. (Colour scheme: Heteroatom (X) = orange, W = teal, removed addenda = transparent, pink = newly exposed X=O group or a lone pair, depending on the heteroatom present).

To this day only one dilacunary species has been isolated which is the $\{\gamma\text{-}XW_{10}\}$ where X = Si,[31] P,[32] Ge.[29] The $\{\gamma\text{-}SiW_{10}\}$ and $\{\gamma\text{-}GeW_{10}\}$ lacunaries are synthesised from their $\{\beta_2\text{-}XW_{11}\}$ precursors and the two vacant positions are former edge-sharing addenda from two different triads (Figure 16).

1.2.1.4 Molybdenum Blues and Browns

The following sections provide an overview of molybdenum-based POMs, which can appear both as isopolymolybdates and hetropolymolybdates, giving an emphasis upon the molybdenum blue wheel-type structure $\{Mo_{154}\}$ and the molybdenum brown spherical structure $\{Mo_{132}\}$. Interestingly, the oldest of all POMs, first reported by Scheele in 1793, fell

into exactly this category although its structure could not be determined until the development of modern X-ray crystallographic analysis.[33] Compared to other polyanions being much more unstable in solution, the increased stability of these polymolybdate clusters allows them to be used as anionic cores or building blocks in the construction of larger supramolecular materials.[34] One example being the largest POM cluster ever recorded with the $\{Mo_{368}\}$ also known as *blue lemon* that is approximately 6 nm in diameter.[10]

However, mostly simple one-pot conditions have been applied which resulted in the formation of high-nuclearity molybdenum-based POMs by acidification of aqueous solutions of metal salts.[41robert] Partial reduction of the acidified aqueous solutions using reducing agents such as Al, Cu, Fe but also $NaBH_4$, Na_2S, cysteine, ascorbic acid, and hydrazine derivatives leads to the formation of the blue wheel-type $\{Mo_{154}\}$ and the brown spherical-type $\{Mo_{132}\}$ under increased reducing conditions.[19] This partial reduction, where a portion of the molybdenum atoms change from a + 6 to a + 5 oxidation state forms solutions of distinct colours which leads to the resulting structural families referred to as the molybdenum-blues and molybdenum-browns. Furthermore, partial reduction is responsible for the formation of a variety of molybdate building blocks, which can link together forming distinct architectures. They can be broken down into small building blocks that repeat within the crystal structures and be placed into a hierarchical order based on their nuclearity. The simplest among them is the $\{Mo_1\}$ unit that can have either an octahedral geometry as $\{MoO_6\}$ or exist as a decahedral $\{MoO_7\}$. The former one also acts as a template for the formation of the pentagonal $\{Mo(Mo)_5\}$ unit being an $\{MoO_7\}$ at its core surrounded by five $\{MoO_6\}$ octahedra which edge-share along the equator of the ten-sided bipyramid.

Regardless of the ultimate composition of the species, the general formula can always be summarised as $\{(\textit{pentagon})_{12}(\textit{linker})_{30}\}$. These clusters are especially significant considering the pores embedded in their surfaces providing them with interesting host-guest properties.[35],[36],[37]

1.2.1.5 The $\{Mo_{154}\}$ Blue Wheel

The first article related to molybdenum blues in aqueous solution was published by Scheele as early as 1778.[33] They are without a doubt widely accepted as remarkable examples of polyoxoanion self-assembly, especially considering the simplicity of their synthetic

procedures. Furthermore, they are defined by containing mixed valence Mo^{V}/Mo^{VI} addenda having delocalised electrons capable of intervalence charge transfer from Mo^{VI} to Mo^{V} enabled by the π-orbitals of the bridging oxo ligands and it is this electronic interaction that gives the clusters their signature intense blue colour.

The self-assembly of molybdenum blues occurs in aqueous Mo^{VI} solutions by interaction of reducing agents and acids as shown by Müller et al. in 1996. They were able to obtain crystalline material of $[Mo_{154}(NO)_{14}O_{448}H_{14}(H_2O)_{70}]^{28-}$ also referred to as $\{Mo_{154}\}$ from one pot reactions of ammonium heptamolybdate tetrahydrate with appropriate reducing agents such as hydrazine sulphate under acidic conditions.[38] This initial discovery quickly led to a rapid expansion in the chemistry of these *big wheel* type clusters based on similar synthetic and structural principles, including even larger $\{Mo_{176}\}$ and $\{Mo_{248}\}$ wheels, in which $\{Mo_{248}\}$ is a so to speak capped version of the $\{Mo_{176}\}$ species.[39],[40]

The $\{Mo_{154}\}$ wheel-type structure consists of $\{Mo_8\}$, $\{Mo_2\}$ and $\{Mo_1\}$ subunits assembled in fourteen $\{Mo_{11}\}$ units with seven on each face comprised of a central $\{(Mo)Mo_5\}$ linked to two additional $\{Mo_1\}$ addenda in a corner-sharing way forming the larger $\{Mo_8\}$ unit, another bridging $\{Mo_1\}$ unit and a linker-type $\{Mo_2\}$ unit which is connected in corner-sharing mode itself. The central $\{(Mo)Mo_5\}$ unit is based on a pentagonal bipyramidal $[MoO_7]$ building block where the equatorial oxo ligands share their five edges with five $[MoO_6]$ octahedra. The {(Mo}Mo5} pentagonal unit is common to all large molybdenum-based POMs and is responsible for the curvature present in these structures. By linking the building blocks together via corner or edge-sharing of the oxygen atoms regular repeating patterns are formed. Ultimately, the formula of the $\{Mo_{154}\}$ anion can be rewritten as $[\{Mo_8\}\{Mo_2\}\{Mo_1\}]_n$ with n = 14 and be considered as a tetradecamer of the three different subunits it consists of. Due to its high nuclearity, it has an outer diameter of 34 Å, an inner diameter of 20 Å and an approximate thickness of 14 Å making it suitable for host-guest chemistry with inorganic compounds.[41]

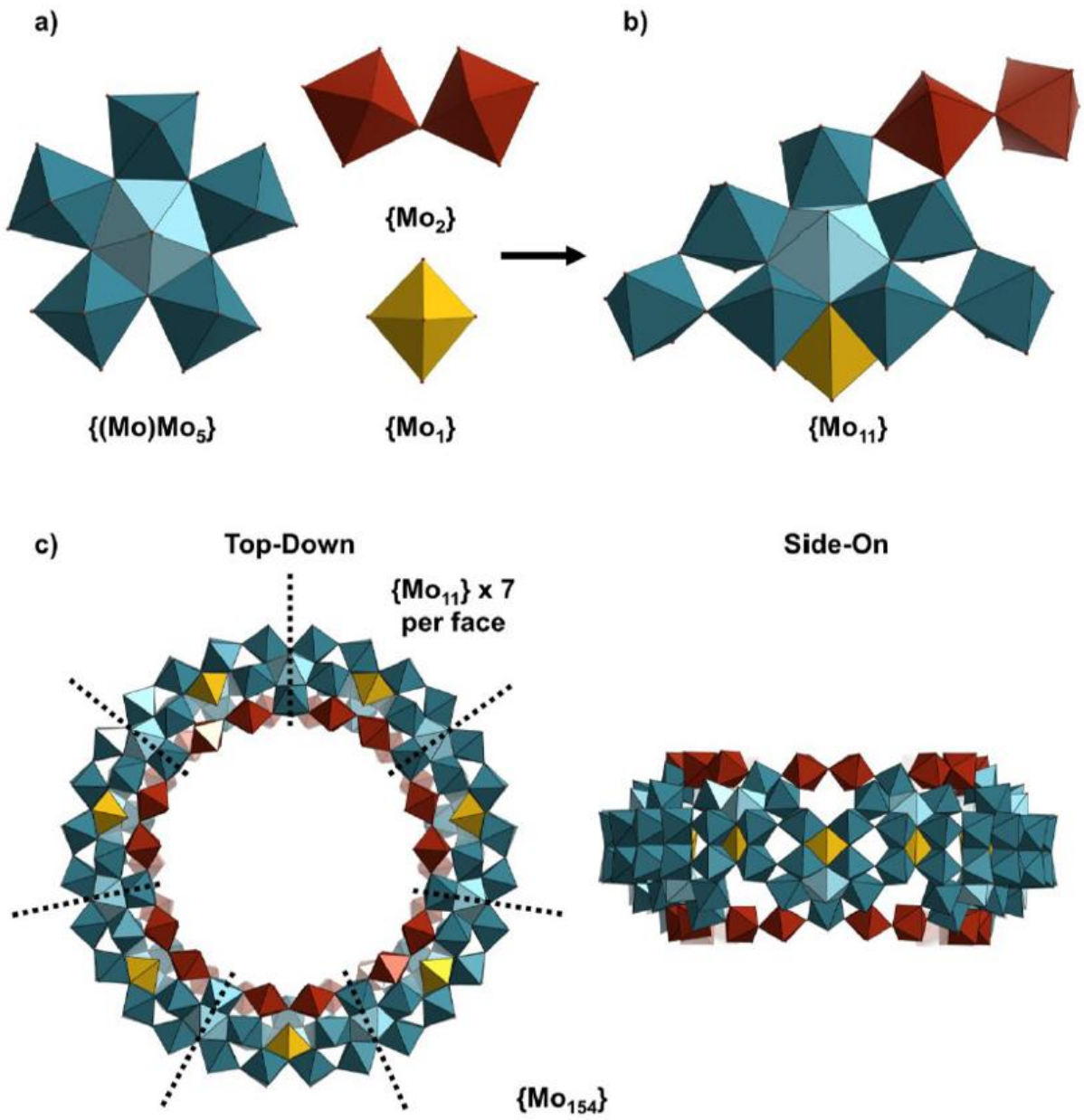

Figure 17

Polyhedral representation of the {Mo*154*} wheel structure shown from a top-down and equatorial perspective and its building blocks highlighting the seven {Mo_{11}} units, where {Mo_1} = yellow, {Mo2} linker-type = red and {(Mo)Mo_5} pentagonal-type = light teal/teal.

1.2.1.6 The {Mo132} Brown Keplerate

In principle, molybdenum browns are further reduced relative to molybdenum blues and, rather than being delocalised throughout the entire molecule, the additional electrons that are found in this species are localised between reduced Mo^V centres in Mo-Mo bonds which contribute to the brown colour of these clusters. That means, when the pH is slightly

increased, the self-assembly tends towards the formation of a remarkable spherical anions colloquially referred to as *Keplerate* clusters due to Johannes Kepler's early model of the cosmos.[42] The $\{Mo_{132}\}$ spherical structure can also be described as twelve $\{Mo_{11}\}$ units which, however, are different to the ones found in $\{Mo_{154}\}$. The central $\{(Mo)Mo_5\}$ building blocks are linked together by five $\{Mo_2\}$ linker-type units connected via edge-sharing among themselves leading to a smaller, fully spherical, icosahedral topology[43],[44],[45],[46]. This structure has an internal cavity size with a diameter of 17 Å and an outer diameter of 25 Å. The building block approach to the formation of the Keplerate structures leaves twenty hexagonal open spaces, referred to as pores, on the sphere's surface. This internal cavity of this Keplerate can be used for the study of guest-host chemistry.

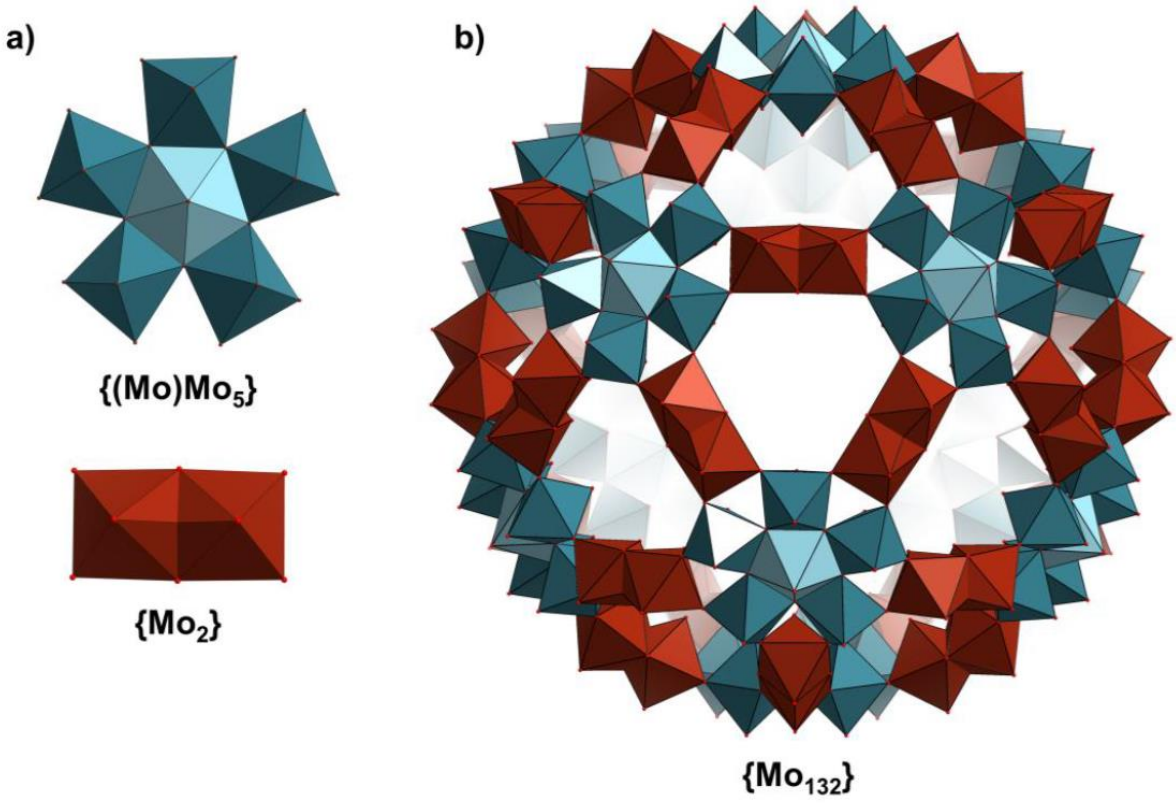

Figure 18

Polyhedral representation of the $\{Mo_{132}\}$ Keplerate structure and its building blocks, where the pentagonal-type $\{(Mo)Mo_5\}$ = light teal/teal and the edge-sharing $\{Mo_2\}$ linker-type = red.

1.2.2 Polyoxometalate-based open Frameworks and POMzites

One of the most notable classification systems to fully categorise POM framework types is the five-category model depicted in Figure 19.[47] POMs can be connected in different ways: Through a transition metal centre via grafted organic units (a-type), directly through transition metal centres (b-type), through an organic linker via transition metal sites within the cluster itself (c-type), through an organic linker via transitions metal centres outside the cluster (d-type) and finally directly by a transitional metal linker within the POM (e-type).

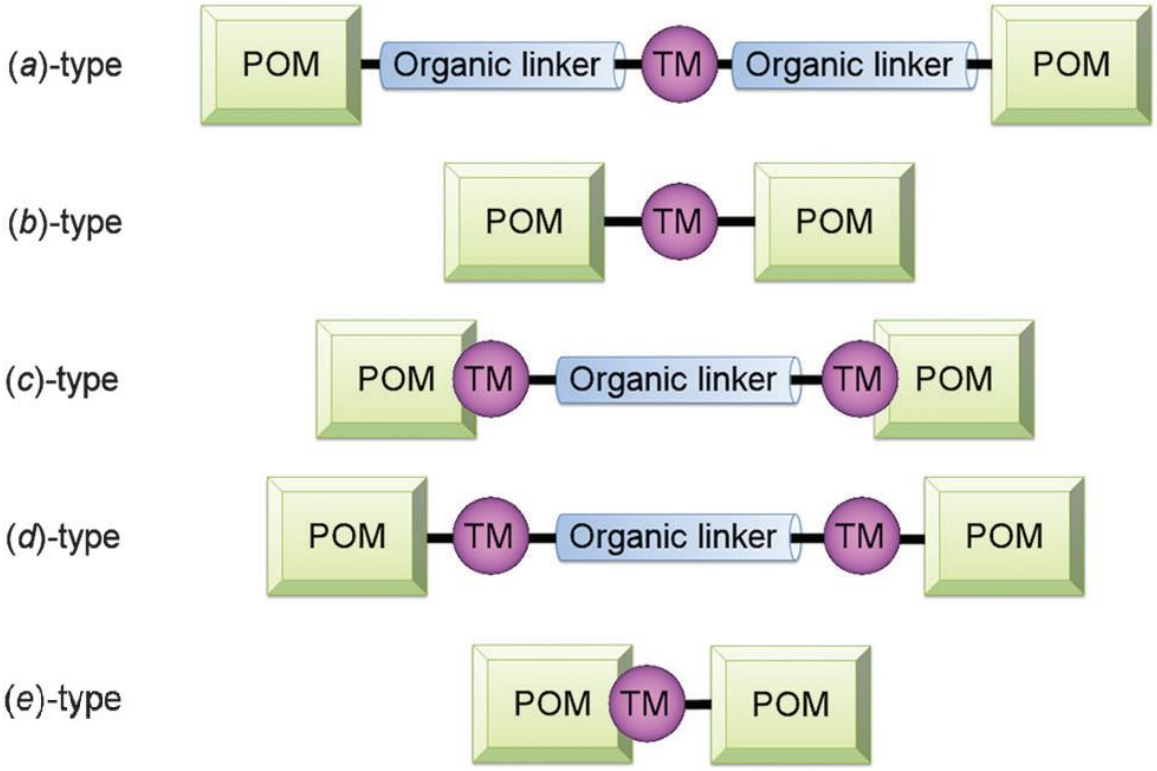

Figure 19

A five-category classification system of POM frameworks: (a) POMs connected to TMs via organic units, (b) POMs connected directly to TMs without any organic components, (c) TMSPs connected through organic linkers via a heterometal, (d) POMs connected through organic linkers via non-embedded TMs and (e) POMs connected via TM linkers within the POM.

The (b)-type consists of POMs connected solely through transition metals without any organic components or involved only as coordinating units not part of the main framework scaffold itself e.g. the {V_{18}}-Network [$M_3V_{18}O_{42}(H_2O)_{12}(XO_4)\cdot 24H_2O$ where M = Fe^{II} or Co^{II} and X = V and S.

Transition metal substituted POMs (TMSPs) are polyoxometalate clusters which incorporate other transition metals within their architectures often occupying the vacant areas of lacunary structures with the potential to link them together. These compounds have the potential to form (c)- and (e)-type networks. For instance, the Kegging network with the overall formula $[(C_4H_{10}NO)_{40}(W_{72}Mn_{12}O_{268}X_7)^n]$ where X = Si or Ge which is based on the substituted Keggin-type POM building blocks.

Also, infinite three-dimensional frameworks can be constructed from molecular precursors of many shapes and sizes including cyclic precursors interconnected by electrophilic linkers. Therefore, some inorganic POM-based frameworks offer the potential to form porous materials which combine the thermal stability of zeolites with the complexity and versatility of metalorganic frameworks.

1.2.2.1 Keggin Network

The so-called “Keggin-Net” belongs to a class of porous materials with an open three-dimensional structure. The formula can be written as $(C_4H_{10}NO)_n[W_{72}M_{12}O_{268}X_7]*zH_2O$ where X represents the heteroatom Si or Ge and M the transition metal Mn or Co.[48]

It is the first example of mesoporous POM based frameworks, where the scaffold consists exclusively of transition metal substituted polyoxometalates (TMSP) which means it is based solely on α-Keggin clusters $[\alpha\text{-}XM_zW_{12-z}O_{40}]^{n-}$ with two different substitution modes ergo two different building blocks. Astonishingly, they are connected to each other directly in absence of any external electrophilic linkers.

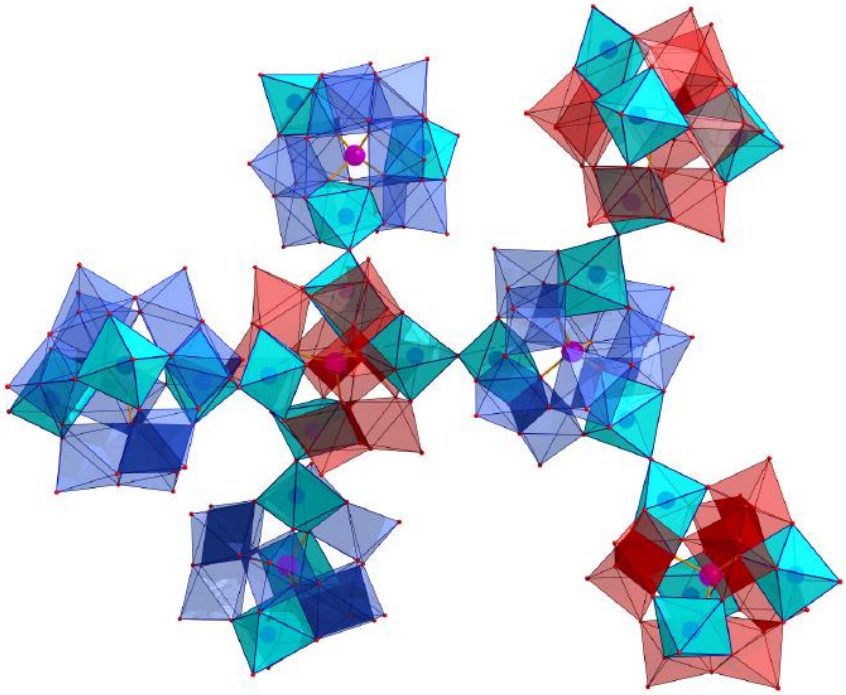

Figure 20

Polyhedral, structural representation of the connectivity of Keggin clusters in the framework material. All octahedra represent [WO_6], of whom the blue ones belong to the three-connected and the red ones to the four-connected cluster. The light-blue corner-sharing octahedra show the connection between two clusters. Half of them are occupied with tungsten and the other half contain the heterometal M, resulting in the [M-O-W] linkage.

The structure provides two different kinds of these substituted building blocks. Depending on the amount of replaced transition metal centres the clusters function as trigonal or tetrahedral (Figure 20) anionic nodes linked alternately to each other by corner-sharing W-O-M bonds. Here, a trigonal node links to three tetrahedral nodes which then each connect to four trigonal building blocks and so on forming this three-dimensional infinite network structure. The positions of the heterometal [MO_6] and the tungsten [WO_6] are not exactly localised because each of them occupy only fifty percent of the connections in the asymmetric unit of the final crystal structure.

The morpholinium cations serve as counterions to stabilise the anionic framework and are added at the beginning of the synthesis so potentially have a templating effect. They are embedded in the large cavities in the crystal structure formed by rings of ten Keggin clusters accompanied by two more SBUs on each side and may be important for crystallisation as without them the framework might stay soluble.

So far, four compounds have been successfully synthesised, while a fifth one was obtained by chemical reduction of the Mn^{III} centres of compound 1 undergoing a reversible single-crystal to single-crystal (SC-SC) redox transformation:

1. $(C_4H_{10}NO)_{40}[W_{72}Mn^{III}_{12}Si_7O_{268}]\cdot 48H_2O$
2. $(C_4H_{10}NO)_{40}H_{12}[W_{72}Mn^{III}_{12}Si_7O_{268}]\cdot 48H_2O$ (reduced)
3. $(C_4H_{10}NO)_{40}[W_{72}Mn^{III}_{12}Ge_7O_{268}]\cdot 48H_2O$
4. $(C_4H_{10}NO)_{46}H_6[W_{72}Co^{II}_{12}Si_7O_{268}]\cdot 68H_2O$
5. $(C_4H_{10}NO)_{46}H_6[W_{72}Co^{II}_{12}Ge_7O_{268}]\cdot 150H_2O)$

1.2.2.2 {V_{18}}-Kegginoid Inorganic Network

This example of a three-dimensional (b)-type framework displays a regular cubic arrangement of kegginoid $\{XV_{18}O_{42}\}$ clusters where X = SO_4 or VO_4 are linked together through either $Fe(H_2O)_4$ or $Co(H_2O)_4$.[49] The high porosity of this scaffold allows the interpenetrations of two slightly shifted frameworks as can be seen in Figure 21. Each POM cluster binds to six transition metal centres $\{M(H_2O)_4\}$ which results in the general formula $[M_3V_{18}O_{42}(H_2O)_{12}(XO_4)]\cdot 24H_2O$ where M = Fe^{II} or Co^{II} and X = V and S. Besides this, the cages host a disordered distribution of both the VO_4 and SO_4 anions for the $\{XO_4\}$ group.

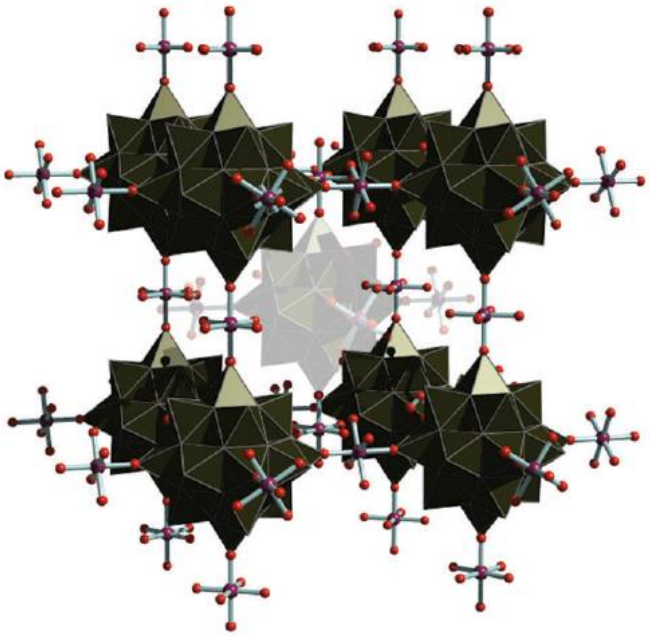

Figure 21

Polyhedral and ball and stick representation of the cubic arrangement of the $\{V_{18}\}$ network linked through Co^{II} or Fe^{II} centres. (Colour scheme: $\{VO_5\}$ polyhedra = black, O = red, Fe or Co = purple).

2 Aims and Abstract

On the following pages, this work presents a new approach to *polyoxometalate* (POM) chemistry by using *design of experiments* (DOE) as a tool to examine the reaction processes of high nuclearity structures. Although DOE has been existing for many decades, there was no major attempt of gathering new information on POM structures or syntheses by using this technique.

Design of experiments is the premier method for investigating and optimising physical processes by altering multiple variables at a time to assess their effect on the outcome. In chemistry, DOE allows access to a wider chemical space than the dominant *one factor at a time* (OFAT) optimisation method providing greater opportunity to find the global, rather than local, yield maximum. Polyoxometalate (POM) chemistry is one such chemical space in which subtle input effects are known to have an outsize impact on the self-assembly of the resulting metal oxide clusters. The formation mechanisms of many complex POM structures are still unclear and due to an insufficient understanding and the many synthetic variables creating a vast chemical space and a wide spectrum of potential products their procedures can lack reliability and reproducibility.

In the light of these issues, DOE analysis was applied to the syntheses of four suitable candidate reactions of large polyoxometalate structures: The Keggin-Net, the V_{18}-Network, the Molybdenum Blue Wheel and the Molybdenum Brown Keplerate. By varying factors such as reducing agent, pH, reaction time and reagent stoichiometry the key factors in the successful synthesis of each family are discovered. Assuming that only few parameters of a reaction are important, these so-called drivers of the system are determined and provide insights into the mechanism of POM self-assembly and the DOE methodology will allow for the reproducible synthesis of complex POMs in the future.

3 Methodology

In the beginning the following four syntheses of POM infinite frameworks were chosen because they were considered as unreliable or irreproducible:

1. The Keggin-Network $(C_4H_{10}NO)_{40}[W_{72}Mn_{12}O_{268}Si_7]\cdot 48H_2O$
2. The $\{V_{18}\}$-Network $[Fe_3V_{18}O_{42}(H_2O)_{12}(XO_4)]\cdot 24H_2O$ where X = V and S
3. The $\{Mo_{154}\}$ Blue Wheel $Na_{15}[Mo_{154}O_{462}H_{14}(H_2O)_{70}]$

4. The {Mo_{132}} Brown Keplerate $(NH_4)_{42}[Mo_{132}O_{372}(CH_3COO)_{30}(H_2O)_{72}]$

Original procedures, which can be found in Section 7.3, were carried out at least once for a better understanding of the experiments' processes and outcomes.

The Keggin-Network and the {Mo_{132}} Keplerate crystals were synthesised successfully whereas the {Mo_{154}} Blue Wheel structure and the {V_{18}}-Network could not be obtained in crystalline form. All compounds were analysed by Inductively Coupled Plasma Optical Emission Spectroscopy (ICP-OES) and two of them, the Keggin-Network and the {Mo_{132}}-Keplerate by Single Crystal X-Ray Diffractometry as well.

3.1 The DOE Approach

For all syntheses, a 12-run, two-level Plackett-Burman design was chosen as a screening design to determine the significant main factors in as few experiments as possible. Several repetitions of each set were carried out, especially when the responses varied considerably, to make sure the results were trustworthy and comparable by their averages. To neutralise any uncontrolled inputs, the running order within the 12 runs was randomly determined for all setups by rolling a dodecahedral die and they were run in two different blocks at different days. Each step of the procedure was assigned to a factor column (controlled inputs A-F) in the design table and the high levels (1) and low levels (-1) were defined. The five remaining columns were assigned to dummy factors (G-K). The original values of each experimental step were taken as a starting point and the factorial levels tried to set as far apart as possible within the syntheses which turned out to be either adding 10 % or deducting 10 % of the original values for most of the factors. The design matrix in the following Table 10Table 10 was elaborated and used as a template for all experiments. A setup was generated that had almost all reagents dissolved in water prior to the synthesis. Six 100 mL round-bottom flasks were chosen sitting on two single magnetic hotplate stirrers containing three heating mantles each to distribute the heat equally. The volumes were kept the same in all experiments by adding small amounts of water.

Afterwards, the minimum significant factor effects were calculated from the experimental error using the effects of the dummy factors and the corresponding t-value and a significance level of 20 % i.e. $\alpha = 0.2$. Before being able to compare the effects with each other they had

to be disentangled because the more the number of experiments is reduced using DOE the more main factors and two-factor interactions are confounded with each other. Higher order interactions could be neglected due to the sparsity-of-effects principle. If the disentangled factor effect was positive, the product yield increased at the factors maximum setting and if it was negative, the product yield increased at the factors minimum setting. The six main factors were then rated by their individual influence on the system expressed by the absolute value of their effect on the yield of the desired POM.

Factors/ Runs	A	B	C	D	E	F	G	H	I	J	K	Response
1	1	1	-1	1	1	1	-1	-1	-1	1	-1	Y_1
2	1	-1	1	1	1	-1	-1	-1	1	-1	1	Y_2
3	-1	1	1	1	-1	-1	-1	1	-1	1	1	Y_3
4	1	1	1	-1	-1	-1	1	-1	1	1	-1	Y_4
5	1	1	-1	-1	-1	1	-1	1	1	-1	1	Y_5
6	1	-1	-1	-1	1	-1	1	1	-1	1	1	Y_6
7	-1	-1	-1	1	-1	1	1	-1	1	1	1	Y_7
8	-1	-1	1	-1	1	1	-1	1	1	1	-1	Y_8
9	-1	1	-1	1	1	-1	1	1	1	-1	-1	Y_9
10	1	-1	1	1	-1	1	1	1	-1	-1	-1	Y_{10}
11	-1	1	1	-1	1	1	1	-1	-1	-1	1	Y_{11}
12	-1	-1	-1	-1	-1	-1	-1	-1	-1	-1	-1	Y_{12}

Table 10

Template for an eleven factor, two-level Plackett-Burman screening design with twelve runs. (A-K = factors, Y_1-Y_{12} = responses, -1 = low setting, 1 = high setting.)

3.1.1 The Keggin-Net 1/3

3.1.1.1 The Keggin-Net 1/3 DOE Preparation

A setup was generated that had almost all reagents added in a dissolved aqueous form. Although the {γ-SiW_{10}} precursor is stable in solutions at pH > 1 and does not convert into {β-SiW_{12}} under the conditions in this setup, it would only dissolve in relatively large amounts of water which would have diluted the reaction mixture too far in this case. That is why the {γ-SiW_{10}} precursor was added in solid form.

Three worksheets (Table 12) were generated, one for each repetition, all in different random running orders and carried out alphabetically from a to l. Each reaction was performed on a scale of approximately 1:4 in comparison with the original synthesis in Section 7.3.4, slight adjustments for the minima and maxima were made which resulted in Table 11 as can be seen below. Furthermore, the volumes were kept the same for all samples by partly adding deionised water always being 55.5 mL at the start of the reaction.

First, 43.83 g and 73.05 g sodium chloride (*NaCl*) were each dissolved in 1 L deionised water to result in a 0.75 M and a 1.25 M solution; 750 mg and 1125 mg manganese sulphate tetrahydrate (*$MnSO_4 \cdot 4H_2O$*) were dissolved in 50 mL deionised water each; 125 mg and 162.5 mg potassium permanganate (*$KMnO_4$*) were dissolved in 25 mL deionised water each; 122.2 mL 98 % sulphuric acid (*H_2SO_4*) was diluted with deionised water and topped up to a volume of 500 mL 4.5 M H_2SO_4.

Factors		-1	+1
A	NaCl [mmol]	0.04	0.06
B	Morpholine [mmol]	17.2	34.4
C	pH_1 by 4.5 M H_2SO_4	7.70	8.10
D	{γ-SiW_{10}} [mmol]	0.10	0.13
E	Stirring time [min]	10.0	20.0
F	$MnSO_4 \cdot 4H_2O$ [mmol]	0,13	0.20
G	$KMnO_4$ [mmol]	0.03	0.04
H	Addition Time [min]	5.0	10.0
I	pH_2 by 4.5 M H_2SO_4	7.6	7.9
J	Reaction Temperature [°C]	RT	75
K	Filter	no	yes

Table 11

All reactions carried out on 55.5 mL scale. The assigned factors A-K with their minimum (-1) and maximum levels (1). All absolute amounts refer to the volumetric scale on the top left.

3.1.1.2 The Keggin-Net 1/3 Synthesis

In this synthesis, (A) 45 mL sodium chloride solution (*NaCl*) was stirring in 100 mL conical flasks, (B) when morpholine (C_4H_9NO) was added including an extra 1.5 mL deionised water to the samples at the lower setting (-1). The pH was between 10.8 and 11.3 at 21 °C, when (C) 4.5 M sulphuric acid (H_2SO_4) was used dropwise to adjust the pH to 7.7 and 8.1. The temperatures of the solutions varied between 24 °C and 28 °C depending on the amount of added acid, which stretched from 1.5 mL to 3.5 mL, this is due to the exothermic reaction during neutralisation. Then, up to 2 mL deionised water was added to the samples containing less acid to even out the volumes. Next, (D) potassium γ-decatungstosilicate ($K_8[\gamma\text{-}SiW_{10}O_{36}]\cdot 12H_2O$) precursor was added in solid form to one half of the samples, (E) ten minutes later to the other half and all stirred for another ten minutes which was plenty of time to dissolve everything. Afterwards, (F) 2 mL manganese sulphate solution ($MnSO_4\cdot 4H_2O$) were added, which turned the colourless solutions yellow immediately and they were stirred for five more minutes. Then, (G) 1 mL potassium permanganate solution ($KMnO_4$) was added in five times 200 µL and the equivalent amount of deionised water (H) over five and ten minutes. The former yellow solution turned brown, became cloudy in some cases and was stirred for another five minutes. Now, (I) the pH was adjusted to 7.6 and 7.9 using drops of 4.5 M sulphuric acid (H_2SO_4) again, before the samples were covered with watch glasses that were fastened with tape on top of the flasks. (J) The samples were heated to 75 °C or left at approximately 20 °C, however, all were stirred for one hour. Next, (K) one half of the samples was filtered through a glass funnel using filter paper whereas the other half was not. All samples were stored unsealed in a shelf at 18 °C for three weeks. Afterwards, they were prepared for ICP analysis as described in Section 3.1.4 whereas the results and their analysis can be found in Section 5.1.1.

Random Orders			Factors	A	B	C	D	E	F	G	H	I	J	K
MAK03-99	**MAK03-101**	**MAK03-103**	**Original Order**	**NaCl**	**Morpho-line**	**pH**	**{γ-SiW_{10}}**	**Stirring Time**	**$MnSO_4$**	**$KMnO_4$**	**Addition time**	**pH_2**	**Reaction Temp**	**Filter**
f	**i**	**a**	**1**	1	1	-1	1	1	1	-1	-1	-1	1	-1
l	**g**	**g**	**2**	1	-1	1	1	1	-1	-1	-1	1	-1	1
i	**l**	**b**	**3**	-1	1	1	1	-1	-1	-1	1	-1	1	1
c	**e**	**i**	**4**	1	1	1	-1	-1	-1	1	-1	1	1	-1
a	**a**	**c**	**5**	1	1	-1	-1	-1	1	-1	1	1	-1	1
h	**j**	**h**	**6**	1	-1	-1	-1	1	-1	1	1	-1	1	1
d	**h**	**f**	**7**	-1	-1	-1	1	-1	1	1	-1	1	1	1
g	**d**	**d**	**8**	-1	-1	1	- 1	1	1	-1	1	1	1	-1
j	**k**	**j**	**9**	-1	1	-1	1	1	-1	1	1	1	-1	-1
k	**b**	**l**	**10**	1	-1	1	1	-1	1	1	1	-1	-1	-1
b	**f**	**e**	**11**	-1	1	1	-1	1	1	1	-1	-1	-1	1
e	**c**	**k**	**12**	-1	-1	-1	-1	-1	-1	-1	-1	-1	-1	-1

Table 12

Twelve run Plackett-Burman screening design with eleven factors, two levels and twelve runs which are in randomly assigned running order a-l for three repetitions. (A-K = factors, -1 low setting, 1 high setting)

3.1.2 The Keggin-Net 2/3

3.1.2.1 The Keggin-Net 2/3 DOE Preparation

A setup was generated that had all reagents added in a dissolved aqueous form except for the {γ-SiW_{10}} precursor. Due to considerably different responses in the first Keggin network setup 1/3 experiments, the decision was made to run another full set of three repetitions with some changes. Three new worksheets (Table 14) were generated, one for each repetition all in random running order and carried out alphabetically from a to l. This time the reactions were carried out in two blocks when the runs a-f were carried out first and g-h afterwards. Therefore six 100 mL round-bottom flasks were chosen sitting on two single magnetic hotplate stirrers containing three heating mantles each to distribute the heat more equally than using two ten-positions magnetic hotplate stirrers and conical flasks. Also, to save time and because of complicated handling the former factors (E) *stirring time* and (H) *addition time* were removed from the setup completely. Instead, two dummy factors took their former space in the worksheet. Furthermore, the total volume was slightly reduced to 53.5 mL and other differences in this were as follows:

The levels of morpholine (C_4H_9NO) were chosen to be closer to each other i.e. 2 mL and 2.5. The low level of pH_1 was raised back to 7.8 because 7.7 using 4.5 M sulphuric acid (H_2SO_4) would get in conflict with the high level of pH_2 set at 8.2 which was a little bit higher than before. The stirring time after the addition of potassium γ-decatungstosilicate ($K_8[\gamma\text{-}SiW_{10}O_{36}]\cdot 12H_2O$) was eliminated as a factor and all samples were stirred for five minutes instead. The addition time of potassium permanganate ($KMnO_4$) was also eliminated as a factor and 1 mL of the potassium permanganate solutions added all at once whereafter all samples were stirred for five minutes. The minimum heating temperature was raised to 30 °C because it could be controlled better than room temperature and the maximum was raised to 80 °C. All samples were stirred for 1.5 h instead of 1 h while heating and all changes resulted in Table 13 can be seen below.

First, 43.83 g and 73.05 g sodium chloride (*NaCl*) were each dissolved in 1 L deionised water to result in a 0.75 M and a 1.25 M solution; 750 mg and 1125 mg manganese sulphate tetrahydrate ($MnSO_4\cdot 4H_2O$) were dissolved in 50 mL deionised water each; 126 mg and 163 mg potassium permanganate ($KMnO_4$) were dissolved in 25 mL deionised water each; 122.2

mL 98 % sulphuric acid (H_2SO_4) was diluted with deionised water and topped up to a volume of 500 mL 4.5 M H_2SO_4.

Factors		-1	+1
A	NaCl [mmol]	0.04	0.06
B	Morpholine [mmol]	22.9	28.7
C	pH_1 by 4.5 M H_2SO_4	7.80	8.20
D	{γ-SiW_{10}} [mmol]	0.10	0.13
F	$MnSO_4 \cdot 4H_2O$ [mmol]	1.30	2.0
G	$KMnO_4$ [mmol]	0.03	0.04
H	pH_2 by 4.5 M H_2SO_4	7.60	7.90
I	Reaction Temp. [°C]	30.0	80.0
J	Filter	no	yes

Table 13

All reactions carried out on 53.5 mL scale. The assigned factors A, B, C, D, F, G, H, I and J with their minimum (-1) and maximum levels (1). All absolute amounts refer to the volumetric scale on the top left.

3.1.2.2 The Keggin-Net 2/3 Synthesis

Thus, (A) 45 mL sodium chloride (*NaCl*) solution were stirring with 500 rpm in 100 mL round-bottom flasks (B) when 2.0 mL and 2.5 mL morpholine (C_4H_9NO) were added including an extra 0.5 mL deionised water to the samples at the lower setting. All samples were approximately at pH 11 and 22 °C, (C) when 4.5 M sulphuric acid (H_2SO_4) was used dropwise to adjust the pH to 7.8 and 8.2. The amounts of acid varied from 2.1 mL to 2.9 mL. Up to 0.9 mL deionised water were added to the samples which contained less acid to even out the volume. (D) Next, 0.3 g and 0.4 g potassium γ-decatungstosilicate ($K_8[\gamma\text{-}SiW_{10}O_{36}]\cdot 12H_2O$) were added in solid form to all samples at the same time and stirred for five minutes which was enough time to dissolve everything. (F) Afterwards, 2 mL manganese sulphate solution ($MnSO_4 \cdot 4H_2O$) was added, which turned the colourless solutions yellow immediately. (G) Then, 1 mL potassium permanganate solution ($KMnO_4$) was added all at once. The former yellow solutions turned brown, became cloudy in some cases and were stirred for another five minutes. (I) Now, the pH was adjusted to 7.6 and 7.9 using drops of 4.5 M sulphuric acid (H_2SO_4) again, before dry condensers were attached on top of the round-bottom flasks. (J) Half of the samples were heated to 30 °C while the other half was heated to 80 °C and all were stirred for one and a half hours. (K) Finally, half of the samples were filtered through a glass

funnel using filter paper and all stored unsealed in a shelf at 18 °C for three weeks. Afterwards, they were prepared for ICP analysis as described in Section 3.1.4 whereas the results and their analysis can be found in Section 5.1.2.

Random Orders			Factors	A	B	C	D	E	F	G	H	I	J	K
MAK03-125	**MAK03-127**	**MAK03-129**	**Original Order**	**NaCl**	**Morpho-line**	**pH_1**	**{γ-SiW_{10}}**	**Dummy 1**	**$MnSO_4$**	**$KMnO_4$**	**pH_2**	**Heating**	**Filter**	**Dummy 2**
g	**j**	**b**	**1**	1	1	-1	1	1	1	-1	-1	-1	1	-1
d	**g**	**g**	**2**	1	-1	1	1	1	-1	-1	-1	1	-1	1
e	**e**	**d**	**3**	-1	1	1	1	-1	-1	-1	1	-1	1	1
a	**d**	**e**	**4**	1	1	1	-1	-1	-1	1	-1	1	1	-1
k	**h**	**l**	**5**	1	1	-1	-1	-1	1	-1	1	1	-1	1
b	**b**	**j**	**6**	1	-1	-1	-1	1	-1	1	1	-1	1	1
j	**a**	**f**	**7**	-1	-1	-1	1	-1	1	1	-1	1	1	1
h	**k**	**i**	**8**	-1	-1	1	-1	1	1	-1	1	1	1	-1
f	**i**	**c**	**9**	-1	1	-1	1	1	-1	1	1	1	-1	-1
i	**l**	**h**	**10**	1	-1	1	1	-1	1	1	1	-1	-1	-1
l	**c**	**a**	**11**	-1	1	1	-1	1	1	1	-1	-1	-1	1
c	**f**	**k**	**12**	-1	-1	-1	-1	-1	-1	-1	-1	-1	-1	-1

Table 14

Twelve run Plackett-Burman screening design with eleven factors (Including two dummy factors), two levels and twelve runs which are in randomly assigned running order a-l for three repetitions. (A-K = factors, -1 low setting, 1 high setting)

3.1.3 Keggin Network 3/3

3.1.3.1 Keggin Network 3/3 DOE Preparation

A setup was generated that had all reagents added in a dissolved aqueous form except for the {γ-SiW_{10}} precursor. Due to the vastly different results of the setups Keggin network 1/3 and 2/3 a third procedure was designed based on the six most important factors of both former sets. Three worksheets (Table 14) were generated, one for each repetition all in random running order and carried out alphabetically from *a* to *l* in six 100 mL round-bottom flasks sitting on two single magnetic hotplate stirrers containing three heating mantles each to distribute the heat equally. Furthermore, the total volume was defined as 55.0 mL and other parameters in this set of three repetitions were the following:

In all experiments 1 M sodium chloride (NaCl) solution was used, the levels of morpholine (*C_4H_9NO*) were chosen to be 2 mL and 3 mL while pH_1 was adjusted to 8.0 using 4.5 M sulphuric acid (*H_2SO_4*) for all reactions. Either 0.3 g or 0.4 g potassium γ-decatungstosilicate (*$K_8[\gamma\text{-}SiW_{10}O_{36}]\cdot 12H_2O$*) were used and 30 mg or 45 mg manganese sulphate (*$MnSO_4\cdot 4H_2O$*) dissolved in 2 mL deionised water were added to the samples. Also, 1 mL potassium permanganate solution was added containing 5 mg and 6.5 mg $KMnO_4$. The final pH_2 was either 7.6 or 7.9 before heating the reaction mixtures for 1.5 h at 30 °C and 80 °C. All samples were stirred for 1.5 h and all changes resulted Table 15 as can be seen below.

First, 58.44 g sodium chloride (*NaCl*) was dissolved in 1 L deionised water to result in a 1 M solution; 750 mg and 1125 mg manganese sulphate tetrahydrate (*$MnSO_4\cdot 4H_2O$*) were dissolved in 50 mL deionised water each; 126 mg and 163 mg potassium permanganate (*$KMnO_4$*) were dissolved in 25 mL deionised water each; 122.2 mL 98 % sulphuric acid (*H_2SO_4*) was diluted with deionised water and topped up to a volume of 500 mL 4.5 M H_2SO_4.

Factors		-1	+1
A	Morpholine [mmol]	22.9	34.4
B	{γ-SiW_{10}} [mmol]	0.10	0.13
C	$MnSO_4\cdot 4H_2O$ [mmol]	0.13	0.20
D	$KMnO_4$ [mmol]	0.03	0.04
E	pH (final) by 4.5 M H_2SO_4	7.60	7.90
F	Reaction Temp. [°C]	30.0	80.0

Table 15

All reactions carried out on 55 mL scale. The assigned factors A, B, C, D, F and G with their minimum (-1) and maximum levels (1). All absolute amounts refer to the volumetric scale on the top left.

3.1.3.2 Keggin Network 3/3 Synthesis

First, 45 mL of 1 M sodium chloride solution (*NaCl*) were stirring with 450 rpm in 100 mL round-bottom flasks (A) when 2 mL and 3 mL morpholine (C_4H_9NO) was added and an extra 1 mL deionised water to the samples with the lower setting. All samples were approximately at pH 11, when 2.44 mL and 3.6 mL 4.5 M sulphuric acid (H_2SO_4) was used to adjust the pH to 8.0. Both solutions were topped up to 52 mL by adding 1.56 mL and 0.4 mL deionised water. (B) Then, 0.3 g and 0.4 g of potassium γ-decatungstosilicate ($K_8[\gamma\text{-}SiW_{10}O_{36}]\cdot 12H_2O$) was added in solid form to the samples at the same time and they were stirred for ten minutes which was enough time to dissolve everything. (C) Afterwards, 2 mL manganese sulphate solution ($MnSO_4\cdot 4H_2O$) was added all at once, which turned the colourless solutions yellow immediately, (D) followed by 1 mL potassium permanganate solution ($KMnO_4$). The former yellow solution turned brown, became cloudy in some cases and was stirred for another five minutes. (E) Now, the pH was adjusted to 7.6 and 7.9 using some drops of 4.5 M sulphuric acid (H_2SO_4), before dry condensers were attached on top of the round-bottom flasks. (F) One half of the samples was heated to 30 °C while the other half was heated to 80 °C and all were stirred for one and a half hours. Finally, they were stored unsealed in a shelf at 18 °C for three weeks and then prepared for ICP analysis as described in Section 3.1.4 whereas the results and their analysis can be found in Section 5.1.3.

Keggin-Network			Factors	A	B	C	D	E	F	G	H	I	J	K
MAK03-149	**MAK03-151**	**MAK03-153**	**Original Order**	**Morpho-line**	**{γ-SiW_{10}}**	**$MnSO_4$**	**$KMnO_4$**	**pH_2**	**Reaction Temp.**	**Dummy 1**	**Dummy 2**	**Dummy 3**	**Dummy 4**	**Dummy 5**
k	**k**	**d**	**1**	1	1	-1	1	1	1	-1	-1	-1	1	-1
l	**j**	**f**	**2**	1	-1	1	1	1	-1	-1	-1	1	-1	1
g	**l**	**i**	**3**	-1	1	1	1	-1	-1	-1	1	-1	1	1
h	**i**	**k**	**4**	1	1	1	-1	-1	-1	1	-1	1	1	-1
f	**e**	**j**	**5**	1	1	-1	-1	-1	1	-1	1	1	-1	1
b	**c**	**b**	**6**	1	-1	-1	-1	1	-1	1	1	-1	1	1
e	**g**	**g**	**7**	-1	-1	-1	1	-1	1	1	-1	1	1	1
j	**h**	**c**	**8**	-1	-1	1	-1	1	1	-1	1	1	1	-1
d	**f**	**e**	**9**	-1	1	-1	1	1	-1	1	1	1	-1	-1
i	**d**	**a**	**10**	1	-1	1	1	-1	1	1	1	-1	-1	-1
c	**a**	**h**	**11**	-1	1	1	-1	1	1	1	-1	-1	-1	1
a	**b**	**l**	**12**	-1	-1	-1	-1	-1	-1	-1	-1	-1	-1	-1

Table 16

Twelve run Plackett-Burman screening design with eleven factors (Including five dummy factors), two levels and twelve runs which are in randomly assigned running order a-l for three repetitions. (A-K = factors, -1 low setting, 1 high setting)

3.1.4 Keggin Net ICP Preparation

Once all runs of one set were completed, all of the Keggin network samples were prepared and analysed by ICP in the following manner:

After 21 days of crystallisation, together with the precipitate the crystals were scratched off the glass-bottom of the conical flask with a plastic spatula and transferred onto a piece of Parafilm lying on a filter paper using a plastic pipette. The samples were covered with watch glasses and left to dry at the air for a couple of days. Once dried, the samples were transferred into 7 mL glass vials which were weighted before. The ones still not completely dry were dried under vacuum overnight. Next, their weights were determined by weighing the vials including the materials which can be found in Section 8.3.

Then, they were prepared for ICP analysis by dissolving about 5-10 mg of each sample in a 100 mL beaker in some deionised water and 2 mL 69 % nitric acid (HNO_3) before transferring it into a 50 mL volumetric flask and topping it up to the total volume of 50 mL with more deionised water. Finally, an elemental analysis of Mn, Si and W was run on the ICP for characterisation and to determine the product's purity. The results and their analysis can be found in Section 5.1

3.2 The {V_{18}} Fe-Linked Network

3.2.1 {V_{18}} Fe-Linked DOE Preparation

A setup was generated that had all reagents added in a dissolved aqueous form except for the vanadium pentoxide V_2O_5. Six reaction steps were chosen to be examined and two worksheets (Table 18) were generated, one for each repetition all in random running order and carried out alphabetically from *a* to *l*. The reactions were carried out in six 100 mL round-bottom flasks sitting on two single magnetic hotplate stirrers containing three heating mantles each to distribute the heat equally. Furthermore, the total volume was defined as 35.0 mL. The parameters in this set of two repetitions were the following:

(A) molarity of the lithium hydroxide (*LiOH*) solution, (B) amount of solid vanadium pentoxide (V_2O_5), (C) heating temperature, (D) addition of hydrazine sulphate ($[N_2H_5][HSO_4]$), (E) addition of iron(II) chloride tetrahydrate ($FeCl_2{\cdot}4H_2O$) and (F) heating time. Factors G, H, I, J and K served as dummies. Once the experimental steps were assigned to the factors the levels were defined as can be seen below in Table 17.

The stock solutions were prepared as follows: 1.437 g and 2.156 g lithium hydroxide (*LiOH*) were dissolved in 50 mL deionised water each; 6.506 g and 13.012 g hydrazine sulphate (*$[N_2H_5][HSO_4]$*) were dissolved in 500 mL deionised water each; and finally, 1.988 g and 2.982 g iron(II) chloride tetrahydrate (*$FeCl_2{\cdot}4H_2O$*) were dissolved in 20 mL deionised water freshly on the day the reactions were carried out.

Factors		-1	+1
A	LiOH [mmol]	4.00	6.00
B	V_2O_5 [mmol]	2.25	2.75
C	Reaction Temp. [°C]	60.0	95.0
D	Hydrazine Sulphate [mmol]	2.0	4.00
E	$FeCl_2{\cdot}4H_2O$ [mmol]	1.00	1.50
F	Reaction Time [h]	3.0	7.0

Table 17

All reactions carried out on 35 mL scale. The assigned factors A-F with their minimum (-1) and maximum levels (1). All absolute amounts refer to the volumetric scale on the top left.

3.2.2 {V_{18}} Fe-Linked Synthesis

(B) First, 0.409 g and 0.500 g solid vanadium pentoxide (*V_2O_5*) were transferred into 100 mL round-bottom flasks, put on two magnetic hotplate stirrers with three heating mantles each and 10 mL deionised water was added. Dry condensers were attached on top of the flasks and (C) the samples heated to 60 °C and 95 °C. (A) After 20 minutes 3 mL lithium hydroxide (*LiOH*) solution was added to the stirring orange slurries. (D) Afterwards, the resulting solution was treated with 20 mL hydrazine sulphate solution (*$[N_2H_5][HSO_4]$*) and stirred for ten minutes, (E) followed by 2 mL iron(II) chloride solution (*$FeCl_2{\cdot}4H_2O$*). (F) The black solutions were heated and stirred for three and seven hours. Then, they were removed from the hotplates, transferred into 50 mL conical flasks and sealed with Parafilm. Finally, they were left in a shelf at 18 °C for 16 h.

The next day, the samples were transferred into 50 mL centrifuge tubes and centrifuged at 4.4 krpm for five minutes. Subsequently, the liquid was pipetted off and the tubes containing black solid material dried under vacuum overnight. Once dried, the samples were transferred into 7 mL glass vials which were weighted before. The ones still not completely dry were dried under vacuum overnight. Next, their weights were determined by weighing the vials including the materials which can be found in Section 8.3.

{V_{18}}-Network		Factors	A	B	C	D	E	F	G	H	I	J	K
MAK03-169	**MAK03-165**	**Original Order**	**LiOH**	**V_2O_5 Solid**	**Reaction Temp.**	**Hydrazine Sulphate Solution**	**FeCl**	**Reaction Time**	**Dummy 1**	**Dummy 2**	**Dummy 3**	**Dummy 4**	**Dummy 5**
d	**b**	**1**	1	1	-1	1	1	1	-1	-1	-1	1	-1
b	**k**	**2**	1	-1	1	1	1	-1	-1	-1	1	-1	1
j	**i**	**3**	-1	1	1	1	-1	-1	-1	1	-1	1	1
e	**a**	**4**	1	1	1	-1	-1	-1	1	-1	1	1	-1
h	**d**	**5**	1	1	-1	-1	-1	1	-1	1	1	-1	1
g	**j**	**6**	1	-1	-1	-1	1	-1	1	1	-1	1	1
k	**f**	**7**	-1	-1	-1	1	-1	1	1	-1	1	1	1
l	**l**	**8**	-1	-1	1	-1	1	1	-1	1	1	1	-1
c	**g**	**9**	-1	1	-1	1	1	-1	1	1	1	-1	-1
a	**h**	**10**	1	-1	1	1	-1	1	1	1	-1	-1	-1
i	**e**	**11**	-1	1	1	-1	1	1	1	-1	-1	-1	1
f	**c**	**12**	-1	-1	-1	-1	-1	-1	-1	-1	-1	-1	-1

Table 18

Twelve run Plackett-Burman screening design with eleven factors (Including five dummy factors), two levels and twelve runs which are in randomly assigned running order a-l for three repetitions. (A-K = factors, -1 low setting, 1 high setting)

3.2.3 {V_{18}} Fe-Linked ICP Preparation

Upon completion, they were prepared for ICP analysis by dissolving about 5-10 mg of each sample in a 100 mL beaker in some deionised water and 2 mL 69 % nitric acid before transferring it into a 50 mL volumetric flask and topping it up to the total volume of 50 mL with more deionised water. Finally, an elemental analysis of Fe, S and V was run on the ICP for characterisation and to determine the product's purity. The results and their analysis can be found in Section 5.2.

3.3 The {Mo_{154}} Blue Wheel

3.3.1 {Mo_{154}} Blue Wheel DOE Preparation

A setup was generated that had all reagents added in a dissolved aqueous form. First, the following six reaction steps were chosen as factors to be examined and one worksheet (Table 20) was generated in random running order and carried out alphabetically from *a* to *l*. The reactions were carried out in six 100 mL round-bottom flasks sitting on two single magnetic hotplate stirrers containing three heating mantles each to distribute the heat equally. Furthermore, the total volume was defined as 27.1 mL. The parameters in this set were the following:

(A) The molarity of the sodium molybdate solution ($Na_2MoO_4{\cdot}2H_2O$), (B) the molarity of the hydrazine sulphate solution ($[N_2H_5][HSO_4]$), (C) the pH of the reaction mixture adjusted by 5 M hydrochloric acid (HCl), (D) the reaction temperature, (E) the stirring time and (F) the evaporation speed. Factors G, H, I, J and K served as dummies. Once the experimental steps were assigned to the factors the levels were defined as can be seen below in Table 19.

The stock solutions were prepared as follows: 3.0 g and 7.5 g sodium molybdate dihydrate ($Na_2MoO_4{\cdot}2H_2O$) were dissolved in 300 mL deionised water each; 0.45 g and 1.50 g hydrazine sulphate ($[N_2H_5][HSO_4]$) were dissolved in 75 mL deionised water each; 215 mL 36 % hydrochloric acid (HCl) was mixed with deionised water and topped up to a volume of 500 mL 5M HCl.

Factors		-1	+1
A	$Na_2MoO_4 \cdot 2H_2O$	0.83	2.07
B	Hydrazine Sulphate	0.23	0.77
C	pH by 5 M HCl	0.80	1.20
D	Reaction Temp. [°C]	20.0	60.0
E	Reaction Time [min]	10.0	60.0
F	Evaporation	Closed	Open

Table 19

All reactions carried out on 27.1 mL scale. The assigned factors A-F with their minimum (-1) and maximum levels (1). All absolute amounts refer to the volumetric scale on the top left.

3.3.2 {Mo_{154}} Blue Wheel Synthesis

First, (A) 20 mL sodium molybdate solution (*$Na_2MoO_4 \cdot 2H_2O$*) were poured into 100 mL round-bottom flasks and stirred at 450 rpm. Then, (B) 5 mL hydrazine sulphate solution (*$[N_2H_5][HSO_4]$*) were added and stirred for five minutes. Subsequently, (C) the pH was adjusted to 0.8 and 1.2 by adding 1.10 mL and 2.10 mL of 5 M hydrochloric acid (*HCl*) to the samples with the higher concentration of sodium molybdate such as 0.65 mL and 1.8 mL to the lower concentrated solutions. Between 0.00 mL and 1.45 mL deionised water was added afterwards to even out the volumes. Now, (D) the temperatures were adjusted to 20 °C and 60 °C and (E) the dark blue solutions stirred for 10 min and 60 min at these settings. (F) All samples were removed from the hotplates, transferred into 50 mL conical flasks and one half sealed with Parafilm whereas the other half was left open to achieve different levels of evaporation. They were put into a shelf at 18 °C and left for four days. Then, they were transferred into 50 mL centrifuge tubes and centrifuged at 4.4 krpm for five minutes, the liquid was pipetted off and the tubes containing dark blue solid material dried under vacuum overnight. Once dried, the samples were transferred into 7 mL glass vials which were weighted before. The ones still not completely dry were dried under vacuum overnight. Next, their weights were determined by weighing the vials including the materials which can be found in Section 8.3.

MAK03-159	A	B	C	D	E	F	G	H	I	J	K
Runs	**Na_2MoO_4**	**Hydrazine Sulphate**	**pH**	**Reaction Temp.**	**Reaction Time**	**Evaporation**	**Dummy 1**	**Dummy 2**	**Dummy 3**	**Dummy 4**	**Dummy 5**
1	1	1	-1	1	1	1	-1	-1	-1	1	-1
2	1	-1	1	1	1	-1	-1	-1	1	-1	1
3	-1	1	1	1	-1	-1	-1	1	-1	1	1
4	1	1	1	-1	-1	-1	1	-1	1	1	-1
5	1	1	-1	-1	-1	1	-1	1	1	-1	1
6	1	-1	-1	-1	1	-1	1	1	-1	1	1
7	-1	-1	-1	1	-1	1	1	-1	1	1	1
8	-1	-1	1	-1	1	1	-1	1	1	1	-1
9	-1	1	-1	1	1	-1	1	1	1	-1	-1
10	1	-1	1	1	-1	1	1	1	-1	-1	-1
11	-1	1	1	-1	1	1	1	-1	-1	-1	1
12	-1	-1	-1	-1	-1	-1	-1	-1	-1	-1	-1

Table 20

Twelve run Plackett-Burman screening design with eleven factors (Including five dummy factors), two levels and twelve runs which are in randomly assigned running order a-l for three repetitions. (A-K = factors, -1 low setting, 1 high setting)

3.3.3 {Mo_{154}} Blue Wheel ICP Prepration

Afterwards, they were prepared for ICP analysis by dissolving about 5-10 mg of each sample in a 100 mL beaker in some deionised water and 2 mL 69 % nitric acid before transferring it into a 50 mL volumetric flask and topping it up to the total volume of 50 mL with more deionised water. Finally, an elemental analysis of Mo was run on the ICP for characterisation and to determine the product's purity. The results and their analysis can be found in Section 5.3.

3.4 The {Mo_{132}} Keplerate

3.4.1 {Mo_{132}} Keplerate DOE Preparation

A setup was generated that had all reagents added in a dissolved aqueous form. First, the following six reaction steps were chosen as factors to be examined and two worksheets (Table 22) were generated, one for each repetition all in random running order and carried out alphabetically from *a* to *l*. The reactions were carried out in six 100 mL round-bottom flasks sitting on two single magnetic hotplate stirrers containing three heating mantles each to distribute the heat equally. Furthermore, the total volume was defined as 47.0 mL. The parameters in this set of two repetitions were the following:

(A) The molarity of the ammonium acetate solution (CH_3COONH_4), (B) the molarity of the ammonium heptamolybdate solution ($(NH_4)_6Mo_7O_{24}\cdot 4H_2O$), (C) the pH of the reaction mixture adjusted by 50 % acetic acid (CH_3COOH), (D) the molarity of the hydrazine sulphate solution ($[N_2H_5][HSO_4]$), (E) the reaction temperature and (F) the stirring time. Factors G, H, I, J and K served as dummies. Once the experimental steps were assigned to the factors the levels were defined as can be seen below in Table 21.

The stock solutions were prepared as follows: 11.55 g and 18.75 g ammonium acetate (CH_3COONH_4) were dissolved in 375 mL deionised water each; 7.5 g and 9.0 g ammonium heptamolybdate tetrahydrate ($(NH_4)_6Mo_7O_{24}\cdot 4H2O$) were dissolved in 75 mL deionised water each; 250 mL glacial acetic acid (CH_3COOH) and 250 mL deionised water were mixed; 1.05 g and 1.35 g hydrazine sulphate ($[N_2H_5][HSO_4]$) were dissolved in 75 mL deionised water each.

Factors		-1	+1
A	CH_3COONH_4	10.0	16.2
B	$(NH_4)_6Mo_7O_{24}{\cdot}4H2O$	0.40	0.49
C	pH by Acetic Acid (50 %)	3.80	4.20
D	Hydrazine Sulphate	0.54	0.69
E	Reaction Temp.	20.0	60.0
F	Reaction Time [min]	10.0	60.0

Table 21

All reactions carried out on 47 mL scale. The assigned factors A-F with their minimum (-1) and maximum levels (1). All absolute amounts refer to the volumetric scale on the top left.

3.4.2 {Mo_{132}} Keplerate Synthesis

First, (A) 25 mL ammonium acetate solution (*CH_3COONH_4*) was poured into 100 mL round-bottom flasks and stirred at 450 rpm. Then, (B) 5 mL ammonium heptamolybdate solution ($(NH_4)_6Mo_7O_{24}{\cdot}4H2O$) was added and subsequently, (C) the pH adjusted to 3.8 and 4.2 by adding 5.2 mL and 11.6 mL of 50 % acetic acid (*CH_3COOH*) to the samples with the higher concentration of ammonium acetate and 3.1 mL and 7.1 mL to the lower concentrated solutions. Between 0.4 mL and 6.9 mL deionised water was added afterwards to even out the volumes. Now, (D) 5 mL hydrazine sulphate solution (*$[N_2H_5][HSO_4]$*) was added to each sample, (E) the temperatures adjusted to 20 °C and 60 °C and the dark brown solutions stirred (F) for either 10 min or 60 min at these settings. Then, all samples were removed from the hotplates, transferred into 50 mL conical flasks and put in a shelf at 18 °C.

Five days later, they were transferred into 50 mL centrifuge tubes and centrifuged at 4.4 krpm for five minutes. Subsequently, the liquid was pipetted off and the tubes containing dark brown solid material dried under vacuum overnight. Once dried, the samples were transferred into 7 mL glass vials which were weighted before. The ones still not completely dry were dried under vacuum overnight. Next, their weights were determined by weighing the vials including the materials which can be found in Section 8.3.

3.4.3 {Mo_{132}} Keplerate Crystals Collection

Four weeks after the aforementioned collection, huge, brown crystals had formed in half of the samples. They were simply collected by Buchner filtration and dried on filter paper covered with watch glasses for two days. Once dried, the samples were transferred into 7 mL

glass vials which were weighted before. The ones still not completely dry were dried under vacuum overnight. Next, their weights were determined by weighing the vials including the materials which can be found in section 8.3.

3.4.4 {Mo_{132}} Keplerate ICP Preparation

Afterwards, they were prepared for ICP analysis by dissolving about 5-10 mg of each sample in a 100 mL beaker in some deionised water and 2 mL 69 % nitric acid before transferring it into a 50 mL volumetric flask and topping it up to the total volume of 50 mL with more deionised water. Finally, an elemental analysis of Mo was run on the ICP for characterisation and to determine the product's purity. The results and their analysis can be found in Section 5.4.

{Mo_{132}}		Factors	A	B	C	D	E	F	G	H	I	J	K
MAK03-161	**MAK03-163**	**Original Order**	**CH_3COONH_4**	**$(NH_4)_6Mo_7O_{24}$**	**Acetic Acid**	**Hydrazine Sulphate**	**Reaction Temp.**	**Reaction Time**	**Dummy 1**	**Dummy 2**	**Dummy 3**	**Dummy 4**	**Dummy 6**
b	l	1	1	1	-1	1	1	1	-1	-1	-1	1	-1
g	j	2	1	-1	1	1	1	-1	-1	-1	1	-1	1
c	e	3	-1	1	1	1	-1	-1	-1	1	-1	1	1
f	c	4	1	1	1	-1	-1	-1	1	-1	1	1	-1
h	k	5	1	1	-1	-1	-1	1	-1	1	1	-1	1
j	a	6	1	-1	-1	-1	1	-1	1	1	-1	1	1
k	i	7	-1	-1	-1	1	-1	1	1	-1	1	1	1
a	f	8	-1	-1	1	-1	1	1	-1	1	1	1	-1
d	b	9	-1	1	-1	1	1	-1	1	1	1	-1	-1
e	h	10	1	-1	1	1	-1	1	1	1	-1	-1	-1
l	g	11	-1	1	1	-1	1	1	1	-1	-1	-1	1
i	d	12	-1	-1	-1	-1	-1	-1	-1	-1	-1	-1	-1

Table 22

Twelve run Plackett-Burman screening design with eleven factors (Including five dummy factors), two levels and twelve runs which are in randomly assigned running order a-l for three repetitions. (A-K = factors, -1 low setting, 1 high setting)

4 The DOE Analysis

4.1 Purity Determination

All sample results were calculated in the exact same way as described below in this section and all yields were tested by weighing and ICP analyses. Purities were based on the smallest appearances of elements in terms of adequate elemental ratios. So, if one element's amount was found the lowest regarding the ratio of the appearance in the molecule, this element became the limiting factor and the yield was based on it. This result was considered to be pure product i.e. the lowest necessary and highest possible yield was calculated.

First, the raw ICP results being provided in ppm (*mg/L*) for each element were divided by its own molar mass (*mg/mmol*) which then resulted in the concentration (*mmol/L*) of the corresponding element in the sample.

$$\textbf{Concentration} = \frac{ppm}{molar\ mass} = \frac{mg/L}{mg/mmol} = \textbf{mmol/L} \qquad \textit{Equation 13}$$

Next, the calculated values (*in mmol/L*) were divided by the atomic quantities of the elements' in the structural formula of the desired compound i.e. for the Keggin network Mn = 12, Si = 7 and W = 72; for the {V_{18}} Fe-linked network Fe = 3, S = 1 and V = 18; for the {Mo_{154}} blue wheel Mo = 154 and Na = 15; for the {Mo_{132}} Keplerate, this step was skipped because there was no other element to compare the amount of Mo to.

$$\textbf{Limiting Element Value} = \frac{concentration\ [mmol/L]}{Element's\ Atomic\ Quantity} \qquad \textit{Equation 14}$$

The smallest value defined the limiting element i.e. the excess of the other elements came from impurities. To find out how high the individual excesses were, the smallest limiting element value was multiplied by the respective atomic quantities of the other elements' in the structural formula and then deducted from their concentration values from Equation 13.

$$\textbf{Element Excess [mmol/L]} = \textbf{Concentration [mmol/L]} - \textbf{Limiting Element Value [mmol/L]} \cdot \textbf{Atomic Quantity} \qquad \textit{Equation 15}$$

Next, the largest impurity was taken and subtracted from the original concentration of the corresponding element. Subsequently this value is divided by the same original concentration value from before and the resulting quotient multiplied by 100 % to get the purity of the sample.

$$\textit{Sample Purity [\%]} = \frac{\textit{Concentration}\ [mmol/L] - \textit{Highest Element Excess}\ [mmol/L]}{\textit{Concentration}\ [mmol/L]} \cdot 100\ \% \qquad \textit{Equation 16}$$

The following steps show how to calculate the amount of W, V and Mo that was transferred from the precursors to the final product. First, we multiply the total yield of each sample with the sample purity divided by 100 %.

$$\textit{Pure Yield [mg]} = \frac{\textit{Sample Yield}\ [mg] \cdot \textit{Sample Purity}\ [\%]}{100\ \%} \qquad \textit{Equation 17}$$

Now, the pure yield values are converted into mmol dividing them by the products' molar mass and then multiplying these values with the atomic quantities of W, V or Mo in the structural formula.

$$\textit{Main Transition Metal Pure Yield [mmol]} = \frac{\textit{Pure Yield}\ [mg]}{M_{POM}\ [mg/mmol]} \cdot \textit{Atomic Quantity} \qquad \textit{Equation 18}$$

Finally, the main transition metal pure yield is divided by the amount of invested main transition metal and multiplied by 100 % to result in how much of it was transferred into the final product.

$$\textit{Final Outcome [\%]} = \frac{\textit{Main Transition Metal Pure Yield}\ [mmol]}{\textit{Invested Main Transition Metal}\ [mmol]} \cdot 100\ \% \qquad \textit{Equation 19}$$

4.2 Factor Effect Calculations

The so-called contrasts (Δ) of the main factors and interactions could be determined by subtracting the averages of the responses ($\bar{y}_{-1}$) at the low level (-1) from the averages of the responses ($\bar{y}_1$) at the high level (1). These contrasts, however, had to be treated further to find the estimated factor effects that were the measure for the significance of the factors, due to the main effects being confounded with two-factor interactions which made it necessary to disentangle them first. To do so, the vector product (e.g. product of columns A and BC = -4) is divided by the number of runs (n = 12) which delivers a quotient of -0.333. An easy way to portray it is given in Table 23 that shows the multiplication of column A and column BC resulting in an imaginary column ABC. If the numerals of this column ABC are summed up and divided by 12 a quotient of -0.333 is received which means that $-\frac{1}{3}$ of the effect of BC had to be added to the effect of A because it is entangled with the interaction by this amount.

Runs/ Factors	1	2	3	4	5	6	7	8	9	10	11	12
A	1	1	-1	1	1	1	-1	-1	-1	1	-1	-1
BC	-1	-1	1	1	-1	1	1	-1	-1	-1	1	1
A*BC	-1	-1	-1	1	-1	1	-1	1	1	-1	-1	-1

Table 23

Visual way of finding the vector product of factor A and interaction BC by multiplying both columns and adding the numerals of A*BC together which equals -4 in this case.

Ergo the correlation (r) is mathematically defined as:

$$r_{A,BC} = \frac{\Sigma_{X_A X_{BC}}}{\sqrt{(\Sigma_{X_A^2})(\Sigma_{X_{BC}^2})}} = -0.333 \qquad \textit{Equation 20}$$

This was repeated for all main factors with all two-factor interactions not containing the correlating main factor themselves because all two-factor interactions that do not include the given main factor are correlated, also called partially confounded with that main effect. This pattern can be found in Section 8.1. The correlations that contain one or more dummy factors as two-factor interactions were defined as 0 which can be found in Section 8.2. Since factor A is aliased with 45 interactions the correlations for all of those must be calculated which determines the confounding and results in the estimated effect of factor A [$E(A_{est})$]. This can be written as the following equation:

$$E(A_{est}) = E(A) + r_{A,BC}E(BC) + r_{A,BD}E(BD) + \ldots + r_{A,JK}E(JK) \qquad \textit{Equation 21}$$

Once all main factors have been disentangled in this manner, they can be checked for their significance in the system.

4.3 Minimum Significant Effect Calculations

The first step was the calculation of the standard deviation (σ) using the effects of the dummy factors by determining the mean of the squared estimated effects of the five dummy factors and then extracting the root of it.

$$\sigma = \sqrt{\frac{\Sigma^2_{Dummies}}{n}} \qquad \textit{Equation 22}$$

The t-value of 1.476 was chosen from a t-table depending on the degrees of freedom, which was the number of dummy factors = 5, and the probability value of α = 0.2. As a final step, the

standard deviation was multiplied by the t-value to find the minimum significant factor effect MIN.

$$MIN = t\text{-}value \cdot \sigma \qquad \textit{Equation 23}$$

The absolute values of an estimated effect had to be higher than the MIN value to be considered as significant.

5 Results and Discussion

5.1 The Keggin Network

5.1.1 Keggin-Net 1/3

After ICP analysis, the yield outcomes [%] for each run relative to the invested amount of tungsten was calculated which was essential to continue the DOE analyses. All values were calculated as shown in the beginning of Section 4.1. which gave the results in Table 25. Surprisingly, the Si/W ratios were inconsistent and, in comparison with previous synthesis, it seemed that working with solids yields a purer product.

	Yield (based on W)			
Runs	**MAK03-99**	**MAK03-101**	**MAK03-103**	**Average**
1	3 %	22 %	7 %	**11 %**
2	7 %	5 %	13 %	**8 %**
3	10 %	11 %	27 %	**16 %**
4	7 %	3 %	12 %	**7 %**
5	6 %	10 %	14 %	**10 %**
6	8 %	15 %	10 %	**11 %**
7	8 %	4 %	7 %	**7 %**
8	4 %	6 %	7 %	**6 %**
9	2 %	4 %	22 %	**9 %**
10	14 %	8 %	10 %	**11 %**
11	2 %	10 %	18 %	**10 %**
12	16 %	4 %	8 %	**9 %**

Table 24

Results of three repetitions of twelve runs. All yields are based on W in percent relative to the invested amount.

Nevertheless, the results were similar enough within the runs to continue with the analysis and calculate the factor effects to find the most important factors. Due to the sparsity of

effects principle, only the three highest effects were chosen to be important and found to belong to factors (I) *pH_2,* (B) *morpholine* and (H) *addition time.*

More changes to the procedure were applied to improve the reliability of the reaction even further. Factor (E) *stirring time* was removed because it consumed a lot of time and the calculated effect was too low to be significant. Furthermore, the way of heating was changed. Having 100 mL conical flasks standing on ten-positions magnetic hotplate stirrers were problematic because the heat was not equally distributed on the hotplate area itself and only the bottoms of the flasks were heated which was an additionally unequal distribution of heat within the sample solutions. So, a setup of three round-bottom flasks sitting in heating mantles on a single magnetic hotplate stirrer was chosen for the next experiments instead. Also, because the room temperature reached from 18 °C to 22 °C the minimum level of the heating temperature was increased to 30 °C to remove another potential source of error.

MAK03-99, 101, 103	A	B	C	D	E	F	G	H	I	J	K	
Runs	**NaCl**	**Morpholine**	**pH_1**	**{γ-SiW_{10}}**	**Reaction Time**	**$MnSO_4$**	**$KMnO_4$**	**Addition Time**	**pH_2**	**Reaction Temp.**	**Filter**	**Average Yield [%]**
1	1	1	-1	1	1	1	-1	-1	-1	1	-1	11
2	1	-1	1	1	1	-1	-1	-1	1	-1	1	8
3	-1	1	1	1	-1	-1	-1	1	-1	1	1	16
4	1	1	1	-1	-1	-1	1	-1	1	1	-1	7
5	1	1	-1	-1	-1	1	-1	1	1	-1	1	10
6	1	-1	-1	-1	1	-1	1	1	-1	1	1	11
7	-1	-1	-1	1	-1	1	1	-1	1	1	1	7
8	-1	-1	1	-1	1	1	-1	1	1	1	-1	6
9	-1	1	-1	1	1	-1	1	1	1	-1	-1	9
10	1	-1	1	1	-1	1	1	1	-1	-1	-1	11
11	-1	1	1	-1	1	1	1	-1	-1	-1	1	10
12	-1	-1	-1	-1	-1	-1	-1	-1	-1	-1	-1	9
$\bar{y}_{-1}$	0,094	0,085	0,094	0,089	0,099	0,101	0,099	0,086	0,112	0,095	0,087	
$\bar{y}_1$	0,096	0,106	0,097	0,102	0,091	0,089	0,091	0,104	0,078	0,095	0,103	
Contrast (Δ)	0,002	0,021	0,003	0,013	-0,008	-0,012	-0,008	0,018	-0,034	0,000	0,016	
Est. Effect	0,002	0,021	0,003	0,013	-0,008	-0,012	-0,008	0,018	-0,034	0,000	0,016	

Table 25

Results including the average yields, the results for the low ($\bar{y}_{-1}$) and high settings ($\bar{y}_1$) within each factor, the contrasts (Δ) and the disentangled effects.

5.1.2 Keggin-Net 2/3

The next Table 26 shows the outcomes [%] for each run relative to the invested amount of tungsten which was essential to continue the DOE analyses. All values were calculated as shown in the beginning of Section 4.1.

	Yield (based on W)			
Runs	**MAK03-125**	**MAK03-127**	**MAK03-129**	**Average**
1	3 %	8 %	5 %	**5 %**
2	6 %	9 %	9 %	**8 %**
3	6 %	9 %	11 %	**9 %**
4	12 %	10 %	6 %	**9 %**
5	3 %	6 %	6 %	**5 %**
6	1 %	0 %	5 %	**2 %**
7	6 %	7 %	9 %	**7 %**
8	2 %	3 %	3 %	**3 %**
9	12 %	11 %	11 %	**11 %**
10	7 %	6 %	10 %	**8 %**
11	3 %	0 %	2 %	**2 %**
12	4 %	2 %	1 %	**2 %**

Table 26

Results of three repetitions of twelve runs. All yields are based on W in percent relative to the invested amount.

The effects were calculated as described in section 4.2 which gave the results in Table 27.
Due to the sparsity of effects principle, only the three highest effects were chosen to be important and found to belong to factors (D) *{γ-SiW_{10}}*, (B) *morpholine*, (I) *reaction temp*.
In comparison with the Keggin net 2/3 results *{γ-SiW_{10}}* and (I) *reaction temp*. but not *pH_2* and *addition time* were significant. The only factor that was important in both experiments was *morpholine*. These were rather contradictory results and to be able to carry out a full factorial design with only three factors later, a third PB design had to be created. However, this time only the five most important factors of both previous tries were selected.

MAK03-125, 127, 129	A	B	C	D	E	F	G	H	I	J	K	
Runs	**NaCl**	**Morpholine**	**pH_1**	**{γ-SiW_{10}}**	**Dummy 1**	**MnSO4**	**KMnO4**	**pH_2**	**Reaction Temp.**	**Filter**	**Dummy 2**	**Average Yield [%]**
1	1	1	-1	1	1	1	-1	-1	-1	1	-1	**5**
2	1	-1	1	1	1	-1	-1	-1	1	-1	1	**8**
3	-1	1	1	1	-1	-1	-1	1	-1	1	1	**9**
4	1	1	1	-1	-1	-1	1	-1	1	1	-1	**9**
5	1	1	-1	-1	-1	1	-1	1	1	-1	1	**5**
6	1	-1	-1	-1	1	-1	1	1	-1	1	1	**2**
7	-1	-1	-1	1	-1	1	1	-1	1	1	1	**7**
8	-1	-1	1	-1	1	1	-1	1	1	1	-1	**3**
9	-1	1	-1	1	1	-1	1	1	1	-1	-1	**11**
10	1	-1	1	1	-1	1	1	1	-1	-1	-1	**8**
11	-1	1	1	-1	1	1	1	-1	-1	-1	1	**2**
12	-1	-1	-1	-1	-1	-1	-1	-1	-1	-1	-1	**2**
$\bar{y}_{-1}$	0,06	0,05	0,06	0,04	0,07	0,07	0,05	0,06	0,05	0,06	0,07	
$\bar{y}_1$	0,06	0,07	0,06	0,08	0,05	0,05	0,07	0,06	0,07	0,06	0,05	
Contrast (Δ)	0,00	0,02	0,01	0,04	-0,01	-0,02	0,01	0,01	0,03	0,00	-0,01	
Est. Effect	0,002	0,014	0,005	0,028	-0,012	-0,011	0,007	0,005	0,019	-0,001	-0,010	

Table 27

Results including the average yields, the results for the low ($\bar{y}_{-1}$) and high settings ($\bar{y}_1$) within each factor, the contrasts (Δ) and the disentangled effects.

5.1.3 Keggin Net 3/3

Three 12-reaction screening experiments were conducted by varying factors A-F as shown in Table 29 at their maximum or minimum setting. Each repeat of the 12-run design was carried out in a randomly assigned and different running order to control for the effect of reaction order.

	Yield (based on W)			
Run	**MAK03-149**	**MAK03-151**	**MAK03-153**	**Average**
1	11 %	6 %	7 %	**8 %**
2	0 %	0 %	0 %	**0 %**
3	0 %	0 %	0 %	**0 %**
4	0 %	0 %	0 %	**0 %**
5	6 %	3 %	3 %	**4 %**
6	7 %	2 %	3 %	**4 %**
7	8 %	4 %	5 %	**6 %**
8	0 %	0 %	0 %	**0 %**
9	9 %	6 %	5 %	**6 %**
10	0 %	5 %	2 %	**2 %**
11	10 %	3 %	1 %	**5 %**
12	0 %	5 %	2 %	**2 %**

Table 28

Keggin net results of transferred W of each run and repetition in percent as well as the averages of each run.

In the Keggin network experiments the minimum significant factor effect was calculated to be 5.3×10^{-3} and the absolute value of any effect had to be equal or higher to be considered as significant. (1) The stoichiometry of manganese sulphate ($MnSO_4{\cdot}4H_2O$) and (2) the heating temperature were found to have significant effects on the outcomes, whereas (3) the concentration of potassium permanganate ($KMnO_4$) did not pass the threshold of being significant, but its effect was still considerably high and worth mentioning here. The negative value of the Factor effect indicates that higher yields were achieved with Factor C at the lower setting demonstrating that the ratio of $MnSO_4.4H_2O$ to {γ-SiW10} should be closer to 1:1 than 2:1 in order to achieve the optimal conditions for self-assembly of the Keggin network. Morpholine has the least effect, likely due to the fact that it exists in significant excess (180-350 equiv.) in solution at either setting, however this may also be a result of its role as a counter cation, rather than integral part of the POM self-assembly process, suggesting that crystallisation is not the limiting factor in the synthesis of this POM.

MAK03-149, 151, 153	A	B	C	D	E	F	G	H	I	J	K	
Runs	**Morpholine**	**{γ-SiW_{10}}**	**$MnSO_4$**	**$KMnO_4$**	**Final pH**	**Reaction Temp.**	**Dummy 1**	**Dummy 2**	**Dummy 3**	**Dummy 4**	**Dummy 5**	**Yield [%]**
1	1	1	-1	1	1	1	-1	-1	-1	1	-1	**8**
2	1	-1	1	1	1	-1	-1	-1	1	-1	1	**0**
3	-1	1	1	1	-1	-1	-1	1	-1	1	1	**0**
4	1	1	1	-1	-1	-1	1	-1	1	1	-1	**0**
5	1	1	-1	-1	-1	1	-1	1	1	-1	1	**4**
6	1	-1	-1	-1	1	-1	1	1	-1	1	1	**4**
7	-1	-1	-1	1	-1	1	1	-1	1	1	1	**6**
8	-1	-1	1	-1	1	1	-1	1	1	1	-1	**0**
9	-1	1	-1	1	1	-1	1	1	1	-1	-1	**6**
10	1	-1	1	1	-1	1	1	1	-1	-1	-1	**2**
11	-1	1	1	-1	1	1	1	-1	-1	-1	1	**5**
12	-1	-1	-1	-1	-1	-1	-1	-1	-1	-1	-1	**2**
$\bar{y}_{-1}$	0,03	0,02	0,05	0,02	0,02	0,02	0,02	0,03	0,04	0,03	0,03	
$\bar{y}_1$	0,03	0,04	0,01	0,04	0,04	0,04	0,04	0,03	0,03	0,03	0,03	
Contrast (Δ)	0,00	0,02	-0,04	0,01	0,02	0,02	0,01	-0,01	-0,01	0,00	0,00	
Est. Effect	**-0,0006**	**0,0041**	**-0,0129**	**0,0048**	**0,0041**	**0,0055**	0,0041	-0,0030	-0,0043	-0,0019	-0,0042	

Table 29

Results including the average yields, the results for the low ($\bar{y}_{-1}$) and high settings ($\bar{y}_1$) within each factor, the contrasts (Δ) and the disentangled effects.

Values in green are significant and values in orange are among the three most important factors.

5.2 The {V_{18}} Network

Two 12-reaction screening experiments were conducted by varying factors A-F as shown in Table 31 at their maximum or minimum setting. Each repeat of the 12-run design was carried out in a randomly assigned and different running order to control for the effect of reaction order.

	Yield (based on V)		
Runs	**MAK03-165**	**MAK03-169**	**Average**
1	34 %	24 %	**29 %**
2	26 %	46 %	**36 %**
3	48 %	33 %	**41 %**
4	15 %	16 %	**16 %**
5	9 %	0 %	**9 %**
6	58 %	60 %	**59 %**
7	34 %	40 %	**37 %**
8	16 %	9 %	**12 %**
9	29 %	29 %	**29 %**
10	38 %	38 %	**38 %**
11	37 %	1 %	**37 %**
12	11 %	21 %	**16 %**

Table 30

{V_{18}} network results of transferred W of each run and repetition in percent as well as the averages of each run.

In the {V_{18}} Fe-linked network experiments the minimum significant factor effect was calculated as 6.9×10^{-2} and the absolute value of any effect had to be equal or higher to be considered as significant. Unfortunately, none of the effects were found to be significant in that respect but three factors had far higher effects than the others: (1) the concentration of vanadium pentoxide (V_2O_5), (2) the concentration of hydrazine sulphate ($[N_2H_5][HSO_4]$) and (3) the reaction time. Increasing the differential between the maximum and minimum settings of these factors may reveal greater insights into their effect on the synthesis in future. Surprisingly, the reaction temperature did not play an important role in the synthesis, whereas a higher yield was achieved when the reaction time was shorter and the concentration of vanadium pentoxide (V_2O_5) lower. The ratio of hydrazine sulphate to vanadium pentoxide seemed to be aiming for 2:1, providing an excess of both reducing electrons and sulphate anions and thus suggesting V reduction may be a key mechanistic step

in the formation of this cluster. However, reactions with separate sulphate sources may be required to disentangle these two possibilities.

MAK03-165, -169	A	B	C	D	E	F	G	H	I	J	K	
Runs	**LiOH**	**V_2O_5**	**Reaction Temp.**	**Hydrazine Sulphate**	**$FeCl_2$**	**Reaction Time**	**Dummy 1**	**Dummy 2**	**Dummy 3**	**Dummy 4**	**Dummy 5**	**Yield [%]**
1	1	1	-1	1	1	1	-1	-1	-1	1	-1	**29**
2	1	-1	1	1	1	-1	-1	-1	1	-1	1	**36**
3	-1	1	1	1	-1	-1	-1	1	-1	1	1	**41**
4	1	1	1	-1	-1	-1	1	-1	1	1	-1	**16**
5	1	1	-1	-1	-1	1	-1	1	1	-1	1	**9**
6	1	-1	-1	-1	1	-1	1	1	-1	1	1	**59**
7	-1	-1	-1	1	-1	1	1	-1	1	1	1	**37**
8	-1	-1	1	-1	1	1	-1	1	1	1	-1	**12**
9	-1	1	-1	1	1	-1	1	1	1	-1	-1	**29**
10	1	-1	1	1	-1	1	1	1	-1	-1	-1	**38**
11	-1	1	1	-1	1	1	1	-1	-1	-1	1	**37**
12	-1	-1	-1	-1	-1	-1	-1	-1	-1	-1	-1	**16**
$\bar{y}_{-1}$	0,29	0,33	0,30	0,25	0,26	0,33	0,24	0,28	0,37	0,28	0,23	
$\bar{y}_{1}$	0,31	0,27	0,30	0,35	0,34	0,27	0,36	0,31	0,23	0,32	0,36	
Contrast (Δ)	0,02	-0,06	0,00	0,10	0,07	-0,06	0,12	0,03	-0,13	0,05	0,13	
Est. Effect	**0,006**	**-0,034**	**0,002**	**0,035**	**0,019**	**-0,034**	0,053	0,026	-0,062	0,019	0,057	

Table 31

Results including the average yields, the results for the low ($\bar{y}_{-1}$) and high settings ($\bar{y}_{1}$) within each factor, the contrasts (Δ) and the disentangled effects.

Values in green are significant and values in orange are among the three most important factors.

5.3 The {Mo_{154}} Blue Wheel

One 12-reaction screening experiment was conducted by varying factors A-F as shown in Table 32 at their maximum or minimum setting. The 12-run design was carried out in a randomly assigned running order to control for the effect of reaction order.

In the {Mo_{154}} blue wheel experiment the minimum significant factor effect was calculated to be 5.6×10^{-2} and the absolute value of any effect had to be equal or higher to be considered as significant. (1) The stoichiometry of hydrazine sulphate (*[N_2H_5][HSO_4]*) was found to have a significant effect on the outcome, whereas (2) the reaction time did not pass the threshold of being significant but was still considerably high. (3) The pH adjustment by 5 M hydrochloric acid (*HCl*) had the third highest effect in this setup.

The positive value of Factor effect B indicates that higher yields were achieved with hydrazine sulphate (*[N_2H_5][HSO_4]*) at the higher setting and that the ratio in comparison with sodium molybdate dihydrate (*$Na_2MoO_4 \cdot 2H_2O$*) should be closer to 1:1 than 1:4 or even lower in order to achieve the optimal conditions for self-assembly of {Mo_{154}}. Although the amounts of sodium molybdate dihydrate (*$Na_2MoO_4 \cdot 2H_2O$*) in the two settings differed a lot from each other, it had barely any effect at all which indicates once more that the main driver of the system was the reducing agent.

MAK03-159	A	B	C	D	E	F	G	H	I	J	K	
Runs	**Na_2MoO_4**	**Hydrazine Sulphate**	**pH**	**Reaction Temp.**	**Reaction Time**	**Evaporation**	**Dummy 1**	**Dummy 2**	**Dummy 3**	**Dummy 4**	**Dummy 5**	**Yield [%]**
1	1	1	-1	1	1	1	-1	-1	-1	1	-1	**53**
2	1	-1	1	1	1	-1	-1	-1	1	-1	1	**3**
3	-1	1	1	1	-1	-1	-1	1	-1	1	1	**0**
4	1	1	1	-1	-1	-1	1	-1	1	1	-1	**21**
5	1	1	-1	-1	-1	1	-1	1	1	-1	1	**1**
6	1	-1	-1	-1	1	-1	1	1	-1	1	1	**7**
7	-1	-1	-1	1	-1	1	1	-1	1	1	1	**7**
8	-1	-1	1	-1	1	1	-1	1	1	1	-1	**0**
9	-1	1	-1	1	1	-1	1	1	1	-1	-1	**47**
10	1	-1	1	1	-1	1	1	1	-1	-1	-1	**0**
11	-1	1	1	-1	1	1	1	-1	-1	-1	1	**28**
12	-1	-1	-1	-1	-1	-1	-1	-1	-1	-1	-1	**1**
$\bar{y}_{-1}$	0,14	0,03	0,19	0,10	0,05	0,13	0,10	0,19	0,15	0,13	0,20	
$\bar{y}_{1}$	0,14	0,25	0,09	0,18	0,23	0,15	0,18	0,09	0,13	0,15	0,08	
Contrast (Δ)	0,00	0,22	-0,11	0,09	0,18	0,02	0,09	-0,10	-0,02	0,01	-0,13	
Est. Effect	**-0,008**	**0,075**	**-0,040**	**0,031**	**0,050**	**0,012**	0,023	-0,030	-0,009	0,005	-0,076	

Table 32

Results including the average yields, the results for the low ($\bar{y}_{-1}$) and high settings ($\bar{y}_{1}$) within each factor, the contrasts (Δ) and the disentangled effects.

Values in green are significant and values in orange are among the three most important factors.

5.4 The {Mo_{132}} Brown Keplerate

Two 12-reaction screening experiments were conducted by varying factors A-F as shown in Table 34 at their maximum or minimum setting. Each repeat of the 12-run design was carried out in a randomly assigned and different running order to control for the effect of reaction order.

	Yield (based on Mo)		
Runs	**MAK03-161**	**MAK03-163**	**Average**
1	36 %	49 %	**42 %**
2	35 %	34 %	**34 %**
3	31 %	30 %	**31 %**
4	18 %	17 %	**17 %**
5	29 %	24 %	**27 %**
6	15 %	22 %	**19 %**
7	2 %	2 %	**2 %**
8	34 %	34 %	**34 %**
9	4 %	2 %	**3 %**
10	31 %	30 %	**31 %**
11	26 %	24 %	**25 %**
12	2 %	1 %	**1 %**

Table 33

{Mo_{132}} brown Keplerate results of transferred Mo of each run and repetition in percent as well as the averages of each run.

In the {Mo_{132}} Keplerate experiments the minimum significant factor effect was calculated to be 4.2×10^{-2} and the absolute value of any effect had to be equal or higher to be considered as significant. Unfortunately, none of the effects were found to be significant in that respect but (1) the pH adjustment by 50 % acetic acid (*CH_3COOH*) almost passed the threshold. The effects of the following two factors were rather close to the minimum significant factor effect and high enough to be mentioned here: (2) the reaction temperature and (3) the concentration of ammonium acetate (*CH_3COONH_4*). The positive value of the Factor effect indicates that higher yields were achieved with Factor C at the higher setting demonstrating that the pH should be higher in order to achieve the optimal conditions for self-assembly of the {Mo_{132}} Keplerate. Interestingly, hydrazine sulphate (*$[N_2H_5][HSO_4]$*) has the least effect here which might be lead back to the small difference between the two settings or the predominant influence of the pH.

MAK03-161, 163	A	B	C	D	E	F	G	H	I	J	K	
Runs	**CH_3COONH_4**	**$(NH_4)_6Mo_7O_{24}$**	**Acetic Acid**	**Hydrazine Sulphate**	**Reaction Temp.**	**Reaction Time**	**Dummy 1**	**Dummy 2**	**Dummy 3**	**Dummy 4**	**Dummy 6**	**Yield [%]**
1	1	1	-1	1	1	1	-1	-1	-1	1	-1	**42**
2	1	-1	1	1	1	-1	-1	-1	1	-1	1	**34**
3	-1	1	1	1	-1	-1	-1	1	-1	1	1	**31**
4	1	1	1	-1	-1	-1	1	-1	1	1	-1	**17**
5	1	1	-1	-1	-1	1	-1	1	1	-1	1	**27**
6	1	-1	-1	-1	1	-1	1	1	-1	1	1	**19**
7	-1	-1	-1	1	-1	1	1	-1	1	1	1	**2**
8	-1	-1	1	-1	1	1	-1	1	1	1	-1	**34**
9	-1	1	-1	1	1	-1	1	1	1	-1	-1	**3**
10	1	-1	1	1	-1	1	1	1	-1	-1	-1	**31**
11	-1	1	1	-1	1	1	1	-1	-1	-1	1	**25**
12	-1	-1	-1	-1	-1	-1	-1	-1	-1	-1	-1	**1**
$\bar{y}_{-1}$	0,16	0,20	0,16	0,20	0,18	0,17	0,28	0,20	0,25	0,20	0,22	
$\bar{y}_1$	0,28	0,24	0,29	0,24	0,26	0,27	0,16	0,24	0,19	0,24	0,23	
Contrast (Δ)	0,12	0,04	0,13	0,03	0,08	0,09	-0,12	0,04	-0,05	0,04	0,01	
Est. Effect	**0,035**	**0,019**	**0,041**	**0,000**	**0,037**	**0,030**	-0,057	0,021	-0,016	0,005	0,011	

Table 34

Results including the average yields, the results for the low ($\bar{y}_{-1}$) and high settings ($\bar{y}_1$) within each factor, the contrasts (Δ) and the disentangled effects.

Values in green are significant and values in orange are among the three most important factors.

5.5 The {Mo_{132}} Brown Keplerate Crystals

Two weeks after the removal and collection of the dark brown {Mo_{132}} Keplerate solid material, huge dark brown crystals had formed. They were analysed in the same manner as the other POM products from all the other reactions.

	Yield (Based on Mo)		
Runs	**MAK03-161**	**MAK03-163**	**Average**
1	27%	10%	**19%**
2	36%	30%	**33%**
3	0%	0%	**0%**
4	37%	35%	**36%**
5	23%	21%	**22%**
6	37%	26%	**32%**
7	0%	0%	**0%**
8	0%	0%	**0%**
9	0%	0%	**0%**
10	35%	28%	**31%**
11	0%	0%	**0%**
12	0%	0%	**0%**

Table 35

{Mo_{132}} brown Keplerate crystals results of transferred Mo of each run and repetition in percent as well as the averages of each run.

In the {Mo_{132}} Keplerate crystals analysis the minimum significant factor effect was calculated to be 1.8×10^{-2} and the absolute value of any effect had to be equal or higher to be considered as significant. (1) The stoichiometry of ammonium acetate (CH_3COONH_4) and (2) the reaction time were found to have significant effects, whereas (3) the reaction temperature almost passed the threshold of being significant as well. The outstanding positive effect of factor A indicates that a higher concentration of ammonium acetate (CH_3COONH_4) leads to higher yields. This could be easily identified because only the samples with the higher setting of factor A formed crystals whereas the others had no yields at all. Surprisingly, a shorter reaction time yielded better results while the opposite was the case in the previous results. This makes sense though because less material reacted and was collected in the former procedure.

Interestingly, the results for the {Mo_{132}} Keplerate precipitate and crystals varied a bit. The concentration of ammonium acetate (*CH_3COONH_4*) and the reaction temperature were among the three most important factors in both cases, only the pH adjustment by 50 % acetic acid (*CH_3COOH*) and the reaction time differed in the results.

It seemed like removing the precipitate after a couple of days could have been examined as a factor as well because huge, seemingly pure crystals formed afterwards in half of the flasks containing only the higher concentration of ammonium acetate (*CH_3COONH_4*).

MAK03-161, 163	A	B	C	D	E	F	G	H	I	J	K	
Runs	**CH_3COONH_4**	**$(NH_4)_6Mo_7O_{24}$**	**Acetic Acid**	**Hydrazine Sulphate**	**Reaction Temp.**	**Reaction Time**	**Dummy 1**	**Dummy 2**	**Dummy 3**	**Dummy 4**	**Dummy 6**	**Yield [%]**
1	1	1	-1	1	1	1	-1	-1	-1	1	-1	**19**
2	1	-1	1	1	1	-1	-1	-1	1	-1	1	**33**
3	-1	1	1	1	-1	-1	-1	1	-1	1	1	**0**
4	1	1	1	-1	-1	-1	1	-1	1	1	-1	**36**
5	1	1	-1	-1	-1	1	-1	1	1	-1	1	**22**
6	1	-1	-1	-1	1	-1	1	1	-1	1	1	**32**
7	-1	-1	-1	1	-1	1	1	-1	1	1	1	**0**
8	-1	-1	1	-1	1	1	-1	1	1	1	-1	**0**
9	-1	1	-1	1	1	-1	1	1	1	-1	-1	**0**
10	1	-1	1	1	-1	1	1	1	-1	-1	-1	**31**
11	-1	1	1	-1	1	1	1	-1	-1	-1	1	**0**
12	-1	-1	-1	-1	-1	-1	-1	-1	-1	-1	-1	**0**
$\bar{y}_{-1}$	0,00	0,16	0,12	0,15	0,15	0,17	0,12	0,15	0,14	0,14	0,14	
$\bar{y}_1$	0,29	0,13	0,17	0,14	0,14	0,12	0,16	0,14	0,15	0,14	0,14	
Contrast (Δ)	0,29	-0,03	0,05	-0,01	-0,01	-0,05	0,04	-0,01	0,02	0,00	0,00	
Est. Effect	**0,100**	**-0,012**	**0,006**	**0,008**	**-0,016**	**-0,025**	0,011	0,000	0,018	-0,008	0,016	

Table 36

Results including the average yields, the results for the low ($\bar{y}_{-1}$) and high settings ($\bar{y}_1$) within each factor, the contrasts (Δ) and the disentangled effects.

Values in green are significant and values in orange are among the three most important factors.

6 Conclusion and Future Work

In all four, different POM syntheses, among the most important and often significant factors were the reducing agent, the reaction temperature, the reaction time, the pH, the conjugate base and the reactants themselves. This shows that no general statement can be made for all POM syntheses, probably due to the different types of structures examined in this work. Although, even among the similar clusters of {Mo_{154}} and {Mo_{132}} the differences were surprising. Nevertheless, the most important main factors for all four syntheses could be revealed and provide a good starting point for further investigation. It is highly likely that there are also significant interaction effects and a full factorial design examining at least the three most important main factors is recommended, since main factors turn out to be significant in screening designs if they are involved in a significant interaction. As soon as all significant main factors and two-factor interactions are unravelled, the optimisation of the procedures can also be explored by pushing the levels of the significant factors in a certain direction to obtain a higher quality and quantity of the desired product. Overall, DOE is an effective tool that aids the chemist into developing strategies for reaction control. In the case of notoriously unpredictable POM formations and syntheses, it provided guidance as to which variables are the most important. Thus, it maximises the potential of a successful synthesis and keeping a record of the significant experimental variables for future generations attempting such procedures.

7 Experimental

7.1 Materials

Unless otherwise mentioned, all solvents and reagents were purchased from commercial sources (primarily Sigma Aldrich and Tokyo Chemical Industry UK) and were used without further purification. The $K_8[\gamma\text{-}SiW_{10}O_{36}]\cdot 12H_2O$ and $K_8[\beta_2\text{-}SiW_{11}O_{39}]\cdot 14H_2O$ starting materials were synthesised following the published procedures in Section 7.3.

7.2 Instrumental

7.2.1 Single-Crystal X-Ray Diffraction

A small amount of Fomblin oil was placed on a glass slide. Some sample solution containing crystals was pipetted onto it and the excess solvent removed. The Fomblin oil serves a dual role of protecting the crystals during mounting and cooling, and as an adhesive during crystal mounting. A suitable single crystal was selected and mounted onto a rubber loop.

Single crystal datasets and unit cells were collected at 150 K on a Bruker Apex II Quasar diffractometer equipped with a graphite monochromator (λ ($Mo_{K\alpha}$) = 0.7107 Å) and a microfocus X-ray source (50 kV, 30 w). Data collection and reduction were performed using the Apex3 or CrysAlisPro software package, structure solution and refinement was carried out by SHELXS-2014 and SHELXL-2014 using WinGX.

7.2.2 Infrared Spectroscopy

The {γ-SiW_{10}} Keggin net precursor was collected in transmission mode using a JASCO FT-IR-410 spectrometer.

7.2.3 pH Measurements

Measurements were taken on a Hanna Instruments HI-2210-02 Bench Top pH Meter with pH electrode (HI 1131B) and temperature probe (HI 7662).

7.2.4 Elemental Analyses

Element analyses for all samples were performed by Inductivity Coupled Plasma Optical Emission Spectroscopy on an Agilent's 5110 ICP-OES using Argon gas and the Synchronous Vertical Dual View
(SVDV).

7.3 Standard Syntheses and Characterisation

7.3.1 Synthesis of $K_8[\beta_2\text{-}SiW_{11}O_{39}]\cdot 14H_2O$

The potassium β_2-undecatungstosilicate was synthesised as in the following procedure from A. Tézé and G. Hervé:[28]

$$11[WO_4]^{2-} + [SiO_3]^{2-} + 16H^+ + 8K^+ + 6H_2O \rightarrow K_8[\beta_2\text{-}SiW_{11}O_{39}]\cdot 14H_2O$$

Sodium metasilicate (11 g, 50 mmol) is dissolved in 100 mL of water (Solution A). Sodium tungstate (182 g, 0.55 mol) is dissolved in 300 mL of water in a separate 1 L beaker containing a magnetic stirring bar. To this solution, 165 mL of 4 M HCl is added in 1 mL portions over 10 min, with vigorous stirring (there is a local formation of hydrated tungstic acid that slowly disappears). Then, Solution A is poured into the tungstate solution, and the pH is adjusted to between 5 and 6 by addition of the 4 M HCl solution (~ 40 mL). This pH is maintained by addition of small amounts of 4 M HCl for 100 min. Solid potassium chloride (90 g) is then added to the solution with gentle stirring. After 15 min, the precipitate is collected by filtering through a sintered glass filter. Purification is achieved by dissolving the product in 850 mL of water. The insoluble material is rapidly removed by filtration on a fine frit, and the salt is precipitated again by addition of solid KCl (80 g). The precipitate is separated by filtration, washed with 2 *M* potassium chloride solution (2 portions of 50 mL), and air dried. Yield: ~ 60 to 80 g (37 - 50%).

Properties

Potassium β_2-undecatungstosilicate is a white solid, which is soluble in water. In solution it slowly converts into the β_3 isomer. It is characterized by polarography in 1 *M* sodium acetate-1 *M* acetic acid buffer. The polarogram shows two two-electron waves at - 0.63 and - 0.77 V *versus* SCE. The visible spectrum of the $[\beta_2\text{-}SiW_{10}O_{39}VO]^{6-}$ complex in aqueous solution shows: $\varepsilon^{sh}_{855} = 130$, $\varepsilon^{sh}_{670} = 420$, $\varepsilon^{max}_{510} = 780$, $\varepsilon^{min}_{370} = 290$.

The polyanion is characterized in the solid state by its IR spectrum (KBr pellet, cm^{-1}): 988, 945, 875, 855, 805, 730, 610 (sh), 530, 460 (sh), 395 (sh), 360, and 325.

7.3.2 Synthesis of $K_8[\gamma\text{-}SiW_{10}O_{36}]\cdot 12H_2O$

The potassium γ-decatungstosilicate was synthesised as in the following procedure from A. Tézé and G. Hervé:[28]

$$[\beta_2\text{-}SiW_{11}O_{39}]^{8-} + 2CO_3^{2-} + 8K^+ + 13H_2O \rightarrow K_8[\gamma\text{-}SiW_{10}O_{36}]\cdot 12H_2O + sHCO_3^- + [WO_4]^{2-}$$

This synthesis requires accurate pH readings on a calibrated pH meter.

The potassium salt of the β_2 isomer of undecatungstosilicate (15 g, 5 mmol), synthesized as described in the procedure in section 7.3.1, is dissolved in 150 mL of water maintained at 25 °C. Impurities in the $K_8[\beta_2\text{-}SiW_{11}O_{39}]$ salt (mainly paratungstate) give insoluble materials, which must be removed rapidly by filtration on a fine frit or through Büchner filtration. The pH of the solution is quickly adjusted to 9.1 by addition of a 2 M aqueous solution of K_2CO_3. The pH of the solution is kept at this value by addition of the K_2CO_3 solution for exactly 16 min. The potassium salt of the γ-decatungstosilicate is then precipitated by addition of solid potassium chloride (40 g). During the precipitation (10 min), the pH must be maintained at 9.1 by addition of small amounts of the K_2CO_3 solution. The solid is removed by filtering, washed with 1 M KCl solution, and air dried. Yield: ~ 10 g (70%).

Properties

The potassium salt of $[\gamma\text{-}SiW_{10}O_{36}]^{8-}$ is soluble in water and stable below pH 8 (in strongly acidic solution, pH < 1, it converts very slowly into $[\beta\text{-}SiW_{12}O_{40}]^{4-}$). A polarogram of the solution exhibits two reversible two-electron waves, with half-wave potentials - 0.75 and - 0.84 V *versus* SCE in 1 M acetic acid - 1 M sodium acetate buffer, pH 4.7. The ^{183}W NMR spectrum of the solution in H_20-D_20 (90/10) mixtures shows three lines with relative intensities 2:2:1, in agreement with the X-ray diffraction determination of the structure of the polyanion in the rubidium salt. The chemical shifts are, respectively, - 96.4, - 137.2, and - 158.2 ppm (external reference 2 M Na_2WO_4 in alkaline D_20).

The compound can be characterized in the solid state by its IR spectrum (KBr pellet, cm^{-1}): 989 (m), 941 (s), 905 (s), 865 (vs), 818 (vs), 740 (vs), 655 (sh), 553 (w), 528 (m), 478 (sh), 390 (sh), 360 (s), 328 (sh), 318 (m), and 303 (sh).

This lacunary polyanion is used to synthetize adduct complexes $[\gamma\text{-}SiW_{10}M_2O_{40}]^{n-}$, especially with V^V, Mo^{VI}, W^{VI}, and di- or trivalent cations of the first transition series.

7.3.3 Reference Synthesis $(C_4H_{10}NO)_{40}[W_{72}Mn_{12}O_{268}Si_7]\cdot 48H_2O$

Morpholine (9.0 g, 103 mmol) was added to 200ml of 1M NaCl and the pH subsequently adjusted to exactly 8.0 using 4.5M H_2SO_4. At this point fresh air dried $K_8[\gamma\text{-}SiW_{10}O_{36}]\cdot 12H_2O$ (1.486 g, 0.5 mmol) is added and stirred vigorously until fully dissolved. $MnSO_4\cdot H_2O$ (0.1267 g, 0.75 mmol) is then added as a solid, resulting in a bright yellow solution. $KMnO_4$ (0.0237 g,

0.15 mmol) is then added crystal by crystal over a period of 10 minutes and the solution stirred for a further 5 mins. At this point a deep brown solution is obtained which is centrifuged to remove any insoluble material. Finally, the pH of the solution is altered to precisely 7.75 using 4.5M H_2SO_4. Tetrahedral diffraction quality crystals begin to form after two weeks. Yield after one month = (350 mg, 15.4 µmol, 22.12 % based on W).

Elemental analysis for $(C_4H_{10}NO)_{40}[W_{72}Mn_{12}O_{268}Si_7]\cdot 48H_2O$, $C_{160}H_{496}Mn_{12}N_{40}O_{356}Si_7W_{72,}$ MW = 22770 g/mol^{-1} calcd (found) : C 8.44, (8.79); H 2.20, (2.16); N 2.46, (2.50); W 58.13, (58.01); Mn 2.90, (2.95) FT-IR (KBr) ṽ/cm^{-1} 1635(m), 1453(sh), 1310(sh), 1102(sh), 1042(sh), 984(sh), 900(sh), 737(br).

7.3.4 Reference Synthesis $[Fe_3V_{18}O_{42}(H_2O)_{12}(XO_4)]\cdot 24H_2O$ (X = V and S)

The following procedure is from Khan *et al:*[49]

An aqueous solution of $LiOH\cdot H_2O$ (3 mL, 5 mmol) was added to a stirred slurry of V_2O_5 (2.5 mmol) in water (10 mL) maintained at 84 - 86 °C. After the resulting solution was treated with hydrazinium sulphate (2.5 mmol), the reaction mixture was heated for another 10 min. The dark coloured solution was diluted to 25 mL (pH = 4.6) and subsequently treated with $FeCl_2\cdot 4H_2O$ (1.25 mmol) and heated for 3 - 7 h. The resultant solution was allowed to stand at room temperature in a stoppered flask for 12 h. Dark prism-shaped crystals were filtered from the mother liquor, washed with cold water to remove amorphous impurity and dried in air at room temperature to give 0.38 g (56 % yield based on vanadium) of 1. FT-IR (KBr; 1200 - 400 cm^{-1}): ṽ = 1131 (m, SO_4), 990 (s, V-O_{term}), 807 (m, VO_4), 689 (m, V-(μ_3-O)), 631 (m, V-(μ_3-O)) cm^{-1}.

8 Supplementary Information

8.1 Full Correlation Pattern of a Plackett-Burman Design

	A	B	C	D	E	F	G	H	I	J	K
AB	0	0	-0,333	-0,333	-0,333	0,333	-0,333	-0,333	0,333	0,333	-0,333
AC	0	-0,333	0	0,333	-0,333	-0,333	0,333	-0,333	0,333	-0,333	-0,333
AD	0	-0,333	0,333	0	0,333	0,333	-0,333	-0,333	-0,333	-0,333	-0,333
AE	0	-0,333	-0,333	0,333	0	-0,333	-0,333	-0,333	-0,333	0,333	0,333
AF	0	0,333	-0,333	0,333	-0,333	0	-0,333	0,333	-0,333	-0,333	-0,333
AG	0	-0,333	0,333	-0,333	-0,333	-0,333	0	0,333	-0,333	0,333	-0,333

AH	0	-0,333	-0,333	-0,333	-0,333	0,333	0,333	0	-0,333	-0,333	0,333
AI	0	0,333	0,333	-0,333	-0,333	-0,333	-0,333	-0,333	0	-0,333	0,333
AJ	0	0,333	-0,333	-0,333	0,333	-0,333	0,333	-0,333	-0,333	0	-0,333
AK	0	-0,333	-0,333	-0,333	0,333	-0,333	-0,333	0,333	0,333	-0,333	0
BC	-0,333	0	0	-0,333	-0,333	-0,333	0,333	-0,333	-0,333	0,333	0,333
BD	-0,333	0	-0,333	0	0,333	-0,333	-0,333	0,333	-0,333	0,333	-0,333
BE	-0,333	0	-0,333	0,333	0	0,333	0,333	-0,333	-0,333	-0,333	-0,333
BF	0,333	0	-0,333	-0,333	0,333	0	-0,333	-0,333	-0,333	-0,333	0,333
BG	-0,333	0	0,333	-0,333	0,333	-0,333	0	-0,333	0,333	-0,333	-0,333
BH	-0,333	0	-0,333	0,333	-0,333	-0,333	-0,333	0	0,333	-0,333	0,333
BI	0,333	0	-0,333	-0,333	-0,333	-0,333	0,333	0,333	0	-0,333	-0,333
BJ	0,333	0	0,333	0,333	-0,333	-0,333	-0,333	-0,333	-0,333	0	-0,333
BK	-0,333	0	0,333	-0,333	-0,333	0,333	-0,333	0,333	-0,333	-0,333	0
CD	0,333	-0,333	0	0	-0,333	-0,333	-0,333	0,333	-0,333	-0,333	0,333
CE	-0,333	-0,333	0	-0,333	0	0,333	-0,333	-0,333	0,333	-0,333	0,333
CF	-0,333	-0,333	0	-0,333	0,333	0	0,333	0,333	-0,333	-0,333	-0,333
CG	0,333	0,333	0	-0,333	-0,333	0,333	0	-0,333	-0,333	-0,333	-0,333
CH	-0,333	-0,333	0	0,333	-0,333	0,333	-0,333	0	-0,333	0,333	-0,333
CI	0,333	-0,333	0	-0,333	0,333	-0,333	-0,333	-0,333	0	0,333	-0,333
CJ	-0,333	0,333	0	-0,333	-0,333	-0,333	-0,333	0,333	0,333	0	-0,333
CK	-0,333	0,333	0	0,333	0,333	-0,333	-0,333	-0,333	-0,333	-0,333	0
DE	0,333	0,333	-0,333	0	0	-0,333	-0,333	-0,333	0,333	-0,333	-0,333
DF	0,333	-0,333	-0,333	0	-0,333	0	0,333	-0,333	-0,333	0,333	-0,333
DG	-0,333	-0,333	-0,333	0	-0,333	0,333	0	0,333	0,333	-0,333	-0,333
DH	-0,333	0,333	0,333	0	-0,333	-0,333	0,333	0	-0,333	-0,333	-0,333
DI	-0,333	-0,333	-0,333	0	0,333	-0,333	0,333	-0,333	0	-0,333	0,333
DJ	-0,333	0,333	-0,333	0	-0,333	0,333	-0,333	-0,333	-0,333	0	0,333
DK	-0,333	-0,333	0,333	0	-0,333	-0,333	-0,333	-0,333	0,333	0,333	0
EF	-0,333	0,333	0,333	-0,333	0	0	-0,333	-0,333	-0,333	0,333	-0,333
EG	-0,333	0,333	-0,333	-0,333	0	-0,333	0	0,333	-0,333	-0,333	0,333
EH	-0,333	-0,333	-0,333	-0,333	0	-0,333	0,333	0	0,333	0,333	-0,333
EI	-0,333	-0,333	0,333	0,333	0	-0,333	-0,333	0,333	0	-0,333	-0,333
EJ	0,333	-0,333	-0,333	-0,333	0	0,333	-0,333	0,333	-0,333	0	-0,333
EK	0,333	-0,333	0,333	-0,333	0	-0,333	0,333	-0,333	-0,333	-0,333	0
FG	-0,333	-0,333	0,333	0,333	-0,333	0	0	-0,333	-0,333	-0,333	0,333
FH	0,333	-0,333	0,333	-0,333	-0,333	0	-0,333	0	0,333	-0,333	-0,333
FI	-0,333	-0,333	-0,333	-0,333	-0,333	0	-0,333	0,333	0	0,333	0,333
FJ	-0,333	-0,333	-0,333	0,333	0,333	0	-0,333	-0,333	0,333	0	-0,333
FK	-0,333	0,333	-0,333	-0,333	-0,333	0	0,333	-0,333	0,333	-0,333	0

GH	0,333	-0,333	-0,333	0,333	0,333	-0,333	0	0	-0,333	-0,333	-0,333
GI	-0,333	0,333	-0,333	0,333	-0,333	-0,333	0	-0,333	0	0,333	-0,333
GJ	0,333	-0,333	-0,333	-0,333	-0,333	-0,333	0	-0,333	0,333	0	0,333
GK	-0,333	-0,333	-0,333	-0,333	0,333	0,333	0	-0,333	-0,333	0,333	0
HI	-0,333	0,333	-0,333	-0,333	0,333	0,333	-0,333	0	0	-0,333	-0,333
HJ	-0,333	-0,333	0,333	-0,333	0,333	-0,333	-0,333	0	-0,333	0	0,333
HK	0,333	0,333	-0,333	-0,333	-0,333	-0,333	-0,333	0	-0,333	0,333	0
IJ	-0,333	-0,333	0,333	-0,333	-0,333	0,333	0,333	-0,333	0	0	-0,333
IK	0,333	-0,333	-0,333	0,333	-0,333	0,333	-0,333	-0,333	0	-0,333	0,000
JK	-0,333	-0,333	-0,333	0,333	-0,333	-0,333	0,333	0,333	-0,333	0	0

Table 37

Full aliasing pattern for a twelve factor Plackett-Burman design with the minimum and maximum settings in Section 3.1 Table 10.

8.2 Correlation Pattern of a Plackett-Burman Design with 5 Dummy Factors

	A	**B**	**C**	**D**	**E**	**F**	**G**	**H**	**I**	**J**	**K**
AB	0	0	-0,333	-0,333	-0,333	0,333	-0,333	-0,333	0,333	0,333	-0,333
AC	0	-0,333	0	0,333	-0,333	-0,333	0,333	-0,333	0,333	-0,333	-0,333
AD	0	-0,333	0,333	0	0,333	0,333	-0,333	-0,333	-0,333	-0,333	-0,333
AE	0	-0,333	-0,333	0,333	0	-0,333	-0,333	-0,333	-0,333	0,333	0,333
AF	0	0,333	-0,333	0,333	-0,333	0	-0,333	0,333	-0,333	-0,333	-0,333
AG	0	0	0	0	0	0	0	0	0	0	0
AH	0	0	0	0	0	0	0	0	0	0	0
AI	0	0	0	0	0	0	0	0	0	0	0
AJ	0	0	0	0	0	0	0	0	0	0	0
AK	0	0	0	0	0	0	0	0	0	0	0
BC	-0,333	0	0	-0,333	-0,333	-0,333	0,333	-0,333	-0,333	0,333	0,333
BD	-0,333	0	-0,333	0	0,333	-0,333	-0,333	0,333	-0,333	0,333	-0,333
BE	-0,333	0	-0,333	0,333	0	0,333	0,333	-0,333	-0,333	-0,333	-0,333
BF	0,333	0	-0,333	-0,333	0,333	0	-0,333	-0,333	-0,333	-0,333	0,333
BG	0	0	0	0	0	0	0	0	0	0	0
BH	0	0	0	0	0	0	0	0	0	0	0
BI	0	0	0	0	0	0	0	0	0	0	0
BJ	0	0	0	0	0	0	0	0	0	0	0
BK	0	0	0	0	0	0	0	0	0	0	0
CD	0,333	-0,333	0	0	-0,333	-0,333	-0,333	0,333	-0,333	-0,333	0,333

CE	-0,333	-0,333	0	-0,333	0	0,333	-0,333	-0,333	0,333	-0,333	0,333
CF	-0,333	-0,333	0	-0,333	0,333	0	0,333	0,333	-0,333	-0,333	-0,333
CG	0	0	0	0	0	0	0	0	0	0	0
CH	0	0	0	0	0	0	0	0	0	0	0
CI	0	0	0	0	0	0	0	0	0	0	0
CJ	0	0	0	0	0	0	0	0	0	0	0
CK	0	0	0	0	0	0	0	0	0	0	0
DE	0,333	0,333	-0,333	0	0	-0,333	-0,333	-0,333	0,333	-0,333	-0,333
DF	0,333	-0,333	-0,333	0	-0,333	0	0,333	-0,333	-0,333	0,333	-0,333
DG	0	0	0	0	0	0	0	0	0	0	0
DH	0	0	0	0	0	0	0	0	0	0	0
DI	0	0	0	0	0	0	0	0	0	0	0
DJ	0	0	0	0	0	0	0	0	0	0	0
DK	0	0	0	0	0	0	0	0	0	0	0
EF	-0,333	0,333	0,333	-0,333	0	0	-0,333	-0,333	-0,333	0,333	-0,333
EG	0	0	0	0	0	0	0	0	0	0	0
EH	0	0	0	0	0	0	0	0	0	0	0
EI	0	0	0	0	0	0	0	0	0	0	0
EJ	0	0	0	0	0	0	0	0	0	0	0
EK	0	0	0	0	0	0	0	0	0	0	0
FG	0	0	0	0	0	0	0	0	0	0	0
FH	0	0	0	0	0	0	0	0	0	0	0
FI	0	0	0	0	0	0	0	0	0	0	0
FJ	0	0	0	0	0	0	0	0	0	0	0
FK	0	0	0	0	0	0	0	0	0	0	0
GH	0	0	0	0	0	0	0	0	0	0	0
GI	0	0	0	0	0	0	0	0	0	0	0
GJ	0	0	0	0	0	0	0	0	0	0	0
GK	0	0	0	0	0	0	0	0	0	0	0
HI	0	0	0	0	0	0	0	0	0	0	0
HJ	0	0	0	0	0	0	0	0	0	0	0
HK	0	0	0	0	0	0	0	0	0	0	0
IJ	0	0	0	0	0	0	0	0	0	0	0
IK	0	0	0	0	0	0	0	0	0	0	0
JK	0	0	0	0	0	0	0	0	0	0	0

Table 38

Aliasing pattern for a twelve factor Plackett-Burman design with the minimum and maximum settings in Section 3.1 Table 10 containing five dummy factors G-K.

8.3 Sample Yields

Keggin Net 1/3	**Yield [mg]**		**{V_{18}} Network**	**Yield [mg]**
MAK03-149b	27,00		MAK03-165a	534,80
MAK03-149c	51,20		MAK03-165b	393,00
MAK03-149d	46,90		MAK03-165c	276,60
MAK03-149e	28,40		MAK03-165d	198,50
MAK03-149f	28,80		MAK03-165e	335,40
MAK03-149k	57,60		MAK03-165f	348,20
MAK03-151a	14,50		MAK03-165g	444,00
MAK03-151b	15,10		MAK03-165h	327,10
MAK03-151c	9,20		MAK03-165i	473,60
MAK03-151d	19,60		MAK03-165j	526,40
MAK03-151e	13,90		MAK03-165k	354,90
MAK03-151f	28,50		MAK03-165l	101,20
MAK03-151g	14,30		MAK03-169a	263,10
MAK03-151k	29,70		MAK03-169b	339,10
MAK03-153a	5,90		MAK03-169c	461,80
MAK03-153b	12,30		MAK03-169d	387,40
MAK03-153d	37,10		MAK03-169e	431,40
MAK03-153e	24,30		MAK03-169f	277,70
MAK03-153g	19,20		MAK03-169g	481,50
MAK03-153h	6,70		MAK03-169h	4,70
MAK03-153j	15,10		MAK03-169i	13,30
MAK03-153l	8,20		MAK03-169j	410,50
Keggin Net 2/3	**Yield [mg]**		MAK03-169k	345,50
MAK03-99a	25,40		MAK03-169l	298,00
MAK03-99b	11,50		**{Mo_{154}} Wheel**	**Yield [mg]**
MAK03-99c	23,60		MAK03-159-a	248,90
MAK03-99d	33,50		MAK03-159-b	15,10
MAK03-99e	83,00		MAK03-159-d	255,00
MAK03-99f	12,20		MAK03-159-e	2,50
MAK03-99g	24,00		MAK03-159-f	46,60
MAK03-99h	51,70		MAK03-159-g	46,80
MAK03-99i	59,50		MAK03-159-i	226,00
MAK03-99j	8,20		MAK03-159-k	174,90
MAK03-99k	87,90		MAK03-159-l	1,90
MAK03-99l	47,20		**{Mo_{132}} Keplerate**	**Yield [mg]**
MAK03-101a	60,60		MAK03-161a	208,40
MAK03-101b	41,80		MAK03-161b	263,00
MAK03-101c	19,30		MAK03-161c	232,00
MAK03-101d	24,30		MAK03-161d	29,90

MAK03-101e	14,40
MAK03-101f	59,40
MAK03-101g	25,90
MAK03-101h	20,60
MAK03-101i	83,10
MAK03-101j	73,20
MAK03-101k	26,10
MAK03-101l	53,06
MAK03-103a	40,27
MAK03-103b	110,15
MAK03-103c	78,25
MAK03-103d	36,64
MAK03-103e	99,11
MAK03-103f	32,93
MAK03-103g	52,74
MAK03-103h	46,09
MAK03-103i	82,02
MAK03-103j	119,21
MAK03-103k	42,03
MAK03-103l	63,13
Keggin Net 3/3	**Yield [mg]**
MAK03-125a	74,30
MAK03-125b	15,80
MAK03-125c	19,10
MAK03-125d	35,80
MAK03-125e	56,60
MAK03-125f	96,50
MAK03-125g	29,60
MAK03-125h	12,30
MAK03-125i	54,50
MAK03-125j	47,00
MAK03-125k	26,50
MAK03-125l	23,50
MAK03-127a	48,00
MAK03-127b	47,30
MAK03-127c	21,70
MAK03-127d	52,80
MAK03-127e	61,30
MAK03-127f	16,70
MAK03-127g	50,90
MAK03-127h	27,70
MAK03-127i	77,30
MAK03-127j	46,50
MAK03-127k	19,10
MAK03-127l	42,10
MAK03-129a	12,70

MAK03-161e	193,30
MAK03-161f	130,70
MAK03-161g	212,10
MAK03-161h	215,80
MAK03-161i	9,40
MAK03-161j	91,50
MAK03-161k	13,50
MAK03-161l	192,20
MAK03-163a	135,70
MAK03-163b	13,30
MAK03-163c	124,80
MAK03-163d	8,60
MAK03-163e	217,60
MAK03-163f	208,50
MAK03-163g	174,00
MAK03-163h	186,80
MAK03-163i	10,10
MAK03-163j	205,70
MAK03-163k	178,10
MAK03-163l	362,10
{Mo_{132}} Crystals	**Yield [mg]**
MAK03-161cryst-b	196,70
MAK03-161cryst-e	213,20
MAK03-161cryst-f	275,40
MAK03-161cryst-g	221,90
MAK03-161cryst-h	165,80
MAK03-161cryst-j	228,40
MAK03-163cryst-a	159,90
MAK03-163cryst-c	258,20
MAK03-163cryst-h	168,90
MAK03-163cryst-j	181,40
MAK03-163cryst-k	156,40
MAK03-163cryst-l	76,70

MAK03-129b	34,30
MAK03-129c	78,20
MAK03-129d	70,60
MAK03-129e	39,70
MAK03-129f	49,00
MAK03-129g	49,00
MAK03-129h	52,70
MAK03-129i	15,70
MAK03-129j	26,20
MAK03-129k	15,90
MAK03-129l	26,50

Table 39

Total impure yields of all analysed samples with their sample codes.

8.4 ICP Results

	Elements [mmol]					**Elements [mmol]**		
Keggin Net Sample Code	**Mn**	**Si**	**W**		**{V_{18}} Sample Code**	**Fe**	**S**	**V**
MAK03-99a	0,04	0,02	0,18		MAK03-165a	0,35	0,02	1,95
MAK03-99b	0,04	0,02	0,18		MAK03-165b	0,21	0,07	1,94
MAK03-99c	0,00	0,00	0,03		MAK03-165c	0,17	0,03	2,07
MAK03-99d	0,04	0,02	0,18		MAK03-165d	0,28	0,03	1,69
MAK03-99e	0,07	0,02	0,25		MAK03-165e	0,30	0,12	1,78
MAK03-99f	0,05	0,03	0,28		MAK03-165f	0,28	0,06	1,89
MAK03-99g	0,00	0,00	0,02		MAK03-165g	0,16	0,06	1,96
MAK03-99h	0,03	0,01	0,11		MAK03-165h	0,22	0,08	1,76
MAK03-99i	0,06	0,03	0,27		MAK03-165i	0,23	0,08	1,75
MAK03-99j	0,06	0,03	0,27		MAK03-165j	0,57	0,10	2,70
MAK03-99k	0,07	0,03	0,28		MAK03-165k	0,46	0,09	3,37
MAK03-99l	0,00	0,00	0,02		MAK03-165l	0,30	0,09	1,73
MAK03-101a	0,06	0,03	0,26		MAK03-169a	0,31	0,14	2,03
MAK03-101b	0,06	0,03	0,27		MAK03-169b	0,49	0,16	3,29
MAK03-101c	0,00	0,00	0,01		MAK03-169c	0,16	0,09	2,03
MAK03-101d	0,05	0,02	0,23		MAK03-169d	0,25	0,06	2,35
MAK03-101e	0,06	0,02	0,22		MAK03-169e	0,55	0,06	3,47
MAK03-101f	0,04	0,02	0,16		MAK03-169f	0,19	0,05	1,98
MAK03-101g	0,05	0,02	0,22		MAK03-169g	0,45	0,08	1,89
MAK03-101h	0,05	0,02	0,21		MAK03-169h	0,06	0,03	0,75
MAK03-101i	0,06	0,03	0,28		MAK03-169i	0,26	0,09	1,83
MAK03-101j	0,00	0,00	0,02		MAK03-169j	0,23	0,11	2,25
MAK03-101k	0,02	0,01	0,06		MAK03-169k	0,24	0,16	1,95
MAK03-101l	0,06	0,02	0,24		MAK03-169l	0,07	0,04	2,41
MAK03-103a	0,00	0,00	0,01		**{Mo_{154}} Sample Code**	**Mo**	**Na**	**S**
MAK03-103b	0,00	0,00	0,02		MAK03-159-a	0,88	0,08	0,04

MAK03-103c	0,05	0,02	0,25		MAK03-159-b	0,66	0,02	0,04
MAK03-103d	0,06	0,02	0,23		MAK03-159-d	1,05	0,04	0,02
MAK03-103e	0,05	0,02	0,23		MAK03-159-e	0,14	0,01	0,01
MAK03-103f	0,05	0,02	0,24		MAK03-159-f	0,83	0,02	0,03
MAK03-103g	0,05	0,03	0,25		MAK03-159-g	0,76	0,02	0,01
MAK03-103h	0,06	0,03	0,27		MAK03-159-i	1,33	0,15	0,07
MAK03-103i	0,05	0,02	0,20		MAK03-159-k	1,01	0,07	0,05
MAK03-103j	0,04	0,02	0,21		MAK03-159-l	0,12	0,01	0,01
MAK03-103k	0,05	0,02	0,24		**{Mo_{132}} Sample Code**	**Mo**	**Na**	**S**
MAK03-103l	0,05	0,02	0,22		MAK03-161a	1,25	0,00	0,01
MAK03-125a	0,04	0,01	0,13		MAK03-161b	0,89	0,00	0,01
MAK03-125b	0,13	0,01	0,10		MAK03-161c	1,04	0,00	0,02
MAK03-125c	0,19	0,08	0,72		MAK03-161d	0,77	0,00	0,02
MAK03-125d	0,12	0,06	0,52		MAK03-161e	0,96	0,00	0,02
MAK03-125e	0,04	0,01	0,10		MAK03-161f	0,78	0,00	0,01
MAK03-125f	0,18	0,06	0,59		MAK03-161g	1,27	0,00	0,02
MAK03-125g	0,08	0,02	0,24		MAK03-161h	1,28	0,00	0,01
MAK03-125h	0,02	0,01	0,09		MAK03-161i	0,85	0,00	0,02
MAK03-125i	0,16	0,06	0,55		MAK03-161j	1,25	0,00	0,01
MAK03-125j	0,29	0,10	0,88		MAK03-161k	1,06	0,00	0,03
MAK03-125k	0,06	0,01	0,12		MAK03-161l	2,05	0,01	0,01
MAK03-125l	0,12	0,03	0,33		MAK03-163a	1,16	0,00	0,01
MAK03-127a	0,05	0,02	0,20		MAK03-163b	1,29	0,00	0,02
MAK03-127b	0,00	0,00	0,01		MAK03-163c	1,23	0,00	0,01
MAK03-127c	0,00	0,00	0,01		MAK03-163d	0,95	0,00	0,01
MAK03-127d	0,06	0,02	0,23		MAK03-163e	1,24	0,00	0,02
MAK03-127e	0,05	0,02	0,20		MAK03-163f	1,58	0,00	0,01
MAK03-127f	0,05	0,01	0,13		MAK03-163g	1,63	0,00	0,01
MAK03-127g	0,04	0,02	0,20		MAK03-163h	1,22	0,00	0,01
MAK03-127h	0,05	0,03	0,24		MAK03-163i	0,95	0,00	0,02
MAK03-127i	0,07	0,03	0,25		MAK03-163j	1,16	0,00	0,01
MAK03-127j	0,05	0,02	0,23		MAK03-163k	1,20	0,01	0,01
MAK03-127k	0,07	0,02	0,22		MAK03-163l	1,64	0,00	0,02
MAK03-127l	0,06	0,02	0,20		**{Mo_{132}} Sample Code**	**Mo**	**Na**	**S**
MAK03-129a	0,07	0,03	0,26		MAK03-161cryst-b	1,27	0,00	0,00
MAK03-129b	0,08	0,03	0,27		MAK03-161cryst-e	1,04	0,00	0,00
MAK03-129c	0,04	0,02	0,15		MAK03-161cryst-f	1,02	0,00	0,00
MAK03-129d	0,08	0,03	0,30		MAK03-161cryst-g	1,19	0,00	0,00
MAK03-129e	0,07	0,02	0,20		MAK03-161cryst-h	1,01	0,02	0,00
MAK03-129f	0,07	0,03	0,32		MAK03-161cryst-j	1,01	0,00	0,00
MAK03-129g	0,05	0,02	0,24		MAK03-163cryst-a	1,04	0,00	0,00
MAK03-129h	0,02	0,01	0,11		MAK03-163cryst-c	1,18	0,00	0,00
MAK03-129i	0,06	0,03	0,25		MAK03-163cryst-h	1,01	0,00	0,00
MAK03-129j	0,08	0,03	0,27		MAK03-163cryst-j	1,00	0,00	0,00
MAK03-129k	0,00	0,00	0,01		MAK03-163cryst-k	1,05	0,00	0,01
MAK03-129l	0,02	0,01	0,09		MAK03-163cryst-l	0,97	0,00	0,00

MAK03-149b	0,07	0,04	0,35
MAK03-149c	0,04	0,02	0,21
MAK03-149d	0,10	0,05	0,49
MAK03-149e	0,00	0,00	0,02
MAK03-149f	0,05	0,03	0,27
MAK03-149k	0,13	0,07	0,63
MAK03-151a	0,05	0,03	0,25
MAK03-151b	0,01	0,00	0,03
MAK03-151c	0,06	0,03	0,29
MAK03-151d	0,01	0,00	0,03
MAK03-151e	0,08	0,05	0,40
MAK03-151f	0,07	0,04	0,36
MAK03-151g	0,06	0,03	0,29
MAK03-151k	0,11	0,06	0,53
MAK03-153a	0,01	0,00	0,03
MAK03-153b	0,06	0,03	0,29
MAK03-153d	0,12	0,07	0,59
MAK03-153e	0,10	0,05	0,49
MAK03-153g	0,12	0,07	0,59
MAK03-153h	0,03	0,01	0,12
MAK03-153j	0,09	0,05	0,48
MAK03-153l	0,02	0,01	0,08

Table 40

Raw ICP results of all DOE experiments in ppm (mg/L).

8.5 Infrared Spectroscopy

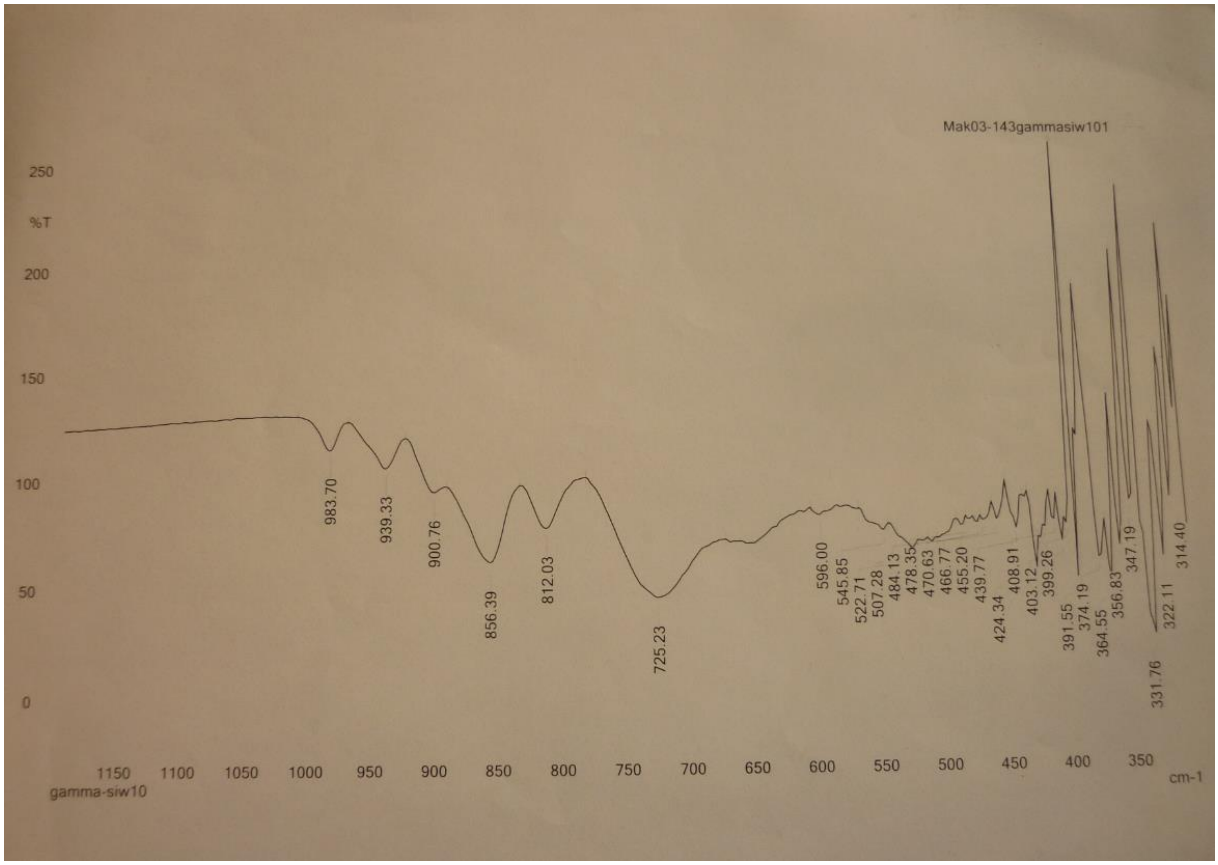

Figure 22

Confirmation of synthesised precursor compound {γ-SiW_{10}} from Section 7.3.2.

9 References

[1] E. Scheffler, *Einführung in die Praxis der statistischen Versuchsplanung*, *DVG*, Leipzig, **1986**.

[2] B. Durakovic, *Periodicals of Engineering and Natural Sciences* **2017**, *5*.

[3] R. P. Niedz, T. J. Evens, *In Vitro Cell. Dev. Biol., Plant* **2016**, *52*, 547-562.

[4] G. H. Bell, J. Ledolter, A. J. Swersey, *Interfaces* **2009**, *39*, 145-158.

[5] G. E. P. Box, R. D. Meyer, *Technometrics* **1986**, *28*, 11-18.

[6] A. K. Das, S. Dewanjee, *Computational Phytochemistry*, **2018**, pp. 75-106.

[7] C. R. Rao, *Supplement to the Journal of the Royal Statistical Society* **1947**, *9*, 128-139.

[8] A. N. Y. Vander Heyden, J. Smeyers-Verbeke, B.G.M. Vandeginste, D.L. Massart, *J. Pharm. Biomed. Anal.* **2001**, *24*, 723-753.

[9] L. B. Barrentine, *Quality Engineering* **1996**, *9*, 11-20.

[10] A. Müller, E. Beckmann, H. Bögge, M. Schmidtmann, A. Dress, *Angew. Chem. Int. Ed.* **2002**, *41*, 1162-1167.

[11] L. C. W. Baker, D. C. Glick, *Chem. Rev.* **1998**, *98*, 3-50.

[12] B. J. Coe, S. J. Glenwright, *Coord. Chem. Rev.* **2000**, *203*, 5-80.

[13] aL. C. W. Baker, T. P. McCutcheon, *J. Am. Chem. Soc.* **1956**, *78*, 4503-4510; bN. Casan-Pastor, P. Gomez-Romero, G. B. Jameson, L. C. W. Baker, *J. Am. Chem. Soc.* **1991**, *113*, 5658-5663.

[14] H. Aoto, K. Matsui, Y. Sakai, T. Kuchizi, H. Sekiya, H. Osada, T. Yoshida, S. Matsunaga, K. Nomiya, *J. Mol. Catal. A: Chem.* **2014**, *394*, 224–231.

[15] L. Ma, S. Liu, J. Zubieta, *Inorg. Chem.* **1989**, *28*, 175-177.
[16] A. Müller, E. Krickemeyer, M. Penk, V. Wittneben, J. Döring, *Angew. Chem. Int. Ed.* **1990**, *29*, 88-90.
[17] M. I. Khan, A. Müller, S. Dillinger, H. Bögge, Q. Chen, J. Zubieta, *Angew. Chem. Int. Ed.* **1993**, *32*, 1780-1782.
[18] M. T. Pope, *Inorg. Chem.* **1972**, *11*, 1973-1974.
[19] M. T. Pope, A. Müller, *Angew. Chem. Int. Ed.* **1991**, *30*, 34-48.
[20] J. M. Poblet, X. López, C. Bo, *Chem. Soc. Rev.* **2003**, *32*, 297-308.
[21] J. Zhang, Q. Li, M. Zeng, Y. Huang, J. Zhang, J. Hao, Y. Wei, *Chem. Commun.* **2016**, *52*, 2378-2381.
[22] A. W. A. Mariotti, J. Xie, B. F. Abrahams, A. M. Bond, A. G. Wedd, *Inorg. Chem.* **2007**, *46*, 2530-2540.
[23] M. Pope, *Heteropoly and Isopoly Oxometalates*, Springer-Verlag Berlin Heidelberg, Berlin, **1983**.
[24] G. Johansson, *Acta Chem. Scand.* **1960**, *14*, 771-773.
[25] S. M. Bradley, R. A. Kydd, R. Yamdagni, *J. Chem. Soc., Dalton Trans.* **1990**, 413-417.
[26] L. C. W. Baker, J. S. Figgis, *J. Am. Chem. Soc.* **1970**, *92*, 3794-3797.
[27] A. Müller, J. Döring, *Z. Anorg. Allg. Chem.* **1991**, *595*, 251-274.
[28] G. H. A. Tézé, R. G. Finke, D. K. Lyon, *Inorg. Synth.* **2007**, *27*, 85-96.
[29] N. H. Nsouli, B. S. Bassil, M. H. Dickman, U. Kortz, B. Keita, L. Nadjo, *Inorg. Chem.* **2006**, *45*, 3858-3860.
[30] G. Herve, A. Teze, *Inorg. Chem.* **1977**, *16*, 2115-2117.
[31] J. Canny, A. Teze, R. Thouvenot, G. Herve, *Inorg. Chem.* **1986**, *25*, 2114-2119.
[32] W. H. Knoth, R. L. Harlow, *J. Am. Chem. Soc.* **1981**, *103*, 1865-1867.
[33] C. W. Scheele, D. S. F. Hermbstädt, M. ed. Sändig, *Sämtliche Physische und Chemische Werke* **1971** (reprint: original **1793**), *Vol. 1*.
[34] D. Hagrman, C. Zubieta, D. J. Rose, J. Zubieta, R. C. Haushalter, *Angew. Chem. Int. Ed.* **1997**, *36*, 873.
[35] A. Müller, C. Serain, *Acc. Chem. Res.* **1999**, *33*, 2-10.
[36] P. Kögerler, B. Tsukerblat, A. Müller, *Dalton Trans.* **2010**, *39*, 21-36.
[37] A. Müller, P. Gouzerh, *Chem. Soc. Rev.* **2012**, *41*, 7431-7463.
[38] A. Müller, J. Meyer, E. Krickemeyer, E. Diemann, *Angew. Chem Int. Ed.* **1996**, *35*, 1206-1208.
[39] A. Müller, E. Krickemeyer, H. Bögge, M. Schmidtmann, C. Beugholt, P. Kögerler, C. Lu, *Angew. Chem. Int. Ed.* **1998**, *37*, 1220-1223.
[40] A. Müller, S. Q. N. Shah, H. Bogge, M. Schmidtmann, *Nature* **1999**, *397*, 48-50.
[41] H. N. Miras, G. J. T. Cooper, D.-L. Long, H. Bögge, A. Müller, C. Streb, L. Cronin, *Science* **2010**, *327*, 72-74.
[42] A. Müller, E. Krickemeyer, H. Bögge, M. Schmidtmann, F. Peters, *Angew. Chem. Int. Ed.* **1998**, *37*, 3359-3363.
[43] A. Müller, S. Sarkar, S. Q. N. Shah, H. Bögge, M. Schmidtmann, S. Sarkar, P. Kögerler, B. Hauptfleisch, A. X. Trautwein, V. Schünemann, *Angew. Chem. Int. Ed.* **1999**, *38*, 3238-3241.
[44] A. Müller, A. M. Todea, J. van Slageren, M. Dressel, H. Bögge, M. Schmidtmann, M. Luban, L. Engelhardt, M. Rusu, *Angew. Chem. Int. Ed.* **2005**, *44*, 3857-3861.
[45] A. Müller, H. Bögge, F. L. Sousa, M. Schmidtmann, D. G. Kurth, D. Volkmer, J. van Slageren, M. Dressel, M. L. Kistler, T. Liu, *Small* **2007**, *3*, 986-992.
[46] A. M. Todea, A. Merca, H. Bögge, J. van Slageren, M. Dressel, L. Engelhardt, M. Luban, T. Glaser, M. Henry, A. Müller, *Angew. Chem. Int. Ed.* **2007**, *46*, 6106-6110.
[47] Y. Wang, L. Ye, T.-g. Wang, X.-B. Cui, S.-Y. Shi, G.-W. Wang, J.-Q. Xu, *Dalton Trans.* **2010**, *39*, 1916-1919.
[48] J. Thiel, P. I. Molina, M. D. Symes, L. Cronin, *Crystal Growth & Design* **2012**, *12*, 902-908.
[49] M. Khan, E. Yohannes, R. Doedens, *Angew. Chem. Int. Ed.* **1999**, *38*, 1292-1294.